University of Alberta

Approaches to the Cryopreservation of Articular Cartilage

by

Nadr Mohamed Jomha ©

A thesis submitted to the Faculty of Graduate Studies and Research in partial fulfillment
of the
requirements for the degree of Doctor of Philosophy

in

Experimental Surgery
Department of Surgery

Edmonton, Alberta

Spring 2003

National Library
of Canada

Acquisitions and
Bibliographic Services

395 Wellington Street
Ottawa ON K1A 0N4
Canada

Bibliothèque nationale
du Canada

Acquisisitons et
services bibliographiques

395, rue Wellington
Ottawa ON K1A 0N4
Canada

Your file Votre référence
ISBN: 0-612-82121-8
Our file Notre référence
ISBN: 0-612-82121-8

The author has granted a non-exclusive licence allowing the National Library of Canada to reproduce, loan, distribute or sell copies of this thesis in microform, paper or electronic formats.

The author retains ownership of the copyright in this thesis. Neither the thesis nor substantial extracts from it may be printed or otherwise reproduced without the author's permission.

L'auteur a accordé une licence non exclusive permettant à la Bibliothèque nationale du Canada de reproduire, prêter, distribuer ou vendre des copies de cette thèse sous la forme de microfiche/film, de reproduction sur papier ou sur format électronique.

L'auteur conserve la propriété du droit d'auteur qui protège cette thèse. Ni la thèse ni des extraits substantiels de celle-ci ne doivent être imprimés ou aturement reproduits sans son autorisation.

Canada

University of Alberta

Library Release Form

Name of Author: Nadr Mohamed Jomha

Title of Thesis: Approaches to the Cryopreservation of Articular Cartilage

Degree: Doctor of Philosophy

Year this Degree Granted: 2003

Permission is hereby granted to the University of Alberta Library to reproduce single copies of this thesis and to lend or sell such copies for private, scholarly or scientific research purposes only.

The author reserves all other publication and other rights in association with the copyright in the thesis, and except as herein before provided, neither the thesis nor any substantial portion thereof may be printed or otherwise reproduced in any material form whatever without the author's prior written permission.

Nadr Mohamed Jomha

2D2.32 WCMC
Department of Surgery
University of Alberta Hospital
8440-112St.
Edmonton, Alberta
T6G 2B7
Canada

Jan 27/03
Date submitted

University of Alberta

Faculty of Graduate Studies and Research

The undersigned certify that they have read, and recommend to the Faculty of Graduate Studies and Research for acceptance, a thesis entitled Approaches to the Cryopreservation of Articular Cartilage submitted by Nadr Mohamed Jomha in partial fulfillment of the requirements for the degree of Doctor of Philosophy in Experimental Surgery.

Dr. Locksley E. McGann
Co-Supervisor

Dr. Marc Moreau
Co-Supervisor

Dr. Keith Bagnall
Committee Member

Dr. Ray Rajotte
Committee Member

Dr. Ron Zernicke
External Examiner

Jan. 24/03
Approval Date

Abstract

Large osteochondral defects degenerate into osteoarthritis and are a significant cause of disability. Current treatment regimens are unable to treat satisfactorily these injuries with successful long-term results. The method that demonstrates satisfactory results with the longest follow-up is osteochondral allografting. However, the use of this technique is limited by loss of chondrocyte viability, matrix damage during the storage period, inability to size accurately and contour match, risk of transmission of infectious disease, and inopportune surgical timing. Successful cryopreservation of intact osteochondral tissue will address all of these issues and provide viable chondrocytes that can maintain the intact cartilage matrix over long periods of time after transplantation.

Seven studies investigated aspects of cryopreserving intact porcine articular cartilage. The initial study validated a computer cell counting method designed to facilitate evaluation of cell recovery used in subsequent studies. This was followed by investigation of a cryopreservation protocol consisting of slow-cooling with low cryoprotectant concentration. Identification of significant obstacles to maintaining intact chondrocytes, as determined by membrane integrity stains, as well as preservation of the cartilage matrix intact led to further investigation of a cryopreservation protocol consisting of rapid-cooling with high cryoprotectant concentration. This technique produced promising results with respect to intact cell recovery and matrix integrity. Further investigations using temperature profiling, scanning electron microscopy and magnetic resonance imaging techniques provided insight into the events occurring within the cartilage matrix during the cryopreservation protocol.

The results of this research demonstrated significant obstacles to successful cryopreservation of intact porcine articular cartilage when using a slow-cool, low cryoprotectant concentration protocol. More promising results were produced when a rapid-cool, high concentration cryopreservation protocol was used as demonstrated by excellent cell recovery in specific areas and significantly less matrix disruption during the cryopreservation procedure. The results of these experiments highlight the possibilities of a rapid-cool, high cryoprotectant concentration protocol to cryopreserve intact articular cartilage. Excellent chondrocyte recovery with maintenance of matrix integrity can be achieved and suggest that use of this cryopreservation method is a viable option. Its use in the treatment of articular cartilage injuries remains a very real possibility.

Acknowledgements

This work could not have been completed without the help of some important people. I would like to thank Dr. Locksley McGann for his guidance throughout the many years of cryobiology research in which I have been involved. Dr. Keith Bagnall was magnificent with his prompt review of my written work and excellent constructive criticism. Dr. Marc Moreau was instrumental in my continued perseverance despite the persistent clinical pressures of my Orthopaedic surgical practice.

I thank Poovadan Anoop, my technician, whose hard work and creative suggestions prodded the research along its winding path. I also would like to thank Bonnie Haugen, my assistant, who has been there consistently and supportively throughout the four years of this research and my clinical practice. I also thank my parents (Alice and Mohamed) and my brothers (Ahmed, Rioth, Salah, and Marwan) and their families who are ever-present and supportive throughout all of my endeavours. Finally, I thank God, who has given me everything I have and blessed me beyond what I could have hoped for.

Table of Contents

Page

Chapter 1 – Introduction and General Literature Review 1

1.1 Introduction 2

1.2 General Literature Review 3

1.2.1 Articular Cartilage 3

1.2.2 Cryobiology 12

1.2.3 Vitrification 19

1.2.4 Viability Assays 27

1.2.5 Indications For Osteochondral Cryopreservation/ Vitrification 30

1.2.6 References 35

Chapter 2 – Validation and Reliability of Computerized Cell-Viability Analysis of Tissue Slices 55

2.1 Introduction 56

2.2 Materials and Methods 57

2.3 Results 63

2.4 Discussion 65

2.5 Acknowledgements 68

2.6 References 69

Chapter 3 – Chondrocyte Recovery in Cryopreserved Porcine Articular Cartilage after Bone Carrier Alteration 71

3.1 Introduction 72

3.2 Materials and Methods 73

3.3 Results 75

3.4 Discussion 77

3.5 Acknowledgements 79

3.6 References 80

Chapter 4 – Effects of Increasing Concentrations of Dimethyl Sulfoxide During Cryopreservation of Porcine Articular Cartilage 83
4.1 Introduction 84
4.2 Materials and Methods 85
4.3 Results 90
4.4 Discussion 92
4.5 Acknowledgements 98
4.6 References 99

Chapter 5 – Cryopreservation of Porcine Articular Cartilage in High Concentrations of Cryoprotectant 102
5.1 Introduction 103
5.2 Materials and Methods 104
5.3 Results 107
5.4 Discussion 113
5.5 Acknowledgements 118
5.6 References 119

Chapter 6 – Comparison of High Cryoprotectant Concentrations For Cryopreservation of Porcine Articular Cartilage 125
6.1 Introduction 126
6.2 Materials and Methods 127
6.3 Results 129
6.4 Discussion 131
6.5 Acknowledgements 134
6.6 References 135

Chapter 7 – MRI and Biochemical Assessments of Changes in Porcine Articular Cartilage after Different Freezing Protocols 138
7.1 Introduction 139
7.2 Materials and Methods 141
7.3 Results 145
7.4 Discussion 151
7.5 Acknowledgements 154
7.6 References 155

Chapter 8 – Intramatrix Events during Cryopreservation of Porcine Articular Cartilage Using Rapid Cooling 160
8.1 Introduction 161
8.2 Materials and Methods 162
8.3 Results 164
8.4 Discussion 169
8.5 Acknowledgements 172
8.6 References 173

Chapter 9 – General Discussion And Conclusion 176
9.1 General Discussion 177
9.2 Conclusion 183
9.3 References 185

List of Tables

		Page
Table 1-1	Articular cartilage environmental values	9
Table 1-2	Classification of viability assays	27
Table 2-1	Intra-rater Intraclass Correlation Coefficient for all evaluators and the computer program	64
Table 2-2	Inter-Rater Intraclass Correlation Coefficient within each group and including the computer program	64
Table 2-3	Pearson's correlation with 95% confidence intervals	65
Table 5-1	Combinations of Me_2SO concentrations and PBS solutions used to create the nine experimental solutions	109
Table 7-1	Biochemical data (mean average ± S.E. for n = 3 in all cases)	150
Table 8-1	Cooling rates for each cryoprotectant concentration determined by the time to cool from -20°C to -120°C for each Me_2SO concentration	166
Table 8-2	Percent of open area as determined by the Batch Processor program	169

List of Figures

Page

Figure 1-1 Phase diagram during cooling of solution containing a cryoprotectant agent 22

Figure 2-1 Computer generated histograms 59

Figure 2-2 Computer generated cumulative histograms 60

Figure 2-3 Digitized images 62

Figure 2-4 Computer generated images after processing by the computer program 62

Figure 3-1 Representation of the dowel with a hole drilled into the bone (a) and 70μm cartilage slices divided into nine equal sections (b) 75

Figure 3-2 Intact cell recovery comparing the nine sections of the two comparison groups 76

Figure 4-1 Schematic diagrams of an osteochondral dowel 87

Figure 4-2 SEM of AC after freeze-substitution of osteochondral dowels cryopreserved in 3*M* and 6*M* Me_2SO solutions using a rapid cooling technique 89

Figure 4-3 Intact chondrocyte recovery relative to fresh controls after 30 minutes exposure to different concentrations of Me_2SO at 4°C 90

Figure 4-4 Intact chondrocyte recovery relative to toxicity controls after proceeding through the cryopreservation protocol 91

Figure 4-5 Intact chondrocyte recovery relative to fresh controls after cryopreservation in different concentrations of Me_2SO 92

Figure 5-1 Schematic diagrams of an osteochondral dowel and 70μm section 109

Figure 5-2 Intact cell recovery after exposure to various Me_2SO concentrations at 4°C 110

Figure 5-3 Intact cell recovery after exposure to various PBS tonicities at 4°C 110

Figure 5-4 Intact cell recovery compared to fresh controls - 6*M* 111

Figure 5-5 Intact cell recovery compared to fresh controls - 5*M* 111

Figure 5-6 Cell recovery compared to toxicity controls – 6*M* 112

Figure 5-7 Cell recovery compared to toxicity controls – 5*M* 112

Figure 6-1 Cell recovery from toxicity controls by layers 130

Figure 6-2 Cell recovery from experimental samples by layers 130

Figure 7-1 Digital images illustrating three distinct bands in the cartilage matrix 143

Figure 7-2 Fixed charge density (FCD – mM) of the CTR group along with the three experimental groups characterizing the superficial, middle and deep bands 146

Figure 7-3 k_m (sec^{-1}) values of AC in the three bands from the CTR group and the three experimental groups 147

Figure 7-4 T_2 (ms) relaxation of AC in the three bands of all four groups 148

Figure 7-5 Diffusion coefficient of water perpendicular to AC surface in the three bands in all four groups 149

Figure 7-6 Diffusion coefficient of water parallel to AC surface in the three bands in all four groups 149

Figure 8-1 Temperature versus time graph of the temperature within the matrix during the rapid-cooling protocol from the different Me_2SO solutions 165

Figure 8-2 Temperature gradient graph using matrix temperature as the reference point 167

Figure 8-3 Representative scanning electron micrographs from the 1*M* Me_2SO, 5*M* Me_2SO, and 6*M* Me_2SO samples 168

Figure 8-4 Computer generated (Batch Processor) images of the open areas from the same samples as seen in Figure 8-3 168

List of Abbreviations

AC	articular cartilage
AFGP	anti-freeze glycoprotein
atm	atmosphere
Cv	concentration required to vitrify
CP	cryoprotectant
CPA	cryoprotectant
CTR	control
D	water diffusion coefficient
DB	deep band
EB	ethidium bromide
ECM	Extracellular matrix
FCD	fixed charge density
FDA	fluorescein diacetate
GAG	glycosaminoglycans
GD-DTPA^2	gadolidium DTPA
HCl	hydrochloric acid
H & E	hematoxylin and eosin
ICC	interclass correlation coefficient
LN/LN$_2$	liquid nitrogen
M	molar
MB	middle band
Me$_2$SO	dimethyl sulfoxide
MPF	Combination solution of 3.1*M* Me$_2$SO, 2.2*M* PD, 3.1*M* formamide
MRI	magnetic resonance imaging
MT	magnetization transfer
MTC	magnetization transfer contrast
OCD	osteochondral dowel
OD	optical density

PBS	phosphate buffered saline
PG	Proteoglycans
PG	1,2-propanediol
PVA	polyvinyl alcohol
SB	superficial band
SC-Me_2SO	slow-cooled in presence of Me_2SO
SC-PBS	slow-cooled in PBS
SD	standard deviation
SE	standard error
SF	snap frozen
SEM	scanning electron micscopy
TE	echo time
T_g	glass transition temperature
T_h	homogenous nucleation temperature
TR	repeat time
T_1	longitudinal relaxation time
T_2	transverse relaxation time
UV	ultraviolet
vol	volume
wt	weight
~	approximately

Chapter One

Introduction and General Literature Review

1.1 Introduction

Osteochondral injury and disease continues to be a significant cause of morbidity. Natural history studies clearly show that large, full-thickness, chondral lesions (greater than 1cm) (6, 42, 90, 222) consistently deteriorate to osteoarthritis, the second leading cause of disability in the United States (95). Approximately 17% of the United States population has osteoarthritis (1) and the disabling and debilitating costs are enormous with an estimated $65 billion dollars spent on treatment in the US in 1997, including direct medical costs of approximately $15 billion (1, 95). The huge personal and economic impact of chondral lesions has led to the investigation of numerous methods to treat this problem including osteochondral allografting.

Osteochondral allografting has been performed with variable results. Fresh allografts would logically seem to be the best solution but they have problems with accurate size and contour matching, testing for infectious diseases, and the timing of the surgical procedure. Frozen allografts have been used with some success but there have been problems with chondrocyte death and matrix disruption. Successful cryopreservation of articular cartilage (AC) allografts would result in viable cells in a minimally altered matrix that could be stored indefinitely. Long-term storage using cryoprotection would also allow accurate size and contour matching as well as extensive infectious disease testing. Furthermore, the surgical procedure could be performed when the surgical staff and patient are optimally prepared. Unfortunately, successful cryopreservation of intact AC has been elusive. The complex nature of the cartilage matrix with interactions between the proteoglycans, collagen, water and chondrocytes has provided barriers to successful cryopreservation that have yet to be overcome.

The objectives of this thesis are: 1) to investigate methods of cryopreservation in an animal model that closely represents human AC in both thickness and structure and 2) to provide insight on the barriers to successful cryopreservation and the subsequent development of methods to enhance current cryopreservation techniques. This thesis will begin with a review of the literature providing basic information on human AC and cryobiology as well as some of the difficulties encountered with cryopreservation of intact AC. It will proceed with a series of experiments designed to investigate mechanisms of damage to the cartilage matrix and cells during the cryopreservation procedure. This will be followed by a description of an alternative method of cryopreservation (vitrification) that has provided promising initial results.

1.2 General Literature Review

1.2.1 Articular Cartilage

Articular cartilage is a complex structure that develops over years with changes in cell shape and volume, collagen diameter and proteoglycan (PG) content depending on the depth in the matrix. Articular cartilage maturity corresponds with skeletal maturity at the time of closure of the growth plates. The constituents of AC are well documented and can be found in standard textbooks (138, 139) and review articles (89, 114, 182). This review will focus on the components of AC known or thought to have significant relevance to cryopreservation.

Articular cartilage can be divided into four zones – superficial, middle (transition), deep, and calcified. The superficial zone comprises 10-20% of the thickness of the cartilage although this percentage increases towards the periphery of the joint. The superficial zone is covered by a 3μm thick "skin" called the lamina splendens (102, 112) that consists of tightly packed small collagen fibers (10-30nm) (168). Below the lamina splendens, the 10-20μm diameter cells lie elongated with the long axis parallel to the joint surface (168). The water content of this zone is approximately 80% of the wet weight of the matrix, the highest of any zone. The collagen fibers are thin and run mainly parallel to the joint surface while the PG content is the lowest of any zone. The superficial zone is less permeable than the deeper zones and may act to resist expansion. This zone is essential for joint function including transmission of compressive forces to bone (32, 198). Fibrillation of the superficial zone can result in early loss of mechanical function (32).

The middle or transition zone is the largest zone, approximately 40-60% of the matrix thickness. The cells are more rounded and active and reside in a "moat" consisting of increased water content contained by sparse collagen fibers; a specific microenvironment exists (79). The collagen fibers are larger (60nm) and lose the orientation seen in the superficial zone. The PG content is the highest of all four zones and they are loosely attached to the collagen fibers.

The deep zone has spherical chondrocytes lined up in a columnar fashion. The water content is the lowest (approximately 65%) while the collagen fibers are thin and become larger (up to 150nm) and more vertically oriented as they reach the tidemark, a thin, well-defined line that demarcates the transition from the deepest uncalcified zone to the calcified zone (138).

The final, deepest zone is the calcified zone, which is separated from the other three zones by the tidemark at skeletal maturity. The chondrocytes are small pyknotic cells which are usually dead. The collagen fibers align perpendicular to the articular surface and progress through the tidemark (168) but are not in continuity with the underlying bone. There is minimal PG content. The tidemark is 2-5μm thick and may provide a tethering mechanism for the collagen fibers to prevent shear stresses. The permeability of the tidemark after skeletal maturity remains controversial. Small gaps in the tidemark may allow passage of nutrients (190) as has been demonstrated on baboons (134). Conversely, hydrogen diffusion through subchondral bone ceases with skeletal maturity indicating an absence of nutrient diffusion at that time (176). Unfortunately, these experiments were performed with only small numbers of animals and definitive conclusions remain to be drawn.

In addition to the four zones described, there is also variation throughout the extracellular matrix (ECM). The ECM consists of a dense stable network of collagen fibers embedded in a very high concentration of PG gel. There are three ECM zones dispersed throughout the four zones just described – pericellular, territorial, and interterritorial (91). The pericellular zone is a thin layer immediately adjacent to the cell membrane. The cell, along with the pericellular zone, is called a chondron (119). The pericellular zone is comprised mainly of PG with small amounts of closely packed collagen. This zone provides hydrodynamic protection to the cell and may reflect topographical differences in metabolic activity (78, 79). The well-defined territorial matrix surrounds the pericellular matrix and contains larger collagen fibers and PGs. The interterritorial matrix is the largest region with a progressive increase in prominence as the matrix progresses from superficial to deep. It contributes the majority of material properties of AC due to large, parallel collagen fibers and PGs.

The chondrocytes within the cartilage matrix constitute approximately 1% of the tissue volume and are 5-20µm in diameter. These metabolically active cells maintain the matrix and are stimulated by many factors including the environment (cytokines, growth factors, hormones, drugs) (110, 214) and current matrix composition (110, 126, 147). Mechanical loads (stresses, strains, flow velocities, osmotic and hydraulic pressures, electrical currents and potentials) (63, 126, 205, 206, 214) can stimulate cells typically through changes in cell shape (81, 101, 102, 214, 225). The cell volume can change 20% with physiologic levels of matrix deformation and when chondroytes are removed from the matrix, they can expand 30-40% (79, 101). The cells survive by diffusion and convective transport of nutrients through the matrix. Chondrocytes are heterogenous and produce matrix at different rates and respond to growth factors differently (81, 111). This complex arrangement with its many components make it difficult for cryopreservation because each component has its own special requirements for effective recovery that may be detrimental, even lethal, for the other components.

Water content varies throughout the matrix (123, 139) ranging from 80% in the superficial zone to 65% in the deep zone. A small proportion of the water is intracellular and approximately 30% is in the intrafibrillar space within the collagen. The water in the cells and collagen fibrils is not available for transport under mechanical loading and is excluded from interaction with the PG molecules resulting in increased density of fixed charges, raised interstitial osmotic pressure and high charge-charge repulsion. The remainder of the water exists in the molecular pores of the ECM. Approximately 94% of the total water is freely available for exchange while the remaining 6% is extremely tightly bound and will not exchange. The hydrophilic nature of PG is especially important due to its effect on matrix mechanical function and is due to the following three factors –

1) Donnan osmotic pressure due to interstitial free floating counter ions required to neutralize charges on the PG, 2) electrostatic repulsive forces between fixed negative charges along the PG, and 3) the entropic tendency of the PGs to gain volume in solution. There is a fine balance between the total swelling pressure of the PG from these forces and the constraint induced by the collagenous network (142). It is by these mechanisms that water is maintained in AC and has the ability to function as a supporter of mechanical loads. The complex interactions of the large volume of water with the solid matrix components provide a formidable obstacle to cryopreservation because ice crystal formation during cooling can cause irreparable damage to occur in the matrix.

Six different types of collagen have been identified in AC making up 50% of the dry weight and 10-20% of the wet weight of the matrix (114, 139). The vast majority is Type II (90-95%) with Types V/VI/IX/X/XI making up the rest. Collagen provides tensile strength to the matrix and immobilizes the PGs. Type II collagen is uniformly distributed throughout the matrix while the other types are more localized. Type VI collagen is localized to the pericellular capsule and may tether the chondrocytes to the matrix. Type IX is also concentrated pericellularly and covalently links Type II collagen fibrils (49, 114). The cross-linking contributes to the tensile strength, allows greater structural stability, less susceptibility to calcification, increased availability for PG linkage and gel formation to maintain the high water content. It also renders the fibers insoluble. These properties highlight the delicate balance that exists within the matrix. Disruption of the cross-linking by ice formation during cryopreservation may result in early degeneration of the cartilage due to the loss of the cross-linking properties. The remaining collagen types likely do not appear to have significant importance in cryopreservation. The collagen fibers constitute a regular arcade with fibers lined up parallel to the joint surface in the superficial zone, more randomly oriented in the intermediate zone and, finally, perpendicular to the articular surface in the deep zone (31, 36, 168) (classically described by Benninghoff in 1925 (13)). Overlying that characteristic arcade is a subpopulation of fibrils and fibril bundles organized more randomly (32). The structured collagen alignment in each zone indicates specific mechanical function for those zones and must not be disrupted by ice formation during any cryopreservation procedure.

The proteoglycans make up 5-10% of the wet weight of the matrix and consist of a protein core with glycosaminoglycan chains (GAG) attached to them (114, 139). Very large groups of PG molecules (aggrecans) can bind together on one hyaluronic acid molecule forming a large PG aggregate and this enhances the immobilization of the PG within the collagenous matrix. The PG concentration is lowest in the superficial zone and higher in the deeper zones (123). The PG have a homogenous distribution in the intermediate zone and a more variable distribution in the deep zone with increased concentrations of PG surrounding individual cells in all zones. The PGs are an important component of AC and maintaining this complex arrangement would seem crucial to reactivating the cartilage after cryopreservation.

The glycosaminoglycans (GAGs) exist in three main types – chondroitin sulfate (4- and 6- isomers), keratin sulfate, and dermatin sulfate. Hyaluronate is also a GAG and is the anchor for the aggrecan. Hyaluronan may also link the ECM with the chondrocytes through receptors found on the cells. The GAGs contain COOH and SO_4 terminals in solution that ionize to COO^- and SO_3^- requiring Na^+ and Ca^{++} to maintain neutrality. The negatively charged COO^- and SO_3^- are closely packed together in the dense solid matrix (PGs are packed into 1/5th of their free solution volume) resulting in strong charge-charge repulsive forces that is important with respect to swelling pressure and affects the compressive stiffness of AC. The swelling pressure due to the fixed charge density inflates the collagen network and helps maintain the ECM organization due to interaction between the collagen and PGs (108). It also allows the collagen to sustain tensile loads and provides shear stiffness. The fixed charge density can determine the transport of electrolytes and electrokinetic properties of AC (143-145). The free floating ions within the interstitial water give rise to the Donnan osmotic effect previously mentioned. The PG molecules are too large to move in the matrix and do not contribute to the tensile stiffness and strength of the cartilage by themselves. These factors allow the collagen/PG network to impart structural rigidity on the matrix and presumable the integrity of these components must be maintained for AC to survive and function. In addition, the strong electrolyte attraction to maintain neutrality complicates cryopreservation due to the potentially lethal effect of increasing electrolyte concentrations as ice forms in the solution.

Integrins are transmembrane molecules on the outer surface of the chondrocytes that are attached to the surrounding matrix (167). The molecules attach inside the cell on cytoskeletal proteins and are important in the transmembrane signalling of environmental and mechanical stimuli. Disruption of membrane attachments could be extremely important if excessive cell dehydration occurs during cryopreservation.

Cartilage thickness is a function of mechanical stress with thicker cartilage found in unconfined, weight-bearing joints in heavier animals (213). Stockwell's study on humans and animals (213) documented cartilage thickness as being proportional to body weight. The one exception was human cartilage, which was exceptionally thick, possibly because humans are not quadrupeds. Shepherd *et. al.* (200) determined that human knee joints contained thicker cartilage than hip and ankle joints and concluded that less constrained joints contained thicker cartilage. Another important factor may be nutrition. Glucose was shown to have a maximal penetration of 3mm into AC matrix (146) and chondrocyte replication has been noted with increased access to nutrients (169). Therefore, cartilage thickness may be limited by diffusion of nutrients. Consistent with this, cell density decreases with increased distance from the articular surface (213). This could indicate less cellular control in thicker AC because of the consistent lower density of cells in the deep portions of the cartilage. Finally, the chondrocytes may act as mechanoreceptors to detect internal stresses and strains of the tissue and react by synthesizing the necessary matrix materials (81, 167).

The ionic environment of AC is significantly different from the serum (80, 144, 223). The cation (Na^+, K^+, H^+, Ca^{++}) concentration is elevated while the anion (Cl^-, $HCO3^-$) concentration is decreased and these concentrations vary from the superficial to the deep zones. Accordingly, the osmotic and pH levels in the matrix are different than the serum levels.

A representative table is presented (144, 223):

Ion	Superficial	Deep	Tissue/serum
Na^+	240-279	300-350	140
K^+	7-9	9-12	5
Ca^{++}	6-9	14-20	1.5
Cl^-	60-90	50-100	145
Osm	310-370	370-480	280-300
pH	7.1-7.3	6.9	7.4

Table 1-1. Articular cartilage environmental values

The low oxygen environment in the matrix results in anaerobic metabolism with lactic acid formation (212). The acid diffuses out but the hydrogen ions are attracted by the polyanionic PG, resulting in a pH as low as 6.9 in the deep zone. The chondrocytes have a resting pH of 7.1. Therefore they contain powerful buffering and proton transport systems such as the Na^+-H^+ antiporter system. The extracellular osmotic environment is high and there is evidence of stretch activated channels. Changes in the intracellular and extracellular environment activate regulatory volume increases/decreases through multiple mechanisms including Na^+-K^+-$2Cl^-$ cotransporter (increase volume), Cl^- dependent K^+ transporter, Ca^{++} activated K^+ channel, and osmolyte channel (main volume decreaser) as reviewed by Hall *et. al.* (80) Changes in the physical environment (such as loading) can alter the activity of membrane transporters as well as the intracellular components of the chondrocytes. This leads to modulation of the matrix metabolism. These mechanisms of cellular modulation are at risk during cryopreservation because the cell membranes, where the transport mechanisms are located, are primary targets for injury during cryopreservation.

Articular cartilage obtains its nutrition primarily from the synovial fluid via the mechanical action of the joint surface interaction (139). In immature joints there is also a contribution from the permeable underlying bony substrate that may be eliminated with skeletal maturity when the tidemark develops (144, 176). The matrix contains pores of approximately 20-65Å (117) that permits the diffusion of only low molecular weight compounds (<20kd). Diffusion is dependent on molecular weight, size/configuration, structure and charge of the particle (143, 144) and can be enhanced by cyclic and intermittent loading. Small solutes and nutrient molecules diffuse rapidly through the matrix. Large molecules may not be able to diffuse through due to the small effective pore size that can decrease in response to matrix compression. For example, the tightly packed matrix prevents access by the monocytes and immunoglobulins and eliminates any immunologic interaction providing AC with an "immunoprivileged" status.

Mechanical loading seems to play an essential role in the maintenance of cartilage composition, structure and mechanical properties. The chondrocytes are pressure or deformation sensitive and loading changes the internal composition of the cells (cell volume, pH, ionic content) resulting in mechanical, electrical, and physiochemical signals (81, 101). High frequency loading stimulates chondrocyte synthetic activity and aids in internal tissue remodeling, which can occur quite quickly. Static loading decreases matrix synthesis (102, 111, 214, 225). Collagen synthesis is slow and final construction is completed outside of the cell. Conversely, PG synthesis is rapid and completed intracellularly with the final product secreted into the "moat" surrounding the cell.

The biphasic nature of AC dictates its mechanical properties (116) during physiologic use. Therefore, its unique structure is essential to normal function. Loading is shared between solid and fluid phases and the proportion of sharing is determined by volumetric ratios of the tissue (porosity/solidity), loading rates, type of loading (tension/compression/shear), and load partition at the surface. In AC, the matrix is porous, permeable and soft. Therefore it has high frictional drag forces that result in high hydrodynamic pressures or large compressive loads to maintain flow (140). This indicates that fluid pressure provides a significant portion of the total load support (90% (66)) with minimal stress on the solid matrix. Therefore, frictional drag forces dominate the compressive viscoelastic behaviour (creep and stress relaxation) and provide a mechanism for energy dissipation (140). The compressive properties of AC change with increasing depth (198) and are provided by PG osmotic pressure with possible help from the collagen fibers or a PG gel network with some solid-like mechanical properties (108).

Chondrocytes also have viscoelastic properties but have an equilibrium modulus three orders of magnitude less than the ECM (63, 78, 79, 101). The pericellular matrix plays an important role in determining the mechanical stress and the deformation behaviour of the chondrocytes (79). Under physiologic loading conditions, chondrocytes undergo significant volume and shape changes and the chondrocytes experience non-uniform, time-varying stress, strain, fluid flow and pressure fields. The mechanical environment of the cells is influenced by the structures and properties of the cells themselves, the pericellular matrix and the extracellular matrix.

It is evident that AC is a complex structure consisting of many interacting components that are required for normal long-term function as has been described. Most importantly, when considering cryopreservation, is the high water content within the matrix. The fact that water is intimately associated with virtually all AC components makes cryopreservation of AC especially difficult. The phase separation that occurs with ice formation poses the most threatening event during cryopreservation. The prevalence of water throughout the matrix and within the chondrocytes means that all components of the cartilage are at risk during cryopreservation with ice formation. Significant alterations of the water properties during cryopreservation will affect the mechanical properties provided by the collagen and PGs. Damage to these matrix components can lead to early cartilage degeneration. Physiological properties due to factors such as electrolyte concentration also will be adversely affected with ice formation because of the removal of pure water when ice forms. In addition, regulatory mechanisms are at risk during cryopreservation due to injuries that occur to the cell membranes. Therefore, it will be essential to limit the amount of damage caused by ice formation, whether it is due to mechanical causes (alterations in the collagen and PG structure and location), or by physiological causes (rising electrolyte concentrations or membrane disruption). Articular cartilage is a highly organized tissue maintained precisely by active chondrocytes. The delicate balance that exists between components such as chondrocytes, collagen and PGs and their effect on the water and electrolytes in the matrix is essential for normal function of AC. The ability to cryopreserve and then warm AC must allow each individual component to function not only individually but also in harmony as an overall unit for good long-term function.

1.2.2 Cryobiology

Cryobiology examines the effects of cold on biologic tissues with emphasis on the interactions of water with cellular components that become intimately involved during the cooling process. More recent investigation has begun to consider the extracellular environment as well. The modern era of cryobiology began in 1937 when Luyet (131) began observing the major biological effects that occurred with the phase change from water to ice. In 1949, Polge *et. al.* (183) discovered the protective action of glycerol. Since then, numerous articles have been written focusing on the cause of cell injury during cryopreservation.

The plasma membrane is an important primary target of freeze injury during slow and rapid cooling (3, 149, 161) possibly by damage to transport channels within the membrane (161, 208), osmotically driven water flux (171, 172) or membrane deformities due to the presence of extracellular ice (2, 221). Early work done by Lovelock (128, 129) focused on high solute concentrations as the primary cause of membrane damage and cell death. Exposure to high salt concentrations induced membrane leakage (exacerbated by slow cooling (41)) with subsequent dilution and intracellular Na^+ buildup (127) leading to intracellular organelle damage and expansion-induced lysis. Similar conclusions about damage due to high electrolyte concentration exposure were related to minimal cell volume (164, 165) (although disputed (209)), membrane leakage (56, 57), and prolonged exposure (156, 157). Further elucidation of Lovelock's theory that high solute concentrations damaged cell membranes incorporated splitting of cytoplasmic salt-bridged proteins (9, 137, 164) to accommodate increased intracellular cations. As the proteins are brought into solution the net effect is to decrease the intracellular ion concentration without changing the osmotic pressure of the cytoplasm resulting in continued influx of Na^+ as the extracellular Na^+ moves down the concentration gradient. Upon thawing, the extracellular solution becomes isotonic and the proteins "salt out" of solution releasing the cations resulting in excessive water influx and expansion-induced lysis causing lethal injury to the cell.

Factors other than high electrolyte concentrations have been considered to affect cryopreservation including the destruction of the relationship between intracellular water and surface proteins by excessive cell dehydration leading to protein denaturation (86), electrical currents at the growing ice interface in aqueous solutions contributing to cell membrane disruption (207, 229) and physical damage to the cellular membranes during ice formation (67, 68). Methods of cell damage such as "cold shock" or "chilling injury" (128, 129) and "thermal shock" (56) take into account other factors such as cell temperature and the interval through which the cell is cooled with emphasis on the stress differential of thermal contraction.

Osmotic pressure has been implicated in producing cell membrane damage (125) as a gradient can develop at the minimum cell volume causing an elastic failure of the membrane while in the shrunken state (164, 165, 226). Further substantiation of osmotic pressure injury was provided by Muldrew *et. al.* (171). Plasma membrane damage occurred at a critical gradient in osmotic pressure across the membrane with and without intracellular freezing and it was concluded that the water flux driven by the osmotic pressure did the damage to the cell membrane.

In addition to the membrane damage theories just discussed, the formation of intracellular ice during the cooling stage has received significant attention. Theories such as differentials in intracellular/extracellular osmotic pressures (125), extracellular ice nucleation via small tip radius (151, 152), and supercooling (120, 122) have provided possible mechanisms of intracellular ice formation. The intracellular ice was proposed to have solution effects inside the cells by concentrating the electrolytes resulting in damaged organelle membranes. It is likely that intracellular ice is generally lethal to cells (2, 3, 105) although some controversy exists (58, 153) and if present, it must be in minimal amounts (< 4% of total intracellular water) for the cell to survive (105).

The majority of the cellular toxicity that has been attributed to cell membrane damage due to high electrolyte concentrations can be considered slow-cooling injury. In effect, if the cooling process is a slow one, there will be ample opportunity for exposure of the cells to the high electrolyte concentrations. For example, once a solution has been cooled below its heterogenous ice-nucleation temperature and a nucleating event occurs, ice will form in the solution surrounding the cells and any solutes will be excluded. The cell membranes are then exposed to an increased concentration of electrolytes. If the process is slow, the membranes will be exposed for a longer period of time and at a relatively high temperature resulting in more opportunity for detrimental interactions as discussed previously. Therefore, it is thought that slow-cooling injury is most likely due to solution effects.

To minimize the effects of increased electrolyte concentration, rapid cooling is required. Rapid-cooling will decrease the time of exposure to the electrolytes but also achieve lower temperatures sooner and this will decrease the rate of biochemical reactions. Unfortunately, rapid cooling does not allow the cells time to dehydrate, thereby the cells retain a significant amount of free water predisposing them to intracellular ice formation.

The concept of a two-factor hypothesis was developed by Mazur in 1972 (154) when he proposed that cell injury can occur at cooling rates where the cell remains close to its osmotic equilibrium or it can occur at rates in which there is supercooled water within the cells. The first type of injury occurs due to solute effects in which high concentrations of solutes can damage the cell membranes. The second type of injury is due to intracellular ice formation occurring in the supercooled cytoplasm. A reduction of the intracellular water may prevent the formation of intracellular ice. Indeed, if 84-90% of the unbound water is removed from the cell, there would be no intracellular freezing at any temperature (203, 228). Therefore, if slow-cooling promotes cellular dehydration (75), the cell can equilibrate and prevent intracellular supercooling as well as maintain the intracellular chemical potential equal to that of the extracellular environment. Conversely, cells that are not slow cooled become extensively supercooled and maintain their hydration, and are thus more susceptible to intracellular freezing as they reach the nucleation temperature (75). Therefore, slow-cooling in the initial stage of cryopreservation is beneficial to cell survival.

Unfortunately, slow-cooling increases the exposure to high electrolyte concentrations at relatively high temperatures, which can be lethal to cells. Therefore, it must be considered that rapid-cooling may eliminate some of the detrimental effects of slow-cooling. Rapid-cooling decreases the length of time of exposure to high concentrations of solutes and any exposure would be at lower temperatures decreasing the biochemical potential. The difficulty with rapid-cooling is that the cells are unable to equilibrate via osmosis. To compensate, the cell becomes increasingly supercooled and eventually equilibrates by freezing intracellularly. This severely restricts rapid-cooling from being used in isolation. Alternatively, it is the sequential application of slow-cooling to dehydrate the cells followed by rapid-cooling to minimize solution effects that appears to have the potential to cryopreserve cells successfully.

Optimal cooling rates that balance slow- and rapid-cooling effects for different cell lines have been determined for some cells (105, 148, 149) supporting the two-factor hypothesis (154). Unfortunately, optimal cooling rates for most mammalian cells have not been determined. Initially Mazur (150) recommended a cooling rate of 1°C/min for most cells except very large ones and this tends to be the rate commonly used (75, 122, 135, 155, 161). Individual cell properties require consideration during the slow-cooling stage (105). Cells with high membrane permeability and/or cells with low volume to surface ratios have an increased ease of water efflux (150). This causes a depression of the freezing point of the solution (129, 227) inside the cell as well as decreases the nucleation and crystallization rates resulting in decreased supercooling (105, 150). These factors result in increased resistance to intracellular ice formation (227). Conversely, these types of cells are more vulnerable to concentration effects because the viscosity of the cell interior increases due to more rapid efflux of water (105). Another factor to consider is that at sufficiently low temperatures, the cell membrane becomes effectively impermeable (106, 150). All these factors must be considered for each cell line for cryopreservation to be effective.

While attention is necessarily focused on cooling the tissue, warming rates also must be considered. With rapid cooling rates, smaller ice crystals are preferentially created (4, 27, 148). A rapid warming rate is considered to be the optimal method of bringing cells to room temperature (58, 105, 154) by limiting the opportunity of small crystals to recrystallize. A slow warming may be equally effective but only after rapid cooling (156) likely due to the smaller numbers of ice crystals present. With slow cooling rates, the warming rate is not as critical (154, 156) because less intracellular water would be present due to dehydration during the cooling period. It is apparent that the presence of fewer and smaller ice crystals within the cells enhances cell recovery and provides some independence from the warming rate but the complete absence of ice would be preferential.

McGann *et. al.* (156, 157) advanced the two-factor hypothesis into a 2-stage cryopreservation technique to help control the difficulties in cryopreserving mammalian cellular systems. The slow-cooling stage was initiated by placing the samples in solution at a relatively high, subzero temperature followed by ice-nucleation. The solution was slow-cooled at 1°C/min to an intermediate holding temperature where it was maintained to allow equilibration of the cells. This stage allowed the extracellular solution to freeze, which caused the cells to dehydrate due to osmotic and chemical effects. Once dehydrated, the cells were plunged into liquid nitrogen (LN), the rapid-cooling stage. Theoretically, insignificant intracellular ice would form as minimal water remained inside the cells after the slow-cooling stage. In this state, the cells could be stored indefinitely. Rapid warming was used to restore the solutions to room temperature.

McGann *et. al.* (156, 157) and Mazur (154) determined that cell damage could be attributed to both stages. In the first stage, with long periods at the intermediate holding temperature, damage could occur due to thermal shock, high osmolarity, or direct toxic effect of high ionic strength conditions – solution effects. McGann *et. al.* (157) demonstrated that protection from damage due to rapid-cooling (intracellular ice formation due to plunging into LN) was enhanced with longer periods at the holding temperature. This was consistent with a time dependent interaction of the hypertonic, extracellular environment on the cell membrane (cellular dehydration). McGann *et. al.* (156, 157) concluded this 2-

stage technique achieved greater cell recovery compared to a constant cooling rate and supported the theory of damage due to both slow-cooling and rapid-cooling.

Penetrating cryoprotective agents (CPA) have been introduced to decrease the effects of freeze injury mainly via colligative properties (129, 165, 186). A compound that displays low toxicity, high water solubility, low molecular weight and ease in penetrating cell membranes can be a good CPA (10). The most commonly used and accepted CPA is dimethyl sulfoxide (Me_2SO) but glycerol and 1,2-propanediol (propylene glycol, PD) also have been used with some success. The main effect of CPAs is on slow-cooling (105, 170). The addition of a CPA results in the reduction of the salt concentration of the solution at a given temperature when ice has formed (129, 186). This decreases the exposure to high electrolyte concentrations that is damaging to the cell membranes and allows more time for the cells to equilibrate (128). The solution can cool to a lower temperature before exposure to high electrolyte concentrations, which decreases the rate of biochemical reactions that the cells experience (87). In addition, the viscosity of the solution is increased, which decreases the rate of nucleation and crystallization (87, 105, 128). Unfortunately, the use of CPAs is not without concerns. The addition and removal of CPAs can cause osmotic shifts that can be damaging to the cells (96) and each CPA has its own mechanism of toxicity at high concentrations that must be considered.

Me_2SO is the most commonly used and most thoroughly investigated CPA (10, 34, 72, 87, 96, 100, 109, 155, 158, 170, 174, 177, 186, 194, 195, 201, 215, 217-219) and seems to have a stronger effect on the thermodynamic properties of the solution than glycerol. PD, on the other hand, has a much higher stability of its wholly amorphous state than either Me_2SO or glycerol (19). PD is more stable in preventing recrystallization at equal concentrations and cooling rates and the crystallization of PD is much more difficult compared to other solutions. Therefore lower concentrations of PD may be as effective as higher concentrations of the other penetrating CPAs and would have lower toxic effects. Furthermore, it can be combined with agents to create more effective cryoprotectant properties (162).

Combinations of these techniques have been used previously and cryopreservation has been successful on a number of tissues including stem cells (160), fibroblasts (155), sperm (29), Islet cells (184), heart valves (88) and other cells and simple tissues (22, 43, 45, 47, 121, 129, 183, 187). Work on chondrocytes began with Smith in 1965 (201) when she isolated chondrocytes from the matrix of rabbits, monkeys and humans and cryopreserved the cells using 10% Me_2SO with cooling down to –79°C. Successful recovery was noted by normal appearing chondrocytes under phase contrast and fluorescence microscopy. Viability was confirmed by homografting the cells. Cryopreservation of isolated chondrocytes in solution has been achieved with numerous techniques (5, 158, 191, 194, 218, 219) using varying concentrations of Me_2SO. Rapid permeation of Me_2SO into the chondrocytes can occur within 2 minutes at 20°C (159, 195) and was not toxic at concentrations of 5-16% at 4°C for up to 100 minutes (195, 218). However, while concentrations of up to 20% Me_2SO, after 30 minutes exposure to chondrocytes, were also not toxic, progressively longer exposure demonstrated increased toxicity (217).

While initial experiments focused on individual chondrocytes, intact AC presented its own difficulties. For example, even though Me_2SO penetration into intact AC matrix has been demonstrated, it can take 30 minutes to 2 hours to penetrate 2mm in porcine AC (170, 174, 217). In addition, while most of the few reports on ultrastructural effects of cryopreservation on AC matrix have not demonstrated any significant effect on the structure or mechanical properties (8, 109, 215), Hunziker (92) did note a substantial increase in the destruction of bovine AC matrix after freezing when compared to vitrified matrix. Intermediary tissues such as very thin slices of cartilage have been able to undergo successful cryopreservation (100, 107, 175), but the recovery of chondrocytes *in situ* after cryopreservation has not been as successful. Of the few studies available after attempted cryopreservation of intact AC, most have demonstrated recovery of minimal numbers (<10%) of intact cells (mainly in the superficial zone) after various cryopreservation procedures (25, 100, 177). One exception has been Muldrew *et. al.* (170) who demonstrated up to 60% intact cell recovery in intact ovine AC after a 2-stage cryopreservation technique using 10% Me_2SO. Higher cell recovery was noted in the superficial and deep zones compared to the intermediate zone. An attempt to reproduce these results using the same technique on intact human AC was unsuccessful (100) as was another attempt using ovine AC (173) casting doubt on the effectiveness of the 2-stage cryopreservation technique on intact AC. Recently Muldrew *et. al.* (173) demonstrated that a step-cooled technique designed to allow improved diffusion of the solute buildup that occurs in front of a planar ice-front was effective in sheep AC. This technique demonstrated recovery of increased numbers of intact cells (approximately 60%) compared to a concurrently tested 2-stage technique, although these results have yet to be reproduced.

The current state of cryopreservation of intact AC proposes that cellular injury occurs due to solution effects and intracellular ice formation. A 2-stage cryopreservation technique has been successful on cells in solution, which takes into consideration slow- and rapid-cooling injury. The addition of a penetrating CPA can reduce the slow-cooling damage by decreasing the solution effects at a given subzero temperature but the toxic effects of the cryoprotectant must be considered. Unfortunately, application of the current knowledge of cryopreserving cells in solution to cells *in situ* has been unsuccessful. The water distribution throughout the matrix introduces complex interactions between cells, ice, cryoprotectant and matrix constituents. The mechanics of ice formation within the matrix remains unknown and therefore uncontrollable. Uniform penetration of cryoprotectant throughout the matrix has not been definitively proven and appears unlikely. Osmotic shifts will be difficult to control due to the different conditions that cells experience within the various layers of the matrix. Indeed, the cartilage matrix introduces unknowns for most of the details of cryopreservation that have been investigated on cells in solution. These details remain to be resolved prior to successful cryopreservation of cells *in situ*.

1.2.3 Vitrification

Vitrification is the process of consolidating aqueous solutions into amorphous solids without the formation of a crystalline matrix. Vitrification allows the cooling of solutions to low subzero temperatures without the effects of phase separation that occur with crystallization. This is a possible alternative to conventional cryopreservation when working with biologic tissues because phase separation with ice crystal formation causes significant damage during cryopreservation procedures.

During cooling, two types of nucleation events cause ice crystal formation. Homogenous nucleation occurs when a critical number of water molecules combine to form an ice-like structure that becomes energetically favourable for more water molecules to grow onto it (227). This nucleus can rapidly propagate throughout the entire solution. In a pure water solution, this requires about 25 molecules at –40°C and this is the lowest temperature that pure water can go to without crystallizing unless solutes are added to block the water-water molecular interaction (227). As the temperature increases, more water molecules are required to form the homogenous nucleus. The probability of nucleation occurring is related to the sample volume, amount of undercooling, and the viscosity of the liquid (55, 227).

The second type of nucleation is heterogenous which is due to the presence of foreign material within the solution. Foreign material within the solution can provide a base for water molecules to attach to so that the critical minimum number of water-water molecular interactions is lowered and ice nucleation can occur at a relatively higher temperature than pure water. Most aqueous solutions are not pure and therefore will heterogenously ice-nucleate at temperatures warmer than their homogenous nucleation temperature. Cells, on the other hand, contain few heterogenous nucleators and can cool to much lower subzero temperatures before nucleation occurs (105).

The problems with ice formation and resultant phase separation include: physical damage to membranes (3), excessively high electrolyte concentrations (128, 129, 156, 157), osmotic shifts with excessive dehydration and shrinkage (86, 164, 165, 171), generation of electrical and chemical gradients (41, 207, 229), increased enzyme catalyzed reactions due to decompartmentalization of enzymes/substrates/activators(164) (60), and destruction of biologic integrity due to disequilibrium of biopolymer/ion/water concentration balance (61). Vitrification can avoid these problems and result in cells and their environment remaining intact.

The process of vitrification is based on the premise of avoiding both types of nucleation altogether so that ice crystals do not form within the solution. This can be accomplished using an extremely rapid cooling rate (at least 1000°C/min (54)) or a very high concentration of penetrating cryoprotectant agent (CPA). The addition of a solute (i.e. penetrating CPA) decreases the probability of nucleation and ice crystal growth due to increased viscosity along with the fact that solutes are incompatible with ice structure and therefore hinder its growth.

Even with the addition of significant amounts of solutes, problems can occur if the cooling rate is slow. Any ice formed during the cooling period causes a phase separation to occur and solutes are excluded, increasing the CPA concentration. This leads to increased CPA toxicity as well as significant osmotic stresses. With a rapid cooling rate and high concentrations of CPAs, very low temperatures can be reached without ice formation (105). Low temperatures decrease the rate of biochemical reactions and limit the toxicity of the CPAs. As well, no phase separation will occur and the CPA concentration can be well controlled (52). Vitrification is useful because cell membranes are protected by limiting further hydration, lowering the probability of crystallization, and allowing the membrane to remain in the liquid phase (227).

Vitrification is not without difficulties. The two main ingredients – rapid cooling rates and high concentrations of CPAs are not easily achieved, especially in large tissues systems. Tissue with any significant mass cannot be effectively and rapidly cooled with an external source only (55). Furthermore, the concentrations of CPAs normally required for vitrification are toxic to cells (100, 217). Additional problems can occur due to cold shock, fracturing, devitrification (formation of ice crystals from vitrified solution upon warming) and dilution of CPAs.

Initial work on cryopreservation was done by Luyet (131) in 1937 but great difficulties in achieving complete vitrification resulted in a hiatus of activity until the late 1960's. Luyet (130) and Rasmussen (188) eventually came to the conclusion that complete vitrification could occur with low cooling rates if a sufficiently high concentration of cryoprotectant was used but, unfortunately, this was not applied to biologic tissues. Extensive work has been done by Fahy since the early 1980's when he demonstrated unambiguous vitrification using a slow-cool technique with high pressures and very high concentrations of cryoprotectant (50, 54). He described a phase diagram to demonstrate the events that can occur during cooling of a solution containing a cryoprotectant agent (Figure 1-1) (54).

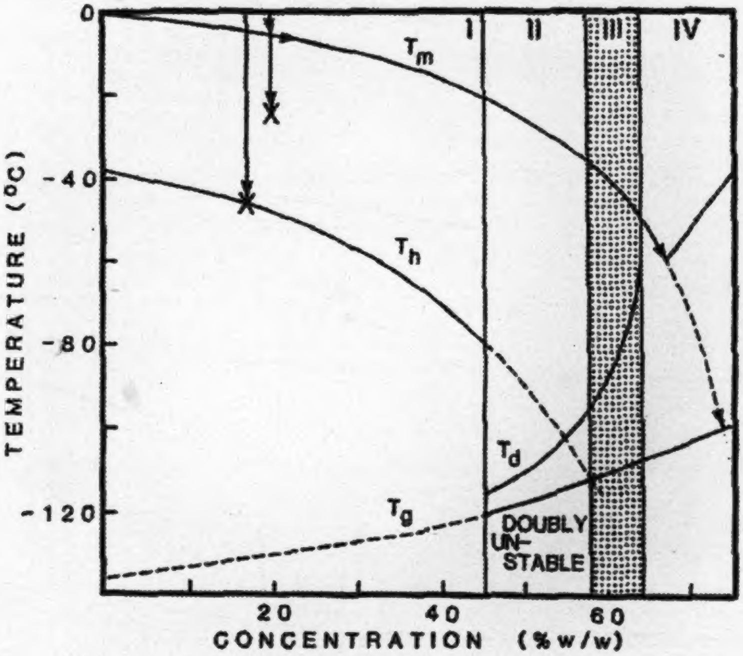

Figure 1-1. Phase diagram during cooling of solution containing a cryoprotectant agent. (Reprinted from Cryobiology, Vol 21, *Vitrification as an approach to cryopreservation*. p408, Fahy, 1984, with permission from Elsevier Science)

The phase diagram is divided into four Regions based on cryoprotectant concentration. Region I at low CPA concentration is the region where vitrification cannot occur due to either heterogenous or homogenous ice nucleation and crystal growth. Region II is a region where the homogenous nucleation temperature (T_h) comes to within 20°C (132)-40°C (188) of the glass transformation temperature (T_g). In this region, a doubly unstable glass occurs and is thought to be heavily laden with ice nuclei due to passing through a large temperature range where heterogenous and homogenous nuclei can form. Glass from this area is inevitably fated to freeze or devitrify upon warming (54). It is impossible to cool large organs through Region II rapidly enough to avoid ice crystal formation.

The critical area is where Region II meets Region III because this is where the T_h meets T_g and neither heterogenous nor homogenous nucleation can occur before the formation of a vitreous state makes crystallization impossible. This concentration of CPA is the lowest concentration able to support complete vitrification (C_v). The C_v values vary with different CPAs and have been determined by Fahy (52). In Region III, the T_h falls below T_g therefore homogenous nucleation cannot occur although ice crystals may be present (due to heterogenous nucleation) as evidenced by recrystallization that can be controlled with rapid warming. Finally, in Region IV, no homogenous nucleation occurs and no devitrification occurs even at the lowest warming rates. Unfortunately there is excessive CPA toxicity and pre-existing ice crystals can grow if already formed. Due to the excessive CPA toxicity, Region IV is not useful for vitrification.

Much work has been performed to investigate the lowest concentration needed to vitrify (C_v) as discussed by Fahy (54). Due to the extreme toxicity noted at high levels of penetrating CPAs, it is necessary to use the lowest concentration of CPA possible when vitrifying biologic tissues. The C_v values for glycerol (65% w/v), Me_2SO (49% w/v), and PD (44% w/v) were determined by Fahy (53) although larger samples may require a higher C_v than initially reported because of slower cooling rates (55). Using 45% PD, vitrification was achieved at cooling rates as low as 10°C/min and Fahy concluded that using high concentrations of penetrating CPAs could achieve vitrification at low cooling rates (54). Boutron (18) confirmed the vitrifying properties of PD at low cooling rates. Boutron (17, 18) also investigated 2,3-butandiol and found that vitrification occurred with 35% at 20°C/min (when a cooling rate of 200-300°C/min was required for 35% PD). Finally, Wusteman (232) performed a direct comparison of common CPAs (2,3-butanediol, 1,2-propanediol, ethanediol, Me_2SO) on human endothelial cells and determined that 2,3-butanediol (32%) and 1,2-propanediol (45%) vitrified at the least toxic levels but it was difficult to warm 2,3-butanediol uniformly. The conclusion was that 1,2-propanediol had the most promising vitrification properties while Me_2SO was significantly more toxic than either of the other two penetrating CPAs.

Even with the lower concentrations of solutions such as 2,3-butanediol and 1,2-propanediol, toxicity still remains a problem with vitrification. Methods to solve this problem have included pressurization (51, 92), combining CPAs at lower concentrations (55, 69, 103, 163, 185, 202), addition of other types of CPAs (7, 54, 69), alteration of CPAs (230), and altering the temperature and methods of addition (16, 103, 202) and dilution (7, 16, 103, 202, 232). Increased pressurization of up to 1000 atm has been noted to decrease the concentration required to vitrify by 5% (51) and can effect some vitrification even without the presence of CPA (92). The high pressure is noted to lower the T_h and elevate the T_g thereby lowering the concentration of CPA where these two temperatures intersect (104). Once the vitrification has occurred, the pressure can be released even during the warming phase.

A popular method of decreasing toxicity effects of CPAs is combining penetrating CPAs at lower concentrations. Penetrating CPAs are thought to have toxicity based on different mechanisms. Combining different CPAs can result in the same viscosity and interference effects as a high concentration of a single CPA (163) and vitrification of different types of tissues has been accomplished with combinations of cryoprotectants (55, 69, 103, 185, 202). In addition, adding a nonpenetrating cryoprotectant can lower the penetrating CPA concentration used by promoting intracellular protein (by cell dehydration) incorporation into the vitrification process. For example, a 6% nonpenetrating cryoprotectant can be added to a 40% penetrating CPA. This combination results in a 46% solution extracellularly and 40% solution inside the cell. Fortunately, the cell contains proteins that have an osmotic and viscous effect as well, and can potentially provide vitrification enhancement to the 40% CPA (7, 54). In addition, some cellular dehydration is beneficial as it concentrates the intracellular proteins thereby enhancing vitrification. Alteration of the CPA itself by adding a methoxyl group to replace the hydroxyl group (230) was noted to increase viscosity, increase permeability and increase glass forming tendency of the cryoprotectant by decreasing CPA-CPA interaction and increasing CPA-water interaction. This allowed lowering of the critical cooling rate and increased stability of vitrification state with warming.

Finally, the temperature and methods of addition and dilution of the CPA is important. Step-wise addition (16, 103, 202) and, more importantly, dilution (7, 16, 103, 202, 232) can decrease the toxicity and osmotic stresses experienced by the cells or tissue. CPAs are more toxic at warmer temperatures (232). Therefore, the addition should be done at cooler temperatures near 0°C. Conversely, increased temperatures enhance penetration of the CPA. Therefore, the dilution may be more beneficial at high temperatures as it may allow quicker removal of the CPA (232). Addition and dilution of CPAs cause significant osmotic shifts on isolated cells (232) that can be maintained within tolerable limits by step-wise addition and dilution and this is recommended during vitrification (7).

Other concerns include ice crystal formation (16, 55), achieving satisfactory cooling rates (55), fracturing (7, 55) and devitrification (7, 103, 185). Even with observed vitrification (direct observation has been reported as an acceptable method to determine vitrification (55, 115, 231) in larger samples (>10ml)), minute ice crystals may form but are unable to grow to visible size. In some cases, the solution surrounding the tissue vitrifies but the sample itself grows ice crystals (16, 55). This is most likely due to incomplete inactivation of heterogenous nucleating agents by the CPA. Potentially successful techniques include increasing the warming rate (232), boiling or ultrafiltration of the solution (231), increasing the cooling rate (55), or blocking ice crystal formation by natural or synthetic anti-freeze glycoproteins (AFGP) (48, 231).

Indeed, Eto *et. al.* (48) demonstrated that AFGPs (even at low concentrations of 1mg/ml, with saturation at 20mg/ml) increased viscosity of all the CPAs that were tested. In addition, AFGPs were noted to decrease the freezing point of the solution. It was determined that 20mg/ml of AFGP was equivalent to 1*M* Me_2SO in viscosity increase. This is important because 20mg/ml AFGP provides only 5*mM* osmol effect compared to the 1*M* osmol effect of 1*M* Me_2SO. Therefore, AFGPs could provide a useful adjunct to current CPAs. The high cost and difficulty obtaining natural AFGPs led Wowk *et. al.* (231)

to investigate synthetic polymer polyvinyl alcohol (PVA) in combination with Me_2SO and ethylene glycol. They found that a low molecular weight PVA in addition to less than 20% vinyl acetate provided inhibition of heterogenous nucleators and enhanced vitrification and minimized devitrification.

Another problem to consider is that satisfactory cooling rates are difficult to achieve with large samples (55). As T_g is approached, there is a steadily declining cooling rate in the sample if the surrounding temperature is just below T_g. The surrounding temperature should be near T_g initially to prevent fracturing which can occur due to thermal stresses if the sample rapidly passes through its T_g (7, 55). In addition, a larger thermal gradient exists across a larger sample despite a slower cooling rate compared to smaller samples. Fortunately, after a period of annealing at low temperatures, slow cooling down to even lower temperatures may occur for longer storage (55). Once a sample is vitrified, it must be warmed and devitrification remains a concern. Devitrification is likely due to ice nuclei that form during the vitrification process that are too small to visualize and do not grow. Upon warming, these nuclei expand to become larger ice crystals that can be damaging to the tissue. Devitrification can be avoided with warming rates (103, 185) in the range of 400-1000°C/min (via microwave) but dielectric heating is also being investigated to provide uniform heating to large samples (232). Reduction of the number of nucleating agents, addition of AFGP (natural or synthetic) as well as the application of pressure may also decrease the incidence and extent of devitrification.

Successful vitrification has been noted since the early 1980's when Shistosoma (97, 98) and Onchocerca (82) demonstrated successful recovery. Over the years, many other cell types and tissues have been successfully vitrified including murine embryos (185), human corneas (7, 16), hematopoietic cells (115), human islet cells (103), vein grafts (202), human skin (69) with variable amounts of cell recovery. Unfortunately, extension to larger tissues/organs has proven difficult for the reasons discussed. With recent insights into methods of mitigating CPA toxicity, vitrification of larger more complex tissues may be possible in the near future.

1.2.4 Viability Assays

Viability can be defined as "ability of a treated sample to exhibit a specific function or functions, expressed as a proportion of the same function exhibited by the same sample before treatment or an identical fresh untreated sample" (180). Provided this definition, it is important to remember that viability is not synonymous with life as exemplified by continued enzymatic function that can occur despite complete cell destruction and death. It is also important to keep in mind that viability index measurements are specific to the damaging mechanism and the biologic sample and measured function (23, 180). Therefore it is important to be cautious when extrapolating results among tissues treated under different experimental conditions using similar assay tests or among different tissues.

Viability assays can be classified according to Pegg (180):

Table 1-2. Classification of viability assays

- I. Physical integrity
  - Gross -appearance
    - -physical property
  - Microscopic -light/electron/fluoresence microscopy
- II. Metabolic activity
  - Uptake of metabolites
  - Production of catabolites
  - Labile metabolites
  - Enzymatic reactions – intracellular, membrane transport
- III. Mechanical activity
  - Motility
  - Phagocytosis
  - Contraction
  - Attachment
  - Aggregation
- IV. Mitotic activity
  - Mitotic index

DNA synthesis

"Plating" tests

Growth and development – tissue culture, embryonic

V. Complete *In Vivo* function

Fertilization and development

Transplantation – cells, tissues, vascularized organs

Each of these tests has advantages and disadvantages depending on the cell type. Physical integrity tests evaluate for normal appearance and usually can only be used as a reference for the maximal number of functioning cells because grossly distorted cells do not function normally. Accuracy can be improved by microscopic viewing with light, fluorescence, or electron microscopy. Metabolic tests evaluate the function of enzymes within the cell but can be positive without intact cell membranes. The most useful metabolic tests are ones that combine the evaluation of intact enzymes within an intact cellular structure. Some fluorescent stains combine the metabolic function with evaluation of intact cell membranes. Fortunately, some of these assays have shown to correlate well with transplantation outcome (179, 196). Mechanical assays usually require a high level of integrated function and are considered more likely to be valuable assays. Reproductive assays assess one of the defining attributes of living things and can be valuable. From DNA synthesis to growth and development assays, many complex processes are required and these may be reliable markers of viability. Finally, *in vivo* function is the ultimate test of viability and transplantation studies are often the ultimate goal of the investigation being performed.

To determine an appropriate viability assay for chondrocyte recovery, it is important to understand the mechanisms of cell death as well as the most likely site of injury during the experimental process. Early reversible changes include alteration of mitochondria and endoplasmic reticulum and lysosomal damage that can initiate chemical reactions within the cell (137, 161). Later irreversible changes include vacuolization of the nucleus followed by nuclear membrane damage. Finally, pyknosis of the nucleus demonstrates death of the cell with nuclear and cellular fragmentation. Irreversible cytoplasmic structural damage facilitates the destruction of the cell and autolysis is a very late event of death.

Freeze injury to chondrocytes is primarily concentrated on cellular membranes (136, 161, 215). Experiments on animal (215) and human (136) chondrocytes after cryopreservation have demonstrated significantly abnormal nuclei with abnormal cell cytoplasm. Cell membrane integrity was also not maintained. Recently Acker *et. al.* (3) confirmed that the cell membrane is a primary target of injury during the formation of extracellular ice.

Based on the information that cell membranes (including nuclear membranes) are a primary site of freeze injury in chondrocytes, fluorescent membrane integrity dyes have been chosen to evaluate chondrocyte recovery after cryopreservation techniques (93, 100, 170, 196). Membrane injury may lead to a loss of selective permeability and this can be used to differentiate between functional and nonfunctional cells. Initial studies employed hematoxylin and eosin (H & E) stains to identify completely disrupted cells. Black *et. al.* (14) tested trypan blue as a more specific stain but interactions with albumin complicated the interpretation of results. Fluorescent stains were initially used by Rotman and Papermaster (192) utilizing fluorescein diacetate (FDA). Viable cells are permeable to the nonpolar fluorogenic ester FDA, which is then hydrolyzed within the cell by nonspecific esterases that release the free fluorescein. Fluorescein is an anionic polar compound that cannot readily leave the cell. Therefore, it accumulates and fluoresces green under ultraviolet (UV) light. With cell membrane damage, the fluorescein quickly leaches out of the cell.

To provide contrast to live cells, Edidin (44) used ethidium bromide (EB) to highlight dead cells. EB is cationic and can only penetrate cells with disrupted membranes, subsequently binding to nuclear DNA and fluorescing red under UV light. The FDA and EB were combined by Dankberg *et. al.* (40) and Patel *et. al.* (178) to allow direct comparison of intact cells with disrupted cells. As FDA is a cytoplasmic stain and EB is a nuclear stain, there were some difficulties in comparing cells identified by these stains. Syto is another nuclear binding stain that concentrates in intact nuclei and fluoresces green under UV light. The effectiveness of Syto compared to FDA and other stains has been confirmed by Yang *et. al.* (233) allowing direct comparison of competing nuclear binding fluorescent stains to evaluate cell membrane integrity.

It should be clear that nuclear binding membrane integrity dyes can provide valuable information regarding intactness of chondrocytes after a cryopreservation protocol but it must be remembered that this assay does not evaluate more subtle forms of cell injury. With this in mind, this assay can be considered as a best case scenario; an intact cell is an essential requirement for cell viability but an intact cell does not conclusively determine that a cell is viable. To complicate matters more, the percent recovery of viable cells required to maintain an AC allograft after transplantation has not been investigated or determined. Most likely, the recovery of cells required will depend, in part, on the amount of matrix damage that occurs during cryopreservation. Further investigations will be required to ultimately determine the viability of intact cells after undergoing a transplantation procedure, as well as the number of viable cells required to maintain the graft.

1.2.5 Indications for Osteochondral Cryopreservation/Vitrification

Natural history studies clearly show that full-thickness chondral lesions of significant size (>1cm in diameter) cause considerable degenerative changes if not treated (6, 42, 90, 222), resulting in osteoarthritis, the second leading cause of work disability in the United States (95). Early, effective treatment of these lesions may eliminate a significant proportion of cases in which osteoarthritis will develop but currently there are no universally accepted treatment options for full thickness chondral defects that provide consistent, excellent, long-term outcomes. Historical treatment options include nonoperative management with protected weight bearing and physical therapy to rehabilitate the musculature around the joint. Failure of nonoperative management (100% in very large defects with up to 70% in smaller defects (26, 42)) usually results in surgical intervention consisting of arthroscopic debridement (6, 99) with or without microfracture technique (204). Unfortunately, failure of this treatment will occur in a significant number of these patients (up to 55% (6, 90) resulting in persisting symptoms and progression to arthritis.

Consequently, there has been intense research into treatment of AC defects including autogenous chondrocyte implantation both without (20, 21, 113, 224) and with synthetic (193, 197)/biologic (62) scaffolds, growth factors (147, 181, 189) and other methods (39, 74, 113, 199). Some of these techniques have shown promise but are limited by an inability to treat large, chondral defects without well-defined borders and an inability to reproduce the complex AC matrix structure. Another technique being investigated is autogenous osteochondral transplantation (mosaicplasty) (83, 85) in which osteochondral autografts are taken from a healthy, relatively non-weight bearing portion of the joint and transferred to the chondral defect. This technique also has reported early success but is limited by size constraints and the possibility of damaging other unaffected portions of the joint (15, 84).

In contrast, osteochondral allografting in which grafts are taken from cadaveric donors and transplanted into the defect are able to treat large, unconfined joint defects (12, 24). This technique has the longest track record with reasonably successful results and may be the most promising approach. Unfortunately, although osteochondral allografting has had some success (11, 33, 35), difficulties persist with both fresh and frozen grafts. Studies have demonstrated that when using fresh (as well as frozen) allografts, size and contour matching is extremely important (24, 35, 59, 71, 141, 166, 210, 211). Other difficulties include the possibility of transmission of infectious diseases (28, 216) (that could be decreased with freezing (59, 216)) and difficult operating conditions due to the irregularity of graft availability. Successful cryopreservation of intact AC matrix would allow long-term storage of osteochondral allografts in a tissue bank and the problems relating to size/contour matching, infection, and graft availability could be readily eliminated.

Fresh osteochondral allografts contain intact chondrocytes with the potential to maintain the matrix over many years (37, 94). In animal studies, fresh osteochondral transplants used as controls had good survival as determined by gross inspection, mechanical properties of the matrix and membrane integrity staining of the chondrocytes (93, 196), examined up to one year post transplantation. It is more difficult to evaluate fresh grafts using human subjects. A number of authors have commented on the clinical outcomes of fresh osteochondral allografts (11, 30, 35, 70, 76, 77, 220) and it is apparent that good to excellent results (up to 90% graft survival (35)) can be obtained using this technique although most are not as successful. In fact, in studies that looked at results 15 years post transplantation, progressive deterioration was noted (12, 73, 133). From the literature, it can be expected that 70-80% of the fresh grafts will be retained and function adequately 10 years after transplantation.

Even though intact cells have been documented to exist within the transplanted allograft for up to 12 years post transplantation (38, 73, 211), clinical and histological deterioration persists. This is most likely due to difficulties in size/contour matching between the donor and recipient. Because of the logistics in harvesting the donor material, the accurate size/contour matching required (preferably within 1-2mm), and time constraints to transplant (preferable within 24 hours) to maintain cell viability, it is very difficult to obtain donor material that is optimal. In addition, time for testing for infectious diseases must be considered. These factors make the practicalities of performing fresh osteochondral allografting in a timely fashion extremely difficult and likely accounts for the long-term deterioration of the fresh allografts. This problem could be resolved with access to viable grafts stored in a tissue bank.

In an attempt to circumvent the problems with fresh osteochondral allografts, investigations on cryopreserving osteochondral tissue have continued. Early cryopreservation techniques consisted of an uncontrolled slow cooling achieved by simply immersing the tissue in cryoprotectant of low concentration and placing into a –80°C freezer (33, 59). This consistently resulted in recovery of low numbers of intact chondrocytes as documented by membrane integrity stains (177) and clinical outcome studies in animals and humans demonstrated deterioration of the grafts after a few years due to loss of cell viability (93, 94, 124, 133). To enhance recovery of intact cells, alterations of the technique to a 2-stage cryopreservation method (initial slow cooling at 1°C/min to an intermediate subzero temperature followed by rapid cooling into LN) with low concentrations of cryoprotectant produced promising results in an ovine model (approximately 60% (170). Unfortunately, these results were not reproducible on human AC (100). Another cryopreservation method being investigated is a stepped procedure using a low concentration of cryoprotectant and prolonged holding at various subzero temperatures (173). Despite all these varying techniques, there is currently no consistently successful method to cryopreserve intact AC and preserve chondrocyte integrity.

Even though slow-cooling cryopreservation techniques have demonstrated recovery of low numbers of intact chondrocytes, transplantation using frozen allografts has had some surprising success. In an animal model, the success was moderate with degenerative changes noted within 3-4 years after transplanting controlled frozen allografts in seven baboons (136). Interestingly, histologic examination demonstrated complete absence of chondrocytes. Hurtig (93) had less successful results on sheep with significant degenerative changes at 6-12 months post transplantation. In human trials, Clohisy *et. al.* (33) and Flynn *et. al.* (59) demonstrated 55-70% good to excellent results of graft survival in the intermediate term (5-10 years) but progressive deterioration was noted over 2-5 years post transplantation and was attributed to poor size and contour matching (59). More recent work on different cryopreservation techniques has produced similar disappointing clinical results even with improved chondrocyte recovery. Schachar *et. al.* (196) examined transplanted ovine osteochondral dowels one year after 2-stage cryopreservation in Me_2SO of low concentration. Even though recovery of a relatively high number of intact cells was noted using this technique (up to 60% (170)), the transplanted dowels deteriorated over one year. The gross morphology, biomechanical testing, membrane integrity, histology, and biochemistry were better than grafts rapidly frozen without cryoprotectant, but the quality of the grafts was not close to fresh grafts inserted as positive controls. Recently, a stepped cooling technique (173) showed even more promising chondrocyte recovery results when compared to the 2-stage technique. Unfortunately, once again, the transplanted dowels developed osteoarthritic changes after one year. This likely indicates that the cells cryopreserved in this manner are not able to maintain the matrix or that the matrix is sufficiently damaged by the cooling technique that it cannot be repaired by the remaining live chondrocytes. Either way, improved preservation techniques are required to enhance long term outcome of osteochondral allograft transplantation.

Immunogenecity is another factor that can be helped with a cryopreserved tissue bank. Cartilage itself is considered "immune privileged" even though antigens present on the collagen and proteoglycans are highly antigenic. The privileged condition of the cartilage matrix is due to prevention of immune components entering the matrix (46). Conversely, bone is highly vascular and immune reactions can occur (141) which stimulate osteoclastic resorption. All types of allografts can have an immune response (118) but fresh grafts provide the most immunogenicity while frozen grafts provide less and freeze dried grafts demonstrate minimal immunogenicity (46, 64, 65), likely due to destruction of the antigen presenting components such as proteins and cells.

An immune reaction can be beneficial after allograft transplantation as the exposed organic contents of the allograft stimulates new bone formation. Unfortunately, this often becomes too aggressive and the increasing inflammatory response can obliterate the new vascular supply causing the death of the new bone and Friedlaender (65) suggests that decreased immunogenicity would increase the chance of transplantation success (35, 59, 116). Tissue matching may also play a role in the future to decrease the immune response (210) although this remains controversial (71). Therefore, establishing a bank of osteochondral grafts would decrease the antigenicity of the grafts and make tissue typing possible if required in the future.

Osteoarthritis is the inevitable sequelae of large osteochondral defects and causes a significant impact on the quality of life for millions of people with a cost of billions of dollars. There are currently no reliable means to treat these large defects. Establishing a method to successfully cryopreserve intact AC while maintaining viable chondrocytes within an intact matrix will provide a source of tissue that can resolve the major difficulties with osteochondral allografting used to treat these defects.

1.2.6 References

1. *Targeting arthritis: Public health takes action* . Center for disease control and prevention. Avail at http://www.cdc.gov/nccdphp/art-aag.htm, 2002.
2. Acker, J.P., A. Larese, H. Yang, A. Petrenko, and L.E. McGann. Intracellular ice formation is affected by cell interactions. *Cryobiology* 38, 4: 363-371, 1999.
3. Acker, J.P. and L.E. McGann. Membrane damage occurs during the formation of intracellular ice. *Cryo Letters* 22, 4: 241-254., 2001.
4. Allenspach, A.L. and T.G. Kraemer. Ice crystal patterns in artificial gels of extracellular matrix macromolecules after quick-freezing and freeze-substitution. *Cryobiology* 26, 2: 170-179, 1989.
5. Almqvist, K.F., L. Wang, C. Broddelez, E.M. Veys, and G. Verbruggen. Biological freezing of human articular chondrocytes. *Osteoarthritis Cartilage* 9, 4: 341-350, 2001.
6. Anderson, A.F. and M.J. Pagnani. Osteochondritis dissecans of the femoral condyles. Long-term results of excision of the fragment. *Am J Sports Med* 25, 6: 830-834, 1997.
7. Armitage, W.J. and S.J. Rich. Vitrification of organized tissues. *Cryobiology* 27, 5: 483-491, 1990.
8. Arnoczky, S.P., M. C.A., S. M.B., V.C. Mow, and R.F. Warren. The effect of cryopreservation on canine menisci: a biochemical, morphologic, and biomechanical evaluation. *J of Orthop Res* 6, 1: 1-12, 1988.
9. Asahina, E. Freezing process and injury in isolated animal cells. *Fed Proc* 24, Suppl 15: S183, 1965.
10. Ashwood-Smith, M.J. Radioprotective and cryoprotective properties of dimethyl sulfoxide in cellular systems. *Ann N Y Acad Sci* 141, 1: 45-62, 1967.
11. Aubin, P.P., H.K. Cheah, A.M. Davis, and A.E. Gross. Long-term followup of fresh femoral osteochondral allografts for posttraumatic knee defects. *Clin Orthop* 391 Suppl: S318-327, 2001.
12. Bell, R.S., A. Davis, D.G. Allan, F. Langer, A.A. Czitrom, and A.E. Gross. Fresh osteochondral allografts for advanced giant cell tumors at the knee. *J Arthroplasty* 9, 6: 603-609, 1994.

13. Benninghoff, A. Form und bau der gelenkknorpel in ihren beziegungen zur funktion. Zweiter teil: der aufbau des gelenkknorpels in sienen bezienhungen zur funktion. *Z Zellforsch* 2, 783, 1925.

14. Black, L. and M.C. Berenbaum. Factors affecting the dye exclusion test for cell viability. *Exp Cell Res* 35, 9-13, 1964.

15. Bobic, V. Arthroscopic osteochondral autograft transplantation in anterior cruciate ligament reconstruction: a preliminary clinical study. *Knee Surg Sports Traumatol Arthrosc* 3, 4: 262-264, 1996.

16. Bourne, W.M. and L.R. Nelson. Human corneal studies with a vitrification solution containing dimethyl sulfoxide, formamide, and 1,2-propanediol. *Cryobiology* 31, 6: 522-530, 1994.

17. Boutron, P. Levo- and dextro-2,3-butanediol and their racemic mixture: Very efficient solutes for vitrification. *Cryobiology* 27, 55-69, 1990.

18. Boutron, P., *Non-equilibrium formation of ice in aqueous solutions: Efficiency of polyalcohol solutions for vitrification*, in *The biophysics of organ cryopreservation*, D.E. Pegg and A.M.J. Karow, Editors. Plenum: New York. p. 201-228, 1987.

19. Boutron, P. and A. Kaufmann. Stability of the amorphous state in the system water--1,2-propanediol. *Cryobiology* 16, 6: 557-568, 1979.

20. Brittberg, M., A. Lindahl, A. Nilsson, C. Ohlsson, O. Isaksson, and L. Peterson. Treatment of deep cartilage defects in the knee with autologous chondrocyte transplantation [see comments]. *N Engl J Med* 331, 14: 889-895, 1994.

21. Brittberg, M., T. Tallheden, B. Sjogren-Jansson, A. Lindahl, and L. Peterson. Autologous chondrocytes used for articular cartilage repair: an update. *Clin Orthop* 391 Suppl: S337-348, 2001.

22. Brockbank, K.G. Effects of cryopreservation upon vein function in vivo. *Cryobiology* 31, 1: 71-81, 1994.

23. Brockbank, K.G. and H.L. Bank. Measurement of postcryopreservation viability. *J Card Surg* 2, 1 Suppl: 145-151, 1987.

24. Bugbee, W.D. and F.R. Convery. Osteochondral allograft transplantation. *Clin Sports Med* 18, 1: 67-75, 1999.

25. Bujia, J., D. Kremer, H. Sudhoff, E. Viviente, C. Sprekelsen, and E. Wilmes. Determination of viability of cryopreserved cartilage grafts. *Eur Arch Otorhinolaryngol* 252, 1: 30-34, 1995.

26. Cahill, B.R. Osteochondritis dissecans of the knee: Treatment of juvenile and adult forms. *J of the American Academy of Orthopaedic Surgeons* 3, 4: 237-247, 1995.

27. Cameron, I.L., K.E. Hunter, and G.D. Fullerton. Quench cooled ice crystal imprint size: a micro-method for study of macromolecular hydration. *Scanning Microsc* 2, 2: 885-898, 1988.

28. CDC. Transmission of HIV through bone transplantation: Case report and public health recommendations. *MMWR* 37, 39: 557-568, 1988.

29. Check, M.L., D.J. Check, J.H. Check, R. Long, and M. Press. Effect of shortened exposure time to the critical period for ice crystal formation on subsequent post-thaw semen parameters from cryopreserved sperm. *Arch Androl* 32, 1: 63-67, 1994.

30. Chu, C.R., F.R. Convery, W.H. Akeson, M. Meyers, and D. Amiel. Articular cartilage transplantation. Clinical results in the knee. *Clin Orthop* 360: 159-168, 1999.

31. Clark, J.M. The organization of collagen in cryofractured rabbit articular cartilage: a scanning electron microscopic study. *J Orthop Res* 3, 1: 17-29, 1985.

32. Clarke, I.C. Articular cartilage: a review and scanning electron microscope study. 1. The interterritorial fibrillar architecture. *J Bone Joint Surg [Br]* 53, 4: 732-750, 1971.

33. Clohisy, D.R. and H.J. Mankin. Osteoarticular allografts for reconstruction after resection of a musculoskeletal tumor in the proximal end of the tibia. *J Bone Joint Surg Am* 76, 4: 549-554, 1994.

34. Cocks, F.H. and W.E. Brower. Phase diagram relationships in cryobiology. *Cryobiology* 11, 4: 340-358, 1974.

35. Convery, F.R., M.H. Meyers, and W.H. Akeson. Fresh osteochondral allografting of the femoral condyle. *Clin Orthop* 273: 139-145, 1991.

36. Curtin, W.A. and W.J. Reville. Ultrastructural observations on fibril profiles in normal and degenerative human articular cartilage. *Clin Orthop* 313: 224-230, 1995.

37. Czitrom, A.A., S. Keating, and A.E. Gross. The viability of articular cartilage in fresh osteochondral allografts after clinical transplantation. *J Bone Joint Surg [Am]* 72, 4: 574-581, 1990.

38. Czitrom, A.A., F. Langer, N. McKee, and A.E. Gross. Bone and cartilage allotransplantation. A review of 14 years of research and clinical studies. *Clin Orthop* 208: 141-145, 1986.

39. Dahlberg, L. and A. Kreicbergs. Demineralized allogeneic bone matrix for cartilage repair. *J Orthop Res* 9, 1: 11-19, 1991.

40. Dankberg, F. and P. M.D. A test of granulocyte membrane integrity and phagocytic function. *Cryobiology* 13, 430-2, 1976.

41. Daw, A., J. Farrant, and G.J. Morris. Membrane leakage of solutes after thermal shock or freezing. *Cryobiology* 10, 2: 126-133, 1973.

42. De Smet, A.A., O.A. Ilahi, and B.K. Graf. Untreated osteochondritis dissecans of the femoral condyles: prediction of patient outcome using radiographic and MR findings. *Skeletal Radiol* 26, 8: 463-467, 1997.

43. Diller, K.R. Intracellular freezing of glycerolized red cells. *Cryobiology* 16, 2: 125-131, 1979.

44. Edidin, M.A. A rapid, quantitative fluorescence assay for cell damage by cytotoxic antibodies. *J Immunol* 104, 1303-1306, 1970.

45. Elliot, K. and J. Whelan, eds. CIBA Foundation Symposium. Vol. 52. Elsevier: Amsterdam, 1977.

46. Elves, M.W. and C.H. Ford. A study of the humoral immune response to osteoarticular allografts in the sheep. *Clin Exp Immunol* 17, 3: 497-508, 1974.

47. Eskew, T.D., J.D. Ollerenshaw, J.M. Philpott, K. Dennis, P. Dawson, Y.S. Sun, W.R. Chitwood, Jr., and R.M. Lust. Successful small diameter arterial grafting using cryopreserved allograft arteries. *Asaio J* 43, 5: M522-526, 1997.

48. Eto, T.K. and B. Rubinsky. Antifreeze glycoproteins increase solution viscosity. *Biochem Biophys Res Commun* 197, 2: 927-931, 1993.

49. Eyre, D.R., J.J. Wu, and P.E. Woods. The cartilage collagens: structural and metabolic studies. *J Rheumatol Suppl* 27, 49-51, 1991.

50. Fahy, G.M., *Prevention of toxicity from high concentrations of cryoprotective agents*, in *Organ preservation, basic and applied sciences*, D.E. Pegg, I.A. Jacobsen, and H. N.A., Editors. MTP Press: Lancaster. p. 367-369, 1982.

51. Fahy, G.M., *Viability concepts in organ preservation*, in *Basic concepts of organ procurement, perfusion, and preservation for transplantation*, L.H. Toledo-Pereyra, Editor. Academic Press: New York. p. 121-158, 1982.

52. Fahy, G.M. Vitrification: a new approach to organ cryopreservation. *Prog Clin Biol Res* 224, 305-335, 1986.

53. Fahy, G.M. and A. Hirsh, *Prospects for organ preservation by vitrification*, in *Organ preservation. Basic and Applied Aspects*, D.E. Pegg, N.A. Jacobsen, and N.A. Halasz, Editors. MTP Press: Lancaster. p. 399-404, 1982.

54. Fahy, G.M., D.R. MacFarlane, C.A. Angell, and H.T. Meryman. Vitrification as an approach to cryopreservation. *Cryobiology* 21, 4: 407-426, 1984.

55. Fahy, G.M., J. Saur, and R.J. Williams. Physical problems with the vitrification of large biological systems. *Cryobiology* 27, 5: 492-510, 1990.

56. Farrant, J. Is there a common mechanism of protection of living cells by polyvinyl pyrrolidone and glycerol during freezing. *Nature (London)* 222, 1175-1176, 1973.

57. Farrant, J. and G.J. Morris. Thermal shock and dilution shock as the causes of freezing injury. *Cryobiology* 10, 134-140, 1970.

58. Farrant, J., C.A. Walter, H. Lee, and L.E. McGann. Use of two-step cooling procedures to examine factors influencing cell survival following freezing and thawing. *Cryobiology* 14, 3: 273-286, 1977.

59. Flynn, J.M., D.S. Springfield, and H.J. Mankin. Osteoarticular allografts to treat distal femoral osteonecrosis. *Clin Orthop* 303: 38-43, 1994.

60. Franks, F. Biological freezing and cryofixation. *J Microsc* 111, 1: 3-16, 1977.

61. Franks, F. and D. Eagland. The role of solvent interactions in protein conformation. *CRC Crit Rev Biochem* 3, 2: 165-219, 1975.

62. Freed, L.E., D.A. Grande, Z. Lingbin, J. Emmanual, J.C. Marquis, and R. Langer. Joint resurfacing using allograft chondrocytes and synthetic biodegradable polymer scaffolds. *J Biomed Mater Res* 28, 8: 891-899, 1994.

63. Freeman, P.M., R.N. Natarajan, J.H. Kimura, and T.P. Andriacchi. Chondrocyte cells respond mechanically to compressive loads. *J Orthop Res* 12, 3: 311-320, 1994.

64. Friedlaender, G.E. Immune responses to osteochondral allografts. Current knowledge and future directions. *Clin Orthop* 174: 58-68, 1983.

65. Friedlaender, G.E. and M.C. Horowitz. Immune responses to osteochondral allografts: nature and significance. *Orthopedics* 15, 10: 1171-1175, 1992.

66. Froimson, M.I., A. Ratcliffe, T.R. Gardner, and V.C. Mow. Differences in patellofemoral joint cartilage material properties and their significance to the etiology of cartilage surface fibrillation. *Osteoarthritis Cartilage* 5, 6: 377-386, 1997.

67. Fujikawa, S. Lamellar to hexagonal II phase transitions in tonoplasts of mushroom hyphae caused by mechanical stress resulting from the formation of extracellular ice crystals. *Cryobiology* 28, 191-202, 1991.

68. Fujikawa, S. and K. Miura. Plasma membrane ultrastructural changes caused by mechanical stress in the formation of extracellular ice as a primary cause of slow freezing injury in fruit-bodies of Basidiomycetes (Lyophyllum ulmarium). *Cryobiology* 23, 371-382, 1986.

69. Fujita, T., Y. Takami, K. Ezoe, T. Saito, A.K. Sato, N. Takeda, Y. Yamamoto, K. Homma. Successful preservation of human skin by vitrification. *J Burn Care Rehabil* 21, 4: 304-309, 2000.

70. Garrett, J.C. Fresh osteochondral allografts for treatment of articular defects in osteochondritis dissecans of the lateral femoral condyle in adults. *Clin Orthop* 303: 33-37, 1994.

71. Garrett, J.C. Treatment of osteochondral defects of the distal femur with fresh osteochondral allografts: a preliminary report. *Arthroscopy* 2, 4: 222-226, 1986.

72. Gerhards, E. and H. Gibian. The metabolism of dimethyl sulfoxide and its metabolic effects in man and animals. *Ann N Y Acad Sci* 141, 1: 65-76., 1967.

73. Ghazavi, M.T., K.P. Pritzker, A.M. Davis, and A.E. Gross. Fresh osteochondral allografts for post-traumatic osteochondral defects of the knee. *J Bone Joint Surg Br* 79, 6: 1008-1013, 1997.

74. Grande, D.A., A.S. Breitbart, J. Mason, C. Paulino, J. Laser, and R.E. Schwartz. Cartilage tissue engineering: current limitations and solutions. *Clin Orthop* 367 Suppl: S176-185, 1999.

75. Griffiths, J.B., C.S. Cox, D.J. Beadle, C.J. Hunt, and D.S. Reid. Changes in cell size during the cooling, warming and post-thawing periods of the freeze-thaw cycle. *Cryobiology* 16, 2: 141-151, 1979.

76. Gross, A.E., Z. Agnidis, and C.R. Hutchison. Osteochondral defects of the talus treated with fresh osteochondral allograft transplantation. *Foot Ankle Int* 22, 5: 385-391, 2001.

77. Gross, A.E., N.H. McKee, K.P. Pritzker, and F. Langer. Reconstruction of skeletal deficits at the knee. A comprehensive osteochondral transplant program. *Clin Orthop* 174: 96-106, 1983.

78. Guilak, F. The deformation behavior and viscoelastic properties of chondrocytes in articular cartilage. *Biorheology* 37, 1-2: 27-44, 2000.

79. Guilak, F., W.R. Jones, H.P. Ting-Beall, and G.M. Lee. The deformation behavior and mechanical properties of chondrocytes in articular cartilage. *Osteoarthritis Cartilage* 7, 1: 59-70, 1999.

80. Hall, A.C., E.R. Horwitz, and R.J. Wilkins. The cellular physiology of articular cartilage. *Exp Physiol* 81, 3: 535-545, 1996.

81. Hall, A.C., J.P. Urban, and K.A. Gehl. The effects of hydrostatic pressure on matrix synthesis in articular cartilage. *J Orthop Res* 9, 1: 1-10, 1991.

82. Ham, P.J., S. Townson, E.R. James, and A.E. Bianco. An improved technique for the cryopreservation of Onchocerca microfilariae. *Parasitol* 83, 139-146, 1981.

83. Hangody, L., P. Feczko, L. Bartha, G. Bodo, and G. Kish. Mosaicplasty for the treatment of articular defects of the knee and ankle. *Clin Orthop* 391 Suppl: S328-336, 2001.

84. Hangody, L., G. Kish, Z. Karpati, I. Szerb, and I. Udvarhelyi. Arthroscopic autogenous osteochondral mosaicplasty for the treatment of femoral condylar

articular defects. A preliminary report. *Knee Surg Sports Traumatol Arthrosc* 5, 4: 262-267, 1997.

85. Hangody, L., G. Kish, L. Modis, I. Szerb, L. Gaspar, Z. Dioszegi, and Z. Kendik. Mosaicplasty for the treatment of osteochondritis dissecans of the talus: two to seven year results in 36 patients. *Foot Ankle Int* 22, 7: 552-558, 2001.

86. Hechter, O. The role of water structure in the molecular organization of cell membranes. *Fed Proc* S15, S91-102, 1965.

87. Hey, J.M. and D.R. MacFarlane. Crystallization of ice in aqueous solutions of glycerol and dimethyl sulfoxide 2: ice crystal growth kinetics. *Cryobiology* 37, 2: 119-130, 1998.

88. Hu, J.F. and L. Wolfinbarger, Jr. Dimethyl sulfoxide concentration in fresh and cryopreserved porcine valved conduit tissues. *Cryobiology* 31, 5: 461-467, 1994.

89. Huber, M., S. Trattnig, and F. Lintner. Anatomy, biochemistry, and physiology of articular cartilage [In Process Citation]. *Invest Radiol* 35, 10: 573-580, 2000.

90. Hughston, J.C., P.T. Hergenroeder, and B.G. Courtenay. Osteochondritis dissecans of the femoral condyles. *J Bone Joint Surg [Am]* 66, 9: 1340-1348, 1984.

91. Hunziker, E.B., M. Michel, and D. Studer. Ultrastructure of adult human articular cartilage matrix after cryotechnical processing. *Microsc Res Tech* 37, 4: 271-284, 1997.

92. Hunziker, E.B., J. Wagner, and D. Studer. Vitrified articular cartilage reveals novel ultra-structural features respecting extracellular matrix architecture. *Histochem Cell Biol* 106, 4: 375-382, 1996.

93. Hurtig, M.B., K. Novak, R. McPherson, S. McFadden, L.E. McGann, K. Mul drew, and N.S. Schachar. Osteochondral dowel transplantation for repair of focal defects in the knee: an outcome study using an ovine model. *Vet Surg* 27, 1: 5-16, 1998.

94. Jackson, D.W., J. Halbrecht, C. Proctor, D. Van Sickle, and T.M. Simon. Assessment of donor cell and matrix survival in fresh articular cartilage allografts in a goat model. *J Orthop Res* 14, 2: 255-264, 1996.

95. Jackson, D.W., T.M. Simon, and H.M. Aberman. Symptomatic articular cartilage degeneration: the impact in the new millennium. *Clin Orthop* 391 Suppl: S14-25, 2001.

96. Jacob, S.W. and R. Herschler. Pharmacology of DMSO. *Cryobiology* 23, 1: 14-27, 1986.

97. James, E.R. Cryopreservation of Schistosoma mansoni schistosomula using 40% v/v (10M) methanol and rapid cooling. *CryoLetters* 1, 535-544, 1980.

98. James, E.R. Schistosoma mansoni: cryopreservation of shistosomula by two-step addition of ethanediol and rapid cooling. *Exper Parasitol* 52, 105-116, 1981.

99. Johnson, L.L. Arthroscopic abrasion arthroplasty: a review. *Clin Orthop* 391 Suppl: S306-317, 2001.

100. Jomha, N.*Cryopreservation of human articular cartilage* in *Experimental Surgery, Masters Thesis*. University of Alberta: Edmonton, 1996.

101. Jones, W.R., H.P. Ting-Beall, G.M. Lee, S.S. Kelley, R.M. Hochmuth, and F. Guilak. Alterations in the Young's modulus and volumetric properties of chondrocytes isolated from normal and osteoarthritic human cartilage. *J Biomech* 32, 2: 119-127, 1999.

102. Jurvelin, J.S., D.J. Muller, M. Wong, D. Studer, A. Engel, and E.B. Hunziker. Surface and subsurface morphology of bovine humeral articular cartilage as assessed by atomic force and transmission electron microscopy. *J Struct Biol* 117, 1: 45-54, 1996.

103. Jutte, N.H., P. Heyse, H.G. Jansen, G.J. Bruining, and G.H. Zeilmaker. Vitrification of human islets of Langerhans. *Cryobiology* 24, 5: 403-411, 1987.

104. Kanno, H. and C.A. Angell. Homogenous nucleatoin and galss formation in aqueous alkali halide solutions at high pressures. *J Phys Chem* 81, 2639-2643, 1977.

105. Karlsson, J.O., E.G. Cravalho, I.H. Borel Rinkes, R.G. Tompkins, M.L. Yarmush, and M. Toner. Nucleation and growth of ice crystals inside cultured hepatocytes during freezing in the presence of dimethyl sulfoxide. *Biophys J* 65, 6: 2524-2536, 1993.

106. Karlsson, J.O.M., E.G. Cravalho, and M. Toner. A model of diffusion-limited ice growth inside biological cells during freezing. *J Appl Phys* 75, 4442-4455, 1994.

107. Kawabe, N. and M. Yoshinao. Cryopreservation of cartilage. *Int Orthop* 14, 3: 231-235, 1990.

108. Khalsa, P.S. and S.R. Eisenberg. Compressive behavior of articular cartilage is not completely explained by proteoglycan osmotic pressure. *J Biomech* 30, 6: 589-594, 1997.

109. Kiefer, G.N., K. Sundby, D. McAllister, and e. al. The effect of cryopreservation on the biomechanical behavior of bovine articular cartilage. *J Orthop Res* 7, 494-501, 1989.

110. Kim, H.A., D.I. Suh, and Y.W. Song. Relationship between chondrocyte apoptosis and matrix depletion in human articular cartilage. *J Rheumatol* 28, 9: 2038-2045, 2001.

111. Kiviranta, I., J. Jurvelin, M. Tammi, A.M. Saamanen, and H.J. Helminen. Weight bearing controls glycosaminoglycan concentration and articular cartilage thickness in the knee joints of young beagle dogs. *Arthritis Rheum* 30, 7: 801-809, 1987.

112. Kobayashi, S., S. Yonekubo, and Y. Kurogouchi. Cryoscanning electron microscopic study of the surface amorphous layer of articular cartilage. *J Anat* 187, Pt 2: 429-444, 1995.

113. Kreklau, B., M. Sittinger, M.B. Mensing, C. Voigt, G. Berger, G.R. Burmester, R. Rahmanzadeh, and U. Gross. Tissue engineering of biphasic joint cartilage transplants. *Biomaterials* 20, 18: 1743-1749, 1999.

114. Kuettner, K.E., M.B. Aydelotte, and E.J. Thonar. Articular cartilage matrix and structure: a minireview. *J Rheumatol Suppl* 27, 46-48, 1991.

115. Kurata, H., K. Takakuwa, and K. Tanaka. Vitrification of hematopoietic progenitor cells obtained from human cord blood. *Bone Marrow Transplant* 14, 2: 261-263, 1994.

116. Kwan, M.K., W.M. Lai, and V.C. Mow. Fundamentals of fluid transport through cartilage in compression. *Ann Biomed Eng* 12, 6: 537-558, 1984.

117. Lai, W.M. and V.C. Mow. Drag-induced compression of articular cartilage during a permeation experiment. *Biorheology* 17, 111-123, 1980.

118. Langer, F., A. Czitrom, K.P. Pritzker, and A.E. Gross. The immunogenicity of fresh and frozen allogeneic bone. *J Bone Joint Surg [Am]* 57, 2: 216-220, 1975.

119. Lee, G.M., C.A. Poole, S.S. Kelley, J. Chang, and B. Caterson. Isolated chondrons: a viable alternative for studies of chondrocyte metabolism in vitro. *Osteoarthritis Cartilage* 5, 4: 261-274, 1997.

120. Leibo, S. Preservation of mammalian cells and embryos by freezing. *Cryoimmunology* 62, 311-334, 1977.

121. Leibo, S.P., *Fundamental cryobiology of mouse ova and embryos*, in *The freezing of mammalian embryos*. Ciba Foundation Symposium: Amsterdam. p. 69-97, 1979.

122. Leibo, S.P., J.J. McGrath, and E.G. Cravalho. Microscopic observation of intracellular ice formation in unfertilized mouse ova as a function of cooling rate. *Cryobiology* 15, 3: 257-271, 1978.

123. Lemperg, R.K., S.E. Larsson, and S.O. Hjertquist. Distribution of water and glycosaminoglycans in different layers of cattle articular cartilage. *Isr J Med Sci* 7, 3: 419-421, 1971.

124. Lester, G.E., L.G. Toussiant, A.D. Blackwood, and G.D. Bos. Cartilaginous extracellular matrix of failed massive osteoarticular allografts. *Clin Orthop* 382: 13-20, 2001.

125. Levitt, J. and G.W. Scarth. Frost hardening studies with living cells. II. Permeability in relation to frost resistance and the seasonal cycle. *Can J Res Sect C Bot Sci* 14, 285-305, 1936.

126. Little, C.B. and P. Ghosh. Variation in proteoglycan metabolism by articular chondrocytes in different joint regions is determined by post-natal mechanical loading. *Osteoarthritis Cartilage* 5, 1: 49-62, 1997.

127. Lovelock, J.E. The denaturation of lipid-protein complexes as a cause of damage by freezing. *Proc Royal Soc London* 147, Ser B: 427-433, 1957.

128. Lovelock, J.E. The haemolysis of human red blood cells by freezing and thawing. *Biochimica Et Biophysica Acta* 10, 414-426, 1953.

129. Lovelock, J.F. The mechanism of the protective action of glycerol against haemolysis by freezing and thawing. *Biochimica et Biophysica Acta* 11, 28-36, 1953.

130. Luyet, B. and D. Rasmussen. Study by differential thermal analysis of the temperatures of instability of rapidly cooled solutions of glycerol, ethylene glycol, sucrose and glucose. *Biodynamica* 10, 210: 167-191, 1968.

131. Luyet, B.J. and M.C. Gibbs. On the mechanism of congelation and of death in the rapid freezing of epidermal plant cells. *Biodynamica* 25, 1-18, 1937.

132. MacFarlane, D.R., R.K. Kadiyala, and C.A. Angell. Cooling rate dependence of the ice nucleation temperature in aqueous LiCl solutions. *J Phys Chem* 87, 235-238, 1983.

133. Mahomed, M.N., R.J. Beaver, and A.E. Gross. The long-term success of fresh, small fragment osteochondral allografts used for intraarticular post-traumatic defects in the knee joint. *Orthopedics* 15, 10: 1191-1199, 1992.

134. Malinin, T. and E.A. Ouellette. Articular cartilage nutrition is mediated by subchondral bone: a long-term autograft study in baboons. *Osteoarthritis Cartilage* 8, 6: 483-491, 2000.

135. Malinin, T.I. Injury of human polymorphonuclear granulocytes frozen in the presence of cryoprotective agents. *Cryobiology* 9, 2: 123-130, 1972.

136. Malinin, T.I., W. Mnaymneh, H.K. Lo, and D.K. Hinkle. Cryopreservation of articular cartilage. Ultrastructural observations and long-term results of experimental distal femoral transplantation. *Clin Orthop* 303: 18-32, 1994.

137. Malinin, T.I. and V.P. Perry. A review of tissue organ viability assay. *Cryobiology* 4, 3: 104-115, 1967.

138. Mankin, H.J., *The articular cartilages, cartilage healing, and osteoarthritis*, in *Adult Orthopaedics*. p. 163-270, 1984.

139. Mankin, H.J., V.C. Mow, J.A. Buckwalter, J.P. Iannotti, and A. Ratcliffe, *Form and function of articular cartilage*, in *Orthopaedic Basic Science*, S.R. Simon, Editor: Chicago. p. 1-44, 1994.

140. Mansour, J.M. and V.C. Mow. The permeability of articular cartilage under compressive strain and at high pressures. *J Bone Joint Surg [Am]* 58, 4: 509-516, 1976.

141. Marco, F., C. Leon, F. Lopez-Oliva, A.J. Perez, A. Sanchez-Barba, and L. Lopez-Duran Stern. Intact articular cartilage cryopreservation. In vivo evaluation. *Clin Orthop* 283: 11-20, 1992.

142. Maroudas, A. Balance between swelling pressure and collagen tension in normal and degenerate cartilage. *Nature* 260, 808-809, 1976.

143. Maroudas, A. Transport of solutes through cartilage: permeability to large molecules. *J Anat* 122, 2: 335-347, 1976.

144. Maroudas, A., M.T. Bayliss, and M.F. Venn. Further studies on the composition of human femoral head cartilage. *Ann Rheum Dis* 39, 5: 514-523, 1980.

145. Maroudas, A., P. Bullough, S.A. Swanson, and M.A. Freeman. The permeability of articular cartilage. *J Bone Joint Surg [Br]* 50, 1: 166-177, 1968.

146. Maroudas, A., P. Bullough, S.A. Swanson, and M.A. Freeman. The permeability of articular cartilage. *J Bone Joint Surg Br* 50, 1: 166-177, 1968.

147. Martin, J.A. and J.A. Buckwalter. The role of chondrocyte-matrix interactions in maintaining and repairing articular cartilage. *Biorheology* 37, 1-2: 129-140, 2000.

148. Mazur, P. Cryobiology: the freezing of biological systems. *Science* 168, 934: 939-949, 1970.

149. Mazur, P. Freezing of living cells: mechanisms and implications. *Am J Physiol* 247, 3 Pt 1: C125-142, 1984.

150. Mazur, P. Kinetics of water loss from cells at subzero temperatures and the likelihood of intracellular freezing. *The Journal of General physiology* 47, 347-369, 1963.

151. Mazur, P. Manifestations of injury in yeast cells exposed to subzero temperatures. *J Bacteriol* 82, 662, 1961.

152. Mazur, P. Physical factors implicated in the death of microorganisms at subzero temperatures. *Ann NY Acad Sci* 85, 610-629, 1960.

153. Mazur, P. The role of intracellular freezing in the death of cells cooled at supraoptimal rates. *Cryobiology* 14, 3: 251-272, 1977.

154. Mazur, P., S.P. Leibo, and E.H. Chu. A two-factor hypothesis of freezing injury. Evidence from Chinese hamster tissue-culture cells. *Exp Cell Res* 71, 2: 345-355, 1972.

155. McGann, L.E. Optimal temperature ranges for control of cooling rate. *Cryobiology* 16, 3: 211-216, 1979.

156. McGann, L.E. and J. Farrant. Survival of tissue culture cells frozen by a two-step procedure to -196 degrees C. I. Holding temperature and time. *Cryobiology* 13, 3: 261-268, 1976.

157. McGann, L.E. and J. Farrant. Survival of tissue culture cells frozen by a two-step procedure to -196 degrees C. II. Warming rate and concentration of dimethyl sulphoxide. *Cryobiology* 13, 3: 269-273, 1976.

158. McGann, L.E., D. McAllister, K. Muldrew, and N.S. Schachar. Permeability of isolated chondrocytes to dimethyl sulfoxide. *Orthop Res Soc* 34 annual meeting, 1988.

159. McGann, L.E., M. Stevenson, K. Muldrew, and N. Schachar. Kinetics of osmotic water movement in chondrocytes isolated from articular cartilage and applications to cryopreservation. *J Orthop Res* 6, 1: 109-115, 1988.

160. McGann, L.E., A.R. Turner, M.J. Allalunis, and J.M. Turc. Cryopreservation of human peripheral blood stem cells: optimal cooling and warming conditions. *Cryobiology* 18, 5: 469-472, 1981.

161. McGann, L.E., H.Y. Yang, and M. Walterson. Manifestations of cell damage after freezing and thawing. *Cryobiology* 25, 3: 178-185, 1988.

162. Mehl, P. and P. Boutron. Cryoprotection of red blood cells by 1,3-butanediol and 2,3-butanediol. *Cryobiology* 25, 1: 44-54, 1988.

163. Mehl, P. and P. Boutron. Glass-forming tendency and stability of the amorphous state in the aqueous solutions of linear polyalcohols with four carbons. II. Ternary systems with water, 1,2-propanediol or 1,3-butanediol or 2,3-butanediol. *Cryobiology* 24, 355-367, 1987.

164. Meryman, H.T., *The exceeding of a minimum tolerable cell volume in hypertonic suspension as a cause of freezing injury*, in *The frozen cell*, G.E.W. Westenholme and M. O'Conner, Editors. Churchill: London. p. 51-64, 1970.

165. Meryman, H.T. Osmotic stress as a mechanism of freezing injury. *Cryobiology* 8, 5: 489-500, 1971.

166. Meyers, M.H., W. Akeson, and F.R. Convery. Resurfacing of the knee with fresh osteochondral allograft. *J Bone Joint Surg [Am]* 71, 5: 704-713, 1989.

167. Millward-Sadler, S.J., M.O. Wright, H. Lee, K. Nishida, H. Caldwell, G. Nuki, and D.M. Salter. Integrin-regulated secretion of interleukin 4: A novel pathway of mechanotransduction in human articular chondrocytes. *J Cell Biol* 145, 1: 183-189, 1999.

168. Minns, R.J. and F.S. Steven. The collagen fibril organization in human articular cartilage. *J Anat* 123, 2: 437-457, 1977.

169. Muldrew, K., M. Chung, K. Novak, N.S. Schachar, R.F. Zernicke, L.E. McGann, J.B. Rattner, and J.R. Matyas. Evidence of chondrocyte repopulation in adult ovine articular cartilage following cryoinjury and long-term transplantation. *Osteoarthritis Cartilage* 9, 5: 432-439, 2001.

170. Muldrew, K., M. Hurtig, K. Novak, N. Schachar, and L.E. McGann. Localization of freezing injury in articular cartilage. *Cryobiology* 31, 1: 31-38, 1994.

171. Muldrew, K. and L.E. McGann. Mechanisms of intracellular ice formation. *Biophys J* 57, 3: 525-532, 1990.

172. Muldrew, K. and L.E. McGann. The osmotic rupture hypothesis of intracellular freezing injury. *Biophys J* 66, 2 Pt 1: 532-541, 1994.

173. Muldrew, K., K. Novak, C. Studholme, G. Wohl, R. Zernicke, N.S. Schachar, and L.E. McGann. Transplantation of articular cartilage following a step-cooling cryopreservation protocol. *Cryobiology* 43, 3: 260-267, 2001.

174. Muldrew, K., B. Sykes, S. N., and L.E. McGann. Permeation kinetics of dimethol sulfoxide in articular cartilage. *Cryo-letters* 17, 311-340, 1996.

175. Oegema, T.R., Jr., L.B. Deloria, M. Fedewa, J. Bischof, and J.L. Lewis. A simple cryopreservation method for the maintenance of cell viability and mechanical integrity of a cultured cartilage analog. *Cryobiology* 40, 4:370-375, 2000.

176. Ogata, K., L.A. Whiteside, and P.A. Lesker. Subchondral route for nutrition to articular cartilage in the rabbit. Measurement of diffusion with hydrogen gas in vivo. *J Bone Joint Surg [Am]* 60, 7: 905-910, 1978.

177. Ohlendorf, C., W.W. Tomford, and H.J. Mankin. Chondrocyte survival in cryopreserved osteochondral articular cartilage. *J Orthop Res* 14, 3: 413-416, 1996.

178. Patel, B.C., J.M. Courtney, J.H. Evans, and J.P. Paul. Biocompatibility assessment: application of fluorescent probe response (FPR) technique. *Biomaterials* 12, 8: 722-726, 1991.

179. Pegg, D.E. In vitro assessment of cell viability in human bone marrow preserved at -79°C. *J Appl Physiol* 19, 123-126, 1964.

180. Pegg, D.E. Viability assays for preserved cells, tissues, and organs. *Cryobiology* 26, 3: 212-231, 1989.

181. Perka, C., O. Schultz, R.S. Spitzer, and K. Lindenhayn. The influence of transforming growth factor beta1 on mesenchymal cell repair of full-thickness cartilage defects [In Process Citation]. *J Biomed Mater Res* 52, 3: 543-552, 2000.

182. Piez, K.A. History of extracellular matrix: a personal view. *Matrix Biol* 16, 3: 85-92, 1997.

183. Polge, C., A.U. Smith, and A.S. Parkes. Revival of spermatozoa after vitrification and dehydration at low temperatures. *Nature* 164, Oct: 666, 1949.

184. Rajotte, R.V., H.L. Stewart, W.A. Voss, and T.K. Shnitka. Viability studies on frozen--thawed rat islets of Langerhans. *Cryobiology* 14, 1: 116-120, 1977.

185. Rall, W.F. and G.M. Fahy. Ice-free cryopreservation of mouse embryos at -196 degrees C by vitrification. *Nature* 313, 6003: 573-575, 1985.

186. Rall, W.F., P. Mazur, and J.J. McGrath. Depression of the ice-nucleation temperature of rapidly cooled mouse embryos by glycerol and dimethyl sulfoxide. *Biophys J* 41, 1: 1-12, 1983.

187. Rall, W.F., P. Mazur, and H. Souzu. Physical-chemical basis of the protection of slowly frozen human erythrocytes by glycerol. *Biophys J* 23, 1: 101-120, 1978.

188. Rasmussen, D. and B. Luyet. Contribution to the establishment of the temperature-concentration curves of homogenous nucleation in solutions of some cryoprotective agents. *Biodynamica* 11, 33-44, 1970.

189. Reddi, A.H. Morphogenesis and tissue engineering of bone and cartilage: inductive signals, stem cells, and biomimetic biomaterials. *Tissue Eng* 6, 4: 351-359, 2000.

190. Redler, I., V.C. Mow, M.L. Zimny, and J. Mansell. The ultrastructure and biomechanical significance of the tidemark of articular cartilage. *Clin Orthop* 112: 357-362, 1975.

191. Rendal-Vazquez, M.E., E. Maneiro-Pampin, M. Rodriguez-Cabarcos, O. Fernandez-Mallo, I. Lopez de Ullibarri, C. Andion-Nunez, and F.J. Blanco. Effect of cryopreservation on human articular chondrocyte viability, proliferation, and collagen expression. *Cryobiology* 42, 1: 2-10, 2001.

192. Rotman, B. and B.W. Papermaster. Membrane properties of living mammalian cells as studied by enzymatic hydrolysis of fluorogenic esters. *Proc Natl Acad Sci U S A* 55, 1: 134-141, 1966.

193. Sams, A.E. and A.J. Nixon. Chondrocyte-laden collagen scaffolds for resurfacing extensive articular cartilage defects. *Osteoarthritis Cartilage* 3, 1: 47-59, 1995.

194. Schachar, N., M. Nagao, T. Matsuyama, D. McAllister, and S. Ishii. Cryopreserved articular chondrocytes grow in culture, maintain cartilage phenotype, and synthesize matrix components. *J Orthop Res* 7, 3: 344-351, 1989.

195. Schachar, N.S. and L.E. McGann. Investigations of low-temperature storage of articular cartilage for transplantation. *Clin Orthop* 208: 146-150, 1986.

196. Schachar, N.S., K. Novak, M. Hurtig, K. Muldrew, R. McPherson, G. Wohl, R.F. Zernicke, and L.E. McGann. Transplantation of cryopreserved osteochondral Dowel allografts for repair of focal articular defects in an ovine model. *J Orthop Res* 17, 6: 909-919, 1999.

197. Schaefer, D., I. Martin, P. Shastri, R.F. Padera, R. Langer, L.E. Freed, and G. Vunjak-Novakovic. In vitro generation of osteochondral composites [In Process Citation]. *Biomaterials* 21, 24: 2599-2606, 2000.

198. Schinagl, R.M., D. Gurskis, A.C. Chen, and R.L. Sah. Depth-dependent confined compression modulus of full-thickness bovine articular cartilage. *J Orthop Res* 15, 4: 499-506, 1997.

199. Schreiber, R.E., B.M. Ilten-Kirby, N.S. Dunkelman, K.T. Symons, L.M. Rekettye, J. Willoughby, and A. Ratcliffe. Repair of osteochondral defects with allogeneic tissue engineered cartilage implants. *Clin Orthop* 367 Suppl: S382-395, 1999.

200. Shepherd, D.E. and B.B. Seedhom. Thickness of human articular cartilage in joints of the lower limb. *Ann Rheum Dis* 58, 1: 27-34, 1999.

201. Smith, A.U. Survival of frozen chondrocytes isolated from cartilage of adult mammals. *Nature* 205, 782-784, 1965.

202. Song, Y.C., P.O. Hagen, F.G. Lightfoot, M.J. Taylor, A.C. Smith, and K.G. Brockbank. In vivo evaluation of the effects of a new ice-free cryopreservation process on autologous vascular grafts. *J Invest Surg* 13, 5: 279-288, 2000.

203. Souza, H., T. Nei, and M. Bito. Water of microorganisms and its freezing, with special reference to the relation between water content and viability of yeast and coli cells. *Low Temp Sci* Sec B, 19: 49-57, 1961.

204. Steadman, J.R., W.G. Rodkey, and J.J. Rodrigo. Microfracture: surgical technique and rehabilitation to treat chondral defects. *Clin Orthop* 391 Suppl: S362-369, 2001.

205. Steinmeyer, J., B. Ackermann, and R.X. Raiss. Intermittent cyclic loading of cartilage explants modulates fibronectin metabolism. *Osteoarthritis Cartilage* 5, 5: 331-341, 1997.

206. Steinmeyer, J. and S. Knue. The proteoglycan metabolism of mature bovine articular cartilage explants superimposed to continuously applied cyclic mechanical loading. *Biochem Biophys Res Commun* 240, 1: 216-221, 1997.

207. Steponkus, P., D. Stout, J. Wolfe, and R. Lovelace. Freeze-induced electrical transients and cryoinjury. *Cryo Lett* 5, 343-348, 1984.

208. Steponkus, P.L., M.P. Garber, S.P. Myers, and R.D. Lineberger. Effects of cold acclimation and freezing on structure and function of chloroplast thylakoids. *Cryobiology* 14, 3: 303-321, 1977.

209. Steponkus, P.L., J. Wolfe, and M.F. Dowgert, *Stresses induced by contraction and expansion during a free-thaw cycle: A membrane perspective*, in *Effects on low temperatures on biological membranes*, G.J. Morris and A. Clarke, Editors. Academic Press: San Francisco. p. 307-322, 1981.

210. Stevenson, S., G.A. Dannucci, N.A. Sharkey, and R.R. Pool. The fate of articular cartilage after transplantation of fresh and cryopreserved tissue-antigen-matched and mismatched osteochondral allografts in dogs. *J Bone Joint Surg [Am]* 71, 9: 1297-1307, 1989.

211. Stockley, I. and A.E. Gross. Bone and osteochondral allograft transplantation. *Surgery* 91, 2223-2229, 1991.

212. Stockwell, R.A. Cartilage failure in osteoarthritis: Relevance of normal structure and function. A review. *Clin Anat* 4, 161-191, 1991.

213. Stockwell, R.A. The interrelationship of cell density and cartilage thickness in mammalian articular cartilage. *J Anat* 109, 3: 411-421, 1971.

214. Suh, J.K., G.H. Baek, A. Aroen, C.M. Malin, C. Niyibizi, C.H. Evans, and A. Westerhausen-Larson. Intermittent sub-ambient interstitial hydrostatic pressure as a potential mechanical stimulator for chondrocyte metabolism. *Osteoarthritis Cartilage* 7, 1: 71-80, 1999.

215. Tavakol, K., R.G. Miller, D.P. Bazett-Jones, W.S. Hwang, L.E. McGann, and N.S. Schachar. Ultrastructural changes of articular cartilage chondrocytes associated with freeze-thawing. *J Orthop Res* 11, 1: 1-9, 1993.

216. Tomford, W.W. Transmission of disease through transplantation of musculoskeletal allografts. *J Bone Joint Surg Am* 77, 11: 1742-1754, 1995.

217. Tomford, W.W., G.P. Duff, and H.J. Mankin. Experimental freeze-preservation of chondrocytes. *Clin Orthop* 197: 11-14, 1985.

218. Tomford, W.W., G.R. Fredericks, and H.J. Mankin. Studies on cryopreservation of articular cartilage chondrocytes. *J Bone Joint Surg [Am]* 66, 2: 253-259, 1984.

219. Tomford, W.W. and H.J. Mankin. Investigational approaches to articular cartilage preservation. *Clin Orthop* 174: 22-27, 1983.

220. Tomford, W.W., D.S. Springfield, and H.J. Mankin. Fresh and frozen articular cartilage allografts. *Orthopedics* 15, 10: 1183-1188, 1992.

221. Toner, M., E.G. Cravalho, and M. Karel. Thermodynamics and kinetics of intracellular ice formation during freezing of biologic cells. *J Appl Phys* 67, 1582-1593, 1990.

222. Twyman, R.S., K. Desai, and P.M. Aichroth. Osteochondritis dissecans of the knee. A long-term study. *J Bone Joint Surg Br* 73, 3: 461-464, 1991.

223. Urban, J. and A. Hall, *Physical modifiers of cartilage metabolism*, in *Articular cartilage and osteoarthritis*, K. K.E., *et al.*, Editors. Raven Press: New York. p. 393-406, 1992.

224. Wakitani, S., T. Kimura, A. Hirooka, T. Ochi, M. Yoneda, N. Yasui, H. Owaki, and K. Ono. Repair of rabbit articular surfaces with allograft chondrocytes embedded in collagen gel. *J Bone Joint Surg [Br]* 71, 1: 74-80, 1989.

225. Wilkins, R.J., J.A. Browning, and J.P. Urban. Chondrocyte regulation by mechanical load. *Biorheology* 37, 1-2: 67-74, 2000.

226. Williams, R.J. Freezing tolerance in Mytilus Edulis. *Comp Biochem Physiol* 35, 145-160, 1970.

227. Wolfe, J. and G. Bryant. Freezing, drying, and/or vitrification of membrane-solute-water systems. *Cryobiology* 39, 2: 103-129, 1999.

228. Wood, T.H. and A.M. Rosenberg. Freezing in yeast cells. *Biochim Biophys Acta* 25, 78-87, 1957.

229. Workman, E. and S. Reynolds. Electrical phenomena occurring during the freezing of dilute aqueous solutions and their possible relationship to thunderstorm electricity. *Phys Rev* 78, 254-259, 1950.

230. Wowk, B., M. Darwin, S.B. Harris, S.R. Russell, and C.M. Rasch. Effects of solute methoxylation on glass-forming ability and stability of vitrification solutions. *Cryobiology* 39, 3: 215-227, 1999.

231. Wowk, B., E. Leitl, C.M. Rasch, N. Mesbah-Karimi, S.B. Harris, and G.M. Fahy. Vitrification enhancement by synthetic ice blocking agents. *Cryobiology* 40, 3: 228-236, 2000.

232. Wusteman, M.C., D.E. Pegg, M.P. Robinson, L.H. Wang, and P. Fitch. Vitrification media: toxicity, permeability, and dielectric properties. *Cryobiology* 44, 1: 24-37., 2002.

233. Yang, H., J. Acker, A. Chen, and L. McGann. In situ assessment of cell viability. *Cell Transplant* 7, 5: 443-451, 1998.

Chapter Two

Validation and Reliability of Computerized Cell-Viability Analysis of Tissue Slices

NM Jomha, PC Anoop, JAW Elliott, K Bagnall, LE McGann

A version of this chapter has been submitted for publication in BioMedCentral – Musculoskeletal Disorders.

2.1 Introduction

Assessment of cell recovery in tissues using membrane integrity dyes has become a frequently used technique. This is especially so with articular cartilage (AC) and chondrocytes *in situ* because the location of cartilage cells within the complex matrix makes other techniques such as cell culture and metabolite production impractical. However, there is minimal literature that documents the effectiveness or reliability of the methods used to count intact cells versus disrupted cells. Such literature is important because the manual counting of cells has the potential for significant variation within/between evaluators, within/between studies and between labs. It is also very time consuming. The development of a reliable, computerized method of cell evaluation after staining with membrane integrity dyes would eliminate many of the variables associated with manual counting. Importantly, the same program could be used by different labs allowing direct comparison of results between labs. Furthermore, a computerized method could perform the task in a small fraction of the time required by a human, resulting in huge time and cost savings.

Membrane integrity stains such as Syto 13, fluorescein diacetate (FDA) and ethidium bromide (EB) have been used successfully in determining cell integrity in intact AC (1, 3, 4, 12, 13, 15) and have demonstrated the best correlation with long-term survival after transplantation in AC (16). Membrane integrity stains aid in evaluating cell viability by inferring that cells with disrupted membranes are dead (6) while those with intact membranes have at least retained the possibility of being intact and viable. By combining the nuclear binding stains Syto 13 and EB, contrasting colours (green and red, respectively) can be observed for differentiation purposes. Intact cells will allow uptake of Syto 13 and exclude the EB resulting in green fluorescence when viewed under fluorescence microscopy. Conversely, cells with disrupted membranes allow uptake and binding of EB as well as the Syto 13 and these cells will stain red or yellow, enhancing the ability to differentiate between cells with intact and disrupted cell membranes. In addition, these stains can be used *in situ* so that cell recovery as a function of location within the matrix can be determined.

Colour differentiation is not always distinct with chondrocytes *in situ* because of the surrounding cartilage matrix. The matrix may partially absorb the stains making the distinction of cells from the background less well defined. Additionally, minor membrane leakage results in less complete EB uptake producing cells of a lighter red or yellow colour further confusing the distinction between intact and disrupted cells. This subjective aspect of the evaluation created inconsistencies between human evaluators, and led to the development of a computer cell-counting program to provide a reproducible determination of the percentage of intact cells versus disrupted cells.

The program design was based on the same principles as colorimetry (11), which measures light intensity at different wavelengths. Colorimetry is a well-established technique and although this technique does not identify individual cells, it is used widely to determine the relative percentage of involved cells when compared to a control group. Based on these principles, a computer program was designed to provide the percentage of green pixels (Syto 13 stain) versus red pixels (EB stain) after elimination of the background in a digitized image.

A reliable method of evaluating intact cell recovery is required to adequately evaluate results from experimental procedures with chondrocytes *in situ*. It was hypothesized that the computer counting program was more reliable than human cell evaluation because of the variability both within and between humans. This study examined the inter-person and intra-person reliability of nine human subjects (divided into three groups) on digitized images of chondrocytes *in situ* stained with fluorescent dyes and compared the results to the computer assessment of the images.

2.2 Materials and Methods

Fifteen digitized images from previous experiments on pig AC were collected. Osteochondral dowels of 10mm diameter had undergone various experimental conditions that included exposure to dimethyl sulfoxide (1*M*, 3*M*, 6*M*) followed by slow cooling (2-stage cryopreservation (8, 9)), or rapid cooling by plunging into liquid nitrogen (4). After the experimental procedures, 70μm slices were removed using a Vibratome® (TPI, St.

Louis, Missouri) sectioning from the articular surface to the cartilage-bone junction across the widest portion of the dowel. The slices were stained using membrane integrity dyes of ethidium bromide (EB; Sigma, St. Louis, MO) and Syto 13 (Molecular Probes, Eugene, OR) (0.1% EB with 0.45% Syto mixed in PBS). Cells with intact membranes stained green due to the absorption of the Syto stain with the exclusion of the EB stain. Cells with disrupted membranes could not exclude the EB stain and therefore stained red. The slices were viewed using a Leitz fluorescence (440-480nm) microscope (Leitz, Germany) at 125X magnification (10X objective and 12.5X eyepiece). The images were recorded using a digital camera (Pixera DiRactor, Pixera Corporation, Los Gatos, CA) and stored on computer.

The custom computer counting program was based on computer-generated histograms of pixel colour intensity for both red and green (Figure 2-1). Cumulative histograms were then constructed from each red and green histogram (Figure 2-2).

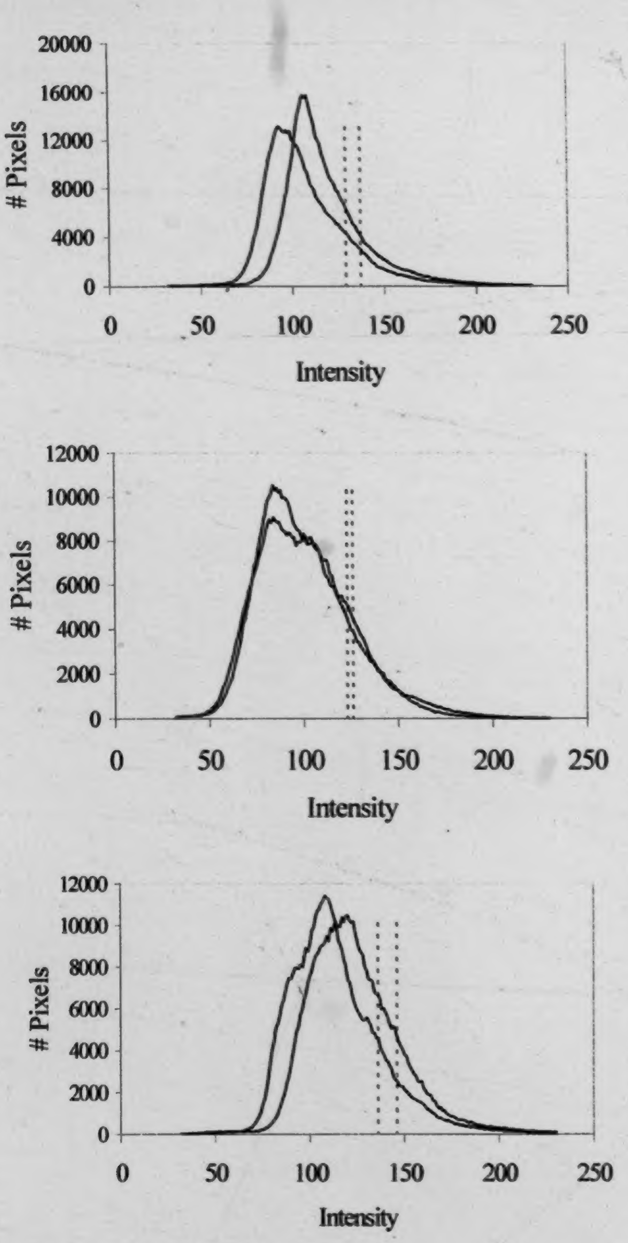

Figure 2-1. Computer generated histograms from 3 images after staining with EB and Syto 13. The red line characterizes the pixel intensity of the red pixels. The green line characterizes the pixel intensity of the green pixels. The vertical red and green dotted lines indicate the threshold determined by the empirical 85% pixel cutoff determined by the cumulative histograms seen in Figure 2-2.

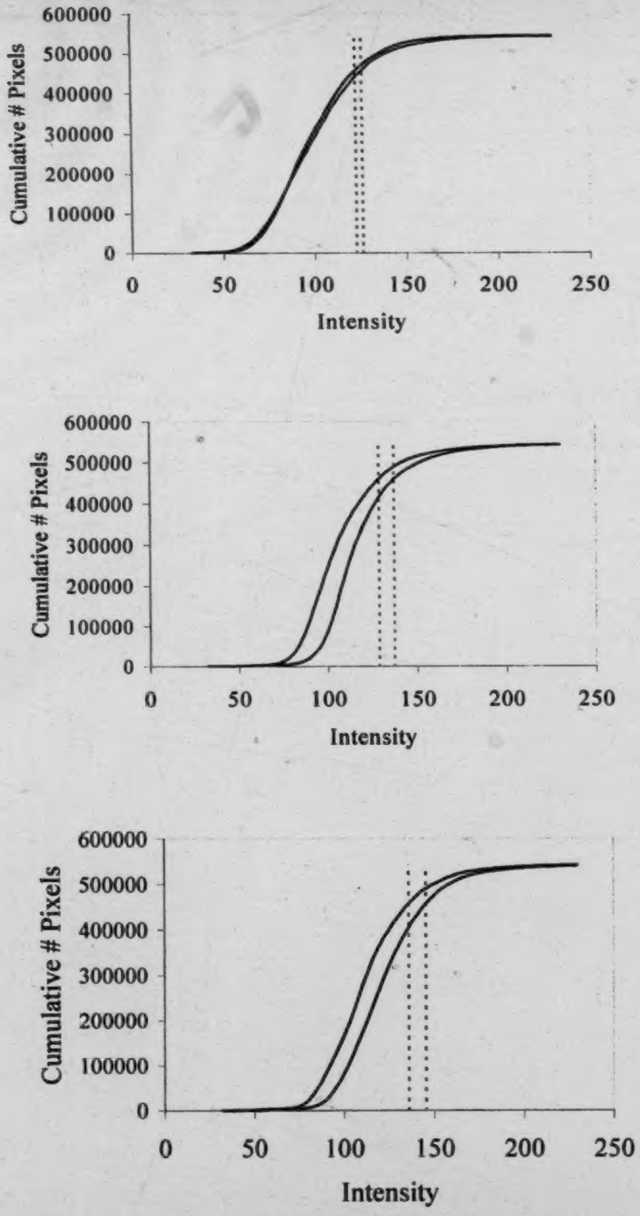

Figure 2-2. Computer generated cumulative histograms corresponding to the histograms seen in Figure 2-1. The red and green dotted lines demarcate the 85th percentile of pixels, which was used as the threshold level for pixel intensity. This threshold intensity, shown in both Figures 2-1 and 2-2, was used to differentiate between the background pixels (to the left of the line) and the cell pixels (to the right of the line). Pixels above the threshold intensity for each colour were designated to be red, green, or black using the following algorithm.

```
If (($I_{red}$ > $Th_{red}$) and ($I_{red}$ > $I_{green}$))
        then $I_{green}$ is set to zero, $I_{blue}$ is set to zero, and $I_{red}$ remains
        else
                if (($I_{green}$ > $Th_{green}$ ) and ($I_{green}$ > $I_{red}$ ))
                        then $I_{red}$ is set to zero, $I_{blue}$ is set to zero, and $I_{green}$ remains
                        else the pixel is set to black
```

where I_{red} , I_{green}, and I_{blue} are the red, green, and blue intensities of a pixel, Th_{red} and Th_{green} are the threshold intensities for red and green. Application of this algorithm to representative images in Figure 2-3 resulted in the processed images in Figure 2-4. The sum of red and green intensities was reported for each image to represent the percentage intact (green) and disrupted (red) cells. This computed percentage recovery was 100%, 55%, and 8% for images A, B, and C, respectively.

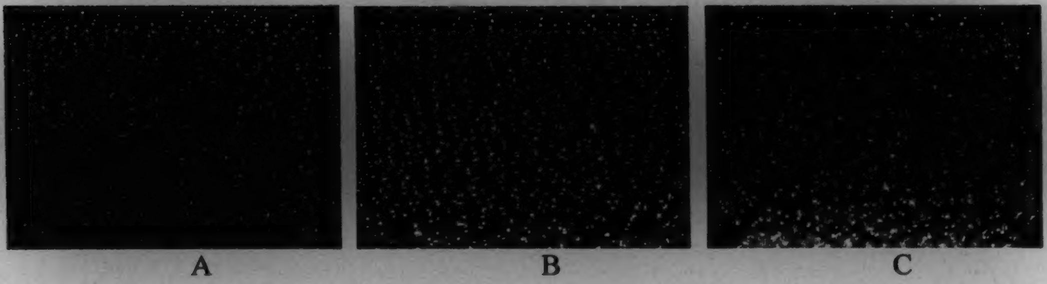

Figure 2-3. Representative digitized images of three different portions of a cartilage slice from which the histograms in Figures 2-1 and 2-2 were generated. These images demonstrate what the human evaluators saw when attempting to quantitatively assess the distribution of red and green cells.

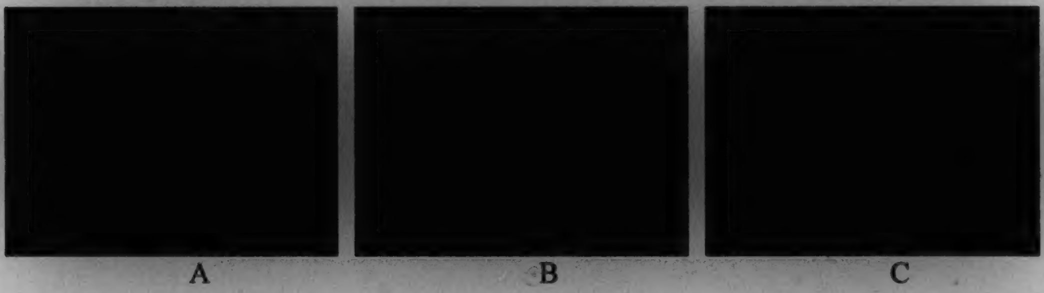

Figure 2-4. Computer generated images after processing by the computer program by application of the algorithm to the images in Figure 2-3. Figure 2-4A shows that he vast majority of cells are intact while Figure 2-4B shows a mixed combination of intact and disrupted cells. Figure 2-4C shows that most cells are disrupted.

Fifteen slices were selected with varying proportions of green and red cells. Three copies of each image were made with one being the original image, one a mirror image, and one rotated 180° to make it difficult for each observer to identify the pictures. The 45 images were arranged in random order for assessment. Three groups of three human evaluators were selected. The "unskilled" group consisted of three people (US1, US2, US3) with computer entry experience but no science research or cell counting background. The "novice" group consisted of three people (NV1, NV2, NV3) with less than one year of science research background but no experience counting cells. The expert group consisted of three people (EX1, EX2, EX3) with a greater than one year science research background and some experience counting cells. All evaluators were provided with the same instructions. The total number of green and red cells for each of the 45 images was recorded by clicking the computer cursor on each cell to demarcate it as green or red with the totals recorded by a data collection program. The computer counting program scanned each of the same 45 images and the percentage of green pixels compared to red pixels was recorded as previously described.

The results were tabulated and statistical analysis was performed including Intraclass Correlation Coefficient (ICC) within (Intra-Rater) human evaluators and between (Inter-Rater) humans and/or computer in addition to Pearson's Correlation and 95% confidence intervals using SPSS-10.07 (SPSS Inc, San Rafael, CA).

2.3 Results

Table 2-1 demonstrates the ICC *within* all evaluators and the computer program and indicates that evaluators with more experience were more reliable when repeating counts on the same image (Intra-Rater) while the computer program was perfectly reliable (ICC = 1.0). Table 2-2 shows the ICC *between* the groups of evaluators (Inter-Rater) and indicates that increased experience of the evaluators resulted in increased correlation *between* individuals. The experienced group had an excellent correlation between the individuals (ICC = .93). When the results from the computer program were included with the results from the experienced human evaluators, the ICC = .84 and indicated a very good correlation between the experienced human evaluators and the computer program.

Evaluator	ICC
US1 – unskilled	0.75
US2 – unskilled	0.78
US3 – unskilled	0.67
NV1 – novice	0.89
NV2 – novice	0.88
NV3 – novice	0.91
EX1 – experienced	0.87
EX2 – experienced	0.97
EX3 – experienced	0.99
Computer program	1.00

Table 2-1. Intra-Rater Intraclass Correlation Coefficient for all human evaluators and the computer program. There was increased reliability, in general, with increased experience. EX3 demonstrated the highest ICC (0.99) while the computer program was perfectly reliable (ICC = 1.00).

	ICC without computer program	ICC with computer program
Unskilled	0.47	0.36
Novice	0.85	0.75
Experienced	0.93	0.84

Table 2-2. Inter-Rater Intraclass Correlation Coefficient within each group and including the computer program. The "ICC with computer program" denotes the ICC when the results from the computer program are included in the results with the human evaluators. The experienced evaluators demonstrated an excellent ICC (0.93) when compared to each other and when the computer program results were included (0.84). The novices also demonstrated a very good correlation (0.85) within their group but there was a further decrease in the ICC when the computer program was included (0.75). The unskilled group had a very low correlation (0.47 and 0.36).

Table 2-3 shows the Pearson's correlation with 95% confidence intervals calculated by comparing the average results within each group for each digitized image with the results from the computer program.

	Pearson's correlation	95% confidence intervals
Unskilled	0.41	-0.19-0.71
Novice	0.79	0.34-0.89
Experienced	0.77	0.44-0.92

Table 2-3. Pearson's correlation with 95% confidence intervals

There was a consistent, although not invariable, correlation of overestimation of the recovery of green cells by the experienced human evaluators when compared to the computer program. The Pearson's correlation of the novice and experienced groups were significant to P = 0.01 with increased 95% confidence intervals in the novice group. The unskilled group had a poor correlation with the computer program.

2.4 Discussion

The purpose of this study was to validate the use of a custom computer counting program to be used in place of human evaluation of chondrocytes *in situ* after staining with membrane integrity dyes. The results of this study supported the hypothesis that the computer counting program was the most reliable method of counting chondrocytes *in situ* after staining with membrane integrity dyes. The computer program had perfect reliability in evaluating the three copies of the 15 digitized pictures (ICC = 1.0) while there was always some error with the human evaluators. The best human evaluator (EX3) came close to the computer program's reliability (ICC = 0.99) but as experience decreased, the reliability decreased (Table 2-1). In addition, the highest correlation between the three most experienced evaluators was ICC = 0.93, with decreasing correlation between evaluators with less experience (Table 2-2). Although the results of this experiment showed that experience in science research and cell counting increased reliability (higher Intra-Rater ICCs and Inter-Rater ICCs), the computer program was consistently the most reliable.

Table 2-3 demonstrates that there was a good correlation between the two methods of cell evaluation (Pearson's Correlation = 0.77) but it was noted that the experienced human evaluators consistently (with occasional exceptions) overestimated the percent recovery of green cells compared to the computer program. The use of membrane integrity dyes is a well-accepted method of preliminary assessment of cell recovery after experimental protocols. Currently, manual counting is the only method of cell evaluation of chondrocytes *in situ* after membrane integrity staining. The custom computer program demonstrated sufficient correlation with the manual counting of experienced human evaluators to warrant its use in the described situation. This program is an improvement over human evaluators because of inherent inconsistencies noted within and between humans. In addition to being more reliable than humans, the program is much quicker and significantly decreases the amount of time required to evaluate the cells.

Membrane integrity has become a popular method of determining cell viability, especially with AC (1, 3, 4, 12-15). This has been supported by evidence of good correlation between a high proportion of cells with membrane integrity and successful outcome after transplantation (16). The difficulty of using membrane integrity dyes with chondrocytes *in situ* stems from the absorption of some stain into the background matrix. The necessity of maintaining the background while evaluating chondrocytes *in situ* can make differentiating colours more difficult and also can provide an optical illusion with respect to the colours seen by different cell counters. The difficulties can be readily appreciated in the Figure 2-3 images.

The computer program was designed to take background interference into account. The use of red and green histograms from the digital image followed by the creation of the cumulative histogram provided information on the distribution and intensity of red and green pixels throughout the image. The threshold intensity was determined by using the intensity of the pixels at the 85th percentile, which was empirically selected by comparing computed results with results from other images previously counted manually, including images of cell monolayers and slices of heart valve. This was the only empirical input used in the computer program.

Figure 2-4 shows that after application of the computed algorithm, the differentiation between red and green becomes much more distinct, and visually correlates with the images seen in Figure 2-3. The selected cutoff at the 85th percentile pixel intensity ensured that variations between absorption of stain into the matrix, minor variations in stain intensity created during mixing, and lighting differences in the microscope were eliminated. The computer program provided a consistent and reliable method of measuring intact cell recovery that can be used to compare results between different experimental techniques and between different labs.

The images in Figure 2-4 demonstrate an advantage of using combined stains. The distribution of the relative amounts of red/green can be visualized and the recovery of cells as a function of location within the matrix can provide valuable information regarding mechanisms of cell injury during cryopreservation. Indeed, characteristic patterns of cell recovery can be consistently found with specific experimental protocols (4, 5).

Cost is an important factor in research. Counting of stained cells in one experiment has taken up to 320 hours when performed by a human evaluator (5). This same cell evaluation can be completed in 16 hours when using the computer program drastically reducing the cost involved but, more importantly, allowing increased numbers of samples to be evaluated which significantly decreases the variability within the experiment (2).

The use of the computer program does raise some concerns but these are the same as for human evaluation. Cells that stain green are considered alive because their membranes are intact. This results in an upper limit for recovery, because the cells may have sustained lethal injury that has not yet resulted in loss of membrane integrity, one the final events of cell death (6, 7, 17). It has been suggested that cells that have some membrane damage, and thus may be permeable to EB, can repair this membrane damage and those cells may survive (10). Conversely, some cell damage may be due to intracellular events and may not have progressed to membrane disruption by the time the stains are applied (10). Nevertheless, assessment of membrane integrity is a useful method in situations where the plasma membrane is a likely target for injury.

In conclusion, this experiment provided evidence that a custom computer counting program was more reliable than human cell evaluators, and was shown to be a valid method for determination of chondrocyte recovery *in situ* after membrane integrity staining. The computer program can provide a useful method of measuring cell outcomes after experimental procedures on tissues systems, while reducing the time and costs involved. It can also allow comparison of results between labs without considering the variations between human evaluators.

2.5 Acknowledgements

The authors thank Lauren Beaupre for statistical analysis. JAW Elliott holds a Canada Research Chair in Interfacial Thermodynamics. Funding was provided by University of Alberta Hospital Foundation, Edmonton Civic Employees Charitable Assistance Fund, and the Edmonton Orthopaedic Research Society.

2.6 References

1. Bujia, J., D. Kremer, H. Sudhoff, E. Viviente, C. Sprekelsen, and E. Wilmes. Determination of viability of cryopreserved cartilage grafts. *Eur Arch Otorhinolaryngol* 252, 1: 30-34, 1995.
2. Gundersen, H.J. and R. Osterby. Optimizing sampling efficiency of stereological studies in biology: or 'do more less well!'. *J Microsc* 121, Pt 1: 65-73, 1981.
3. Jomha, N. *Cryopreservation of human articular cartilage*, in *Experimental Surgery, Masters Thesis*. University of Alberta: Edmonton, 1996.
4. Jomha, N.M., P.C. Anoop, K. Bagnall, and L.E. McGann. Effects of increasing concentrations of dimethyl sulfoxide during cryopreservation of porcine articular cartilage. *Cell Pres Tech* 1, 2: 111-120, 2002.
5. Jomha, N.M., P.C. Anoop, and L.E. McGann. Chondrocyte recovery in cryopreserved porcine articular cartilage after bone carrier alteration. *Cryo Letters* 23, 4: 263-268, 2002.
6. Malinin, T.I. Injury of human polymorphonuclear granulocytes frozen in the presence of cryoprotective agents. *Cryobiology* 9, 2: 123-130, 1972.
7. Malinin, T.I., W. Mnaymneh, H.K. Lo, and D.K. Hinkle. Cryopreservation of articular cartilage. Ultrastructural observations and long-term results of experimental distal femoral transplantation. *Clin Orthop* 303: 18-32, 1994.
8. McGann, L.E. and J. Farrant. Survival of tissue culture cells frozen by a two-step procedure to -196 degrees C. I. Holding temperature and time. *Cryobiology* 13, 3: 261-268, 1976.
9. McGann, L.E. and J. Farrant. Survival of tissue culture cells frozen by a two-step procedure to -196 degrees C. II. Warming rate and concentration of dimethyl sulphoxide. *Cryobiology* 13, 3: 269-273, 1976.
10. McGann, L.E., H.Y. Yang, and M. Walterson. Manifestations of cell damage after freezing and thawing. *Cryobiology* 25, 3: 178-185, 1988.
11. Mosmann, T. Rapid colorimetric assay for cellular growth and survival: Application to proliferation and cytotoxicity assays. *J Immunol Methods* 65, 55-63, 1963.

12. Muldrew, K., M. Chung, K. Novak, N.S. Schachar, R.F. Zernicke, L.E. McGann, J.B. Rattner, and J.R. Matyas. Evidence of chondrocyte repopulation in adult ovine articular cartilage following cryoinjury and long-term transplantation. *Osteoarthritis Cartilage* 9, 5: 432-439, 2001.

13. Muldrew, K., M. Hurtig, K. Novak, N. Schachar, and L.E. McGann. Localization of freezing injury in articular cartilage. *Cryobiology* 31, 1: 31-38, 1994.

14. Muldrew, K., K. Novak, C. Studholme, G. Wohl, R. Zernicke, N.S. Schachar, and L.E. McGann. Transplantation of articular cartilage following a step-cooling cryopreservation protocol. *Cryobiology* 43, 3: 260-267, 2001.

15. Ohlendorf, C., W.W. Tomford, and H.J. Mankin. Chondrocyte survival in cryopreserved osteochondral articular cartilage. *J Orthop Res* 14, 3: 413-416, 1996.

16. Schachar, N.S., K. Novak, M. Hurtig, K. Muldrew, R. McPherson, G. Wohl, R.F. Zernicke, and L.E. McGann. Transplantation of cryopreserved osteochondral Dowel allografts for repair of focal articular defects in an ovine model. *J Orthop Res* 17, 6: 909-919, 1999.

17. Tavakol, K., R.G. Miller, D.P. Bazett-Jones, W.S. Hwang, L.E. McGann, and N.S. Schachar. Ultrastructural changes of articular cartilage chondrocytes associated with freeze-thawing. *J Orthop Res* 11, 1: 1-9, 1993.

Chapter Three

Chondrocyte Recovery in Cryopreserved Porcine Articular Cartilage after Bone Carrier Alteration

NM Jomha, PC Anoop, LE McGann

A version of this chapter has been published in Cryo-Letters.
Jomha, N.M., P.C. Anoop, and L.E. McGann. Chondrocyte recovery in cryopreserved porcine articular cartilage after bone carrier alteration. *Cryo Letters* 23, 4: 263-8, 2002.

3.1 Introduction

Osteochondral disease and injuries are a significant cause of disability that negatively impacts quality of life and ability to work productively. Cryopreservation of osteochondral tissue with preservation of intact chondrocytes may provide an alternative to current treatment methods (1-5, 8, 9, 12, 25, 27). For successful long-term matrix maintenance, the chondrocytes must survive the cryopreservation process.

Successful cryopreservation with high cell recovery has been achieved for cells in suspension (13, 23) including chondrocytes (24, 26, 28) as well as in simple multi-cell tissues like very early embryos (6). Cryopreservation of more complex intact tissues has proven much more difficult (11, 15, 22). A 2-stage cryopreservation technique has been established by McGann (17, 18) and used with moderate success with intact 10mm osteochondral dowels (OCDs) of ovine articular cartilage (AC) (50-60% intact cells) by Muldrew *et. al.* (20). These studies showed that the most difficult area in which to retain intact chondrocytes was the intermediate or middle zone of the dowel. Unfortunately, Muldrew was unable to enhance cell recovery in this region by minor alterations in the cryopreservation process. Reproduction of Muldrew's methodolgy using the same cryopreservation protocol and intact human cartilage was unsuccessful (<10%) (10).

Articular cartilage is composed mainly of collagen and proteoglycans (16) that form complex interactions with extracellular water in the matrix. The complex nature of osteochondral tissue (AC matrix supported on a bone base) has an, as yet, unknown effect on the penetration of cryoprotectants and the subsequent ice formation during the cryopreservation process. After skeletal maturity, the bone base blocks access (14, 21) to cryoprotectant solution and ice nucleators on one side of the osteochondral tissue during the freezing process. The mechanical and physiological effect of this construct on low temperature responses has not been determined.

The purpose of this study was to investigate the influence of altering the structural configuration of the osteochondral tissue on the low-temperature responses of osteochondral tissue. We hypothesized that drilling a 2mm diameter hole in the center of the bone base of the 10mm diameter osteochondral dowel would increase the chondrocyte recovery and alter the distribution of intact chondrocytes throughout the matrix because of the physical alteration of the bone base.

3.2 Materials and Methods

Tissues

Intact stifle joints from pigs of reproductive age sacrificed for meat consumption were harvested within 12 hours of death. Osteochondral dowels (10mm diameter) were harvested using a powered coring device (Delta 10" Drill Press, Delta International Machinery, Ontario, Canada) with the cartilage submerged in 1X PBS (pH = 7.0) (Gibco BRL, MD) maintained at 4°C to minimize thermal damage to the cartilage during the drilling process. The dowels were harvested from the central portion of the weight bearing surface of the medial femoral condyle and contained the full thickness (3-4mm) of AC on a 5-10mm thick bone base. Each joint provided three osteochondral dowels that were randomly placed into three groups: Group 1) control OCD without cryopreservation, 2) intact OCD cryopreserved, and 3) OCD cryopreserved with a 2mm hole drilled through the center of the bone base.

Group 1 was the positive control group and the OCDs from this group were held at 4°C and did not undergo any treatment prior to slicing and staining. The percentage of intact cells from this group was used as a reference for comparison with the other two groups. Negative controls from OCDs plunged directly into liquid nitrogen (LN) have consistently demonstrated very low recovery (<10%). Group 2 consisted of the intact OCDs cryopreserved. These dowels were intact 10mm diameter OCDs that underwent the cryopreservation procedure described below. Group 3 had a 2mm hole drilled in the bone portion of the dowel, drilling from the bone surface towards the bone-cartilage junction. The drilling was completed when the tip of the drill bit breached the subchondral bone (limiting thermal or mechanical damage to the cartilage) exposing the overlying cartilage. These samples then went through the same cryopreservation protocol as Group 2.

Cryopreservation Protocol

The 10mm OCDs were placed in polypropylene test-tubes and immersed in 1M (7.8%) dimethyl sulfoxide (Me_2SO) solution at 4°C for 30 min. The dowels were transferred to an ice-water bath at 0°C for 10 min, then cooled to –7°C in a methanol bath. At –7°C, the dowels were held for 10 min to allow for temperature equilibration and then the solution was ice nucleated with ice crystals from forceps dipped into LN. After 15 minutes to allow dissipation of the latent heat of fusion, the samples were cooled at 1°C/min to –30°C and then plunged into LN (100°C/min cooling rate). It took approximately 50 minutes to proceed through the slow cooling process and another 2 to 3 minutes for the rapid cooling after plunging into LN to achieve a temperature between -180°C and -190°C within the matrix. Once completely frozen and held for a minimum of 12 hours (range 12-48 hours), the samples were warmed in a 37°C water bath until the ice just began to melt (approximately 30 seconds, 100°C/min warming rate) and then were placed in 1X PBS solution until the sample warmed to room temperature (22°C) (approximately 30 minutes).

Cell Assessment

Immediate post-thaw recovery was determined by assessement with membrane integrity stains. Samples were cut using a vibratome (Vibratome Series 1000, TPI, St. Louis, Missouri) cutting perpendicularly from the articular surface towards the cartilage-bone junction. 70μm slices were taken from across the widest portion of the dowels. Each slice was stained using fluorescent dyes of ethidium bromide (EB; Sigma, St. Louis, MO) and Syto 13 (Molecular Probes, Eugene, OR) (0.1% EB with 0.45% Syto mixed in PBS). Cells with intact membranes stained green due to the absorption of the Syto stain with the exclusion of the EB stain. Cells with disrupted membranes could not exclude the EB stain and stained red. The slices were viewed under a Leitz fluorescence (440-480nm) microscope (Leitz, Germany) at 125X magnification (10X objective and 12.5X eyepiece). The images were recorded by digital camera (Pixera DiRactor, Pixera Corporation, Los Gatos, CA) and stored on computer for later manual cell counting.

The digitized pictures from each slice were divided into nine equal sections (Figure 3-1). The most peripheral edges of the slices were excluded due to artifact and handling damage that occurred with the processing of the dowels. All cells were counted as having either intact (green) or disrupted (red) membranes and the percent intact cell recovery were related to fresh controls. The percent recovery of intact cells in each of the nine sections was compared between the three Groups. Statistical analysis was performed using a two-tailed Independent Samples T-test with $P < 0.05$ determined as significant confirmed by 95% confidence intervals using SPSS-10.07 (SPSS Inc, San Rafael, CA).

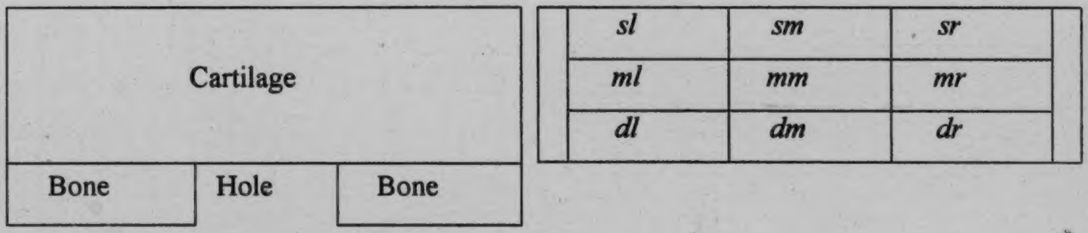

(a) (b)

Figure 3-1. Representation of the dowel with a hole drilled into the bone (a) and 70µm cartilage slices divided into nine equal sections (b).

a) A 2mm hole drilled into the bone portion to the bone-cartilage junction

b) The peripheral edges were excluded due to artifact and handling damage during preparation of dowels. The areas are designated as *sl* = superficial left, *sm* = superficial middle, *sr* = superficial right, *ml* = middle left, *mm* = middle middle, *mr* = middle right, *dl* = deep left, *dm* = deep middle, *dr* = deep right.

3.3 Results

Ten sets of three OCDs from ten donors were used in this study. The intact cell recovery from the slices collected from the control dowels of these ten joints was greater than 95% and overall cell counts were similar between the control and treated samples. Cell recovery from the cryopreserved intact group (Group 2) was evenly distributed throughout the 70µm slice with moderately increased recovery from the deep layer.

There was a significant overall increase in intact cells in the dowels with the 2mm hole (Group 3) when compared to the intact dowels without the hole (Group 2) (48.3 ± 4.8% : 28.6 ± 3.0%, P = 0.003). There was a trend of increased cell recovery in all nine sections from Group 3 versus Group 2 when comparing specific sections within each group (i.e. comparing section *mm* from Group 3 to section *mm* from Group 2). This was statistically significant in the central sections including *sm* (P = 0.033), *mm* (P = 0.002), *mr* (P = 0.026), and *dl* (P = 0.022) (Figure 3-2). There was increased variation in the OCD with the hole as noted by the larger standard errors.

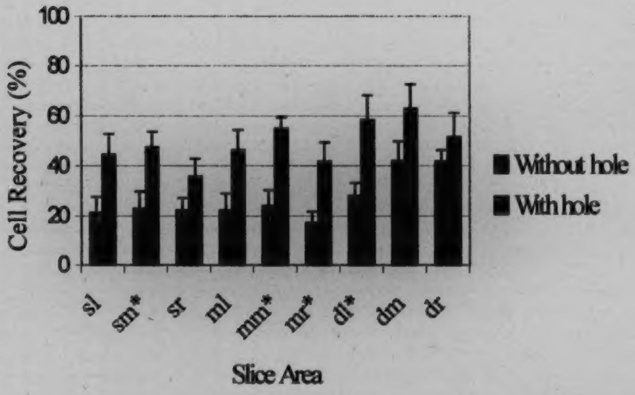

	sl	*sm*	*sr*	
	ml	*mm*	*mr*	
	dl	*dm*	*dr*	

Figure 3-2. Intact cell recovery comparing the nine sections of the two comparison groups with schematic of the most affected sections. The osteochondral dowels cryopreserved intact (Group 2) compared with the osteochondral dowels cryopreserved with the 2mm hole drilled through the center of the bone base (Group 3). The abbreviations are the same as in Figure 3-1 and error bars denote standard error. Areas with * (figure on the left) and shaded areas (figure on the right) denote a statistically significant increase ($P < 0.05$) in intact cell recovery when the area in Group 3 is compared to the same area in Group 2.

3.4 Discussion

This study was designed to provide information on the possible mechanical and physiological mechanisms of cell injury during the cryopreservation process. The effect of altering the OCD configuration was examined to determine its effect on the recovery of intact chondrocytes from intact AC. This study demonstrated an increase in the intact cell recovery in 10mm diameter OCDs that had a 2mm hole drilled centrally through the bone to expose the overlying cartilage. Although higher recovery was noted in all sections of the slice, the most significant increase was noted in the central areas of the cartilage. Because there was a more significant increase in central portions of the cartilage, the overall distribution of the cell recovery changed when the 2mm hole was used. This result supported the hypothesis that altering the bone configuration of the OCD would increase the intact cell recovery and alter the pattern of intact cell recovery.

The reason for the increased cell recovery and altered pattern of cell recovery cannot be conclusively delineated by this study alone but possible reasons include 1) altered intra-matrix ice formation, 2) altered cryoprotectant penetration and 3) altered physical interactions between matrix components.

During this cryopreservation procedure, the solution surrounding the tissue is ice nucleated to induce ice formation. This increases the extracellular solute concentration due to exclusion of the solutes from the ice, leading to cell dehydration, which reduces the risk of intracellular ice formation at lower temperatures. When the ice crystals in the solution contact the osteochondral tissue, ice formation will be induced in the cartilage matrix from all exposed surfaces including the superficial surface as well as the cut edges. Ice will not form initially in the deepest portions of the matrix due to the impermeability of the bone-cartilage junction (14, 21). The 2mm drill hole through the bone into the deep portion of the cartilage potentially permits another point of ice crystal contact with the matrix and may alter the pathway for ice growth within the matrix. The results of this study were consistent with this hypothesis.

Another important factor may be the diffusion of the cryoprotectant and the solutes. Articular cartilage is a complex tissue comprised mainly of collagen, proteoglycans and water with strong bonds between these constituents. Also of note is a negative charge associated with the proteoglycans and the high electrolyte concentrations present within the matrix (7). It is likely that these factors play an important role in the penetration and distribution of the Me_2SO during the 30 minute exposure time prior to cryopreservation. The proteoglycan concentration is higher in the middle and deep zones of the cartilage and the increase in negative charges may inhibit Me_2SO penetration. Therefore, the direct exposure of the deep layer to Me_2SO due to the 2mm drill hole may alter the distribution of the cryoprotectant with increased cell recovery in an altered distribution as shown in this study.

The electrolyte concentration and the osmolarity are highest in the deep layer as well. High solute concentrations (19) are detrimental to cells and ice formation will increase the solute concentration to even higher levels. With an impermeable bone-cartilage junction blocking the diffusion of the solutes out of the cartilage as ice forms within the matrix from the periphery (superficial surfaces and cut edges), extremely high (and injurious) solute concentrations would be expected in the deep portions of the cartilage. The 2mm drill hole may alter the pathway and final location of the solutes during the ice formation and could be responsible for the altered pattern of cell recovery noted in this study. Furthermore, the 2mm hole also may alter the osmotic properties of the deep cartilage by releasing the impermeable deep bone boundary, making this area more available for Me_2SO penetration and/or more amenable to protective ice formation.

The ultimate objective of this work is to cryopreserve osteochondral tissues for transplantation in humans. Pigs were selected due to the thickness of the cartilage in the stifle joint, which is closest to human knee joints. The increased thickness of human AC compared with other animals such as sheep and cows may exacerbate difficulties with cryoprotectant diffusion, high electrolyte concentrations and osmolarity. This is a possible explanation as to why the recovery from the porcine AC in this study was lower than that achieved by Muldrew using ovine cartilage (20).

In conclusion, alteration of the bone configuration of 10mm pig osteochondral dowels by drilling a 2mm hole through the bone to the cartilage resulted in a significant increase in intact chondrocyte recovery, but this did not approach the high recovery seen in the controls. In addition, drilling the 2mm hole altered the pattern of the recovery of the intact cells as determined by the increased recovery in the central portions of the cartilage in the group with the 2mm hole when compared to the group without the hole. These results support the hypothesis that the bone is a significant impediment to successful cryopreservation of AC using the method in this study. Methods of cryopreservation will have to be developed that negate this limiting factor and increase the intact chondrocyte recovery before transplantation of cryopreserved osteochondral fragments should be attempted.

3.5 Acknowledgements

This research was supported by the Canadian Institute of Health Research, Edmonton Civic Employees Charitable Assistance Fund, and the Edmonton Orthopaedic Research Society. The authors thank Lauren Beaupre for the statistical analysis and Dr. Keith Bagnall for review of the manuscript and Ouellette Packers Ltd Edmonton for supplying the tissue.

3.6 References

1. Anderson, A.F. and M.J. Pagnani. Osteochondritis dissecans of the femoral condyles. Long-term results of excision of the fragment. *Am J Sports Med* 25, 6: 830-834, 1997.
2. Aubin, P.P., H.K. Cheah, A.M. Davis, and A.E. Gross. Long-term followup of fresh femoral osteochondral allografts for posttraumatic knee defects. *Clin Orthop* 391 Suppl: S318-327, 2001.
3. Brittberg, M., T. Tallheden, B. Sjogren-Jansson, A. Lindahl, and L. Peterson. Autologous chondrocytes used for articular cartilage repair: an update. *Clin Orthop* 391 Suppl: S337-348, 2001.
4. Chu, C.R., F.R. Convery, W.H. Akeson, M. Meyers, and D. Amiel. Articular cartilage transplantation. Clinical results in the knee. *Clin Orthop* 360: 159-168, 1999.
5. Clohisy, D.R. and H.J. Mankin. Osteoarticular allografts for reconstruction after resection of a musculoskeletal tumor in the proximal end of the tibia. *J Bone Joint Surg Am* 76, 4: 549-554, 1994.
6. Elliot, K. and J. Whelan, eds. CIBA Foundation Symposium. Vol. 52. Elsevier: Amsterdam, 1977.
7. Hall, A.C., E.R. Horwitz, and R.J. Wilkins. The cellular physiology of articular cartilage. *Exp Physiol* 81, 3: 535-545, 1996.
8. Hangody, L., P. Feczko, L. Bartha, G. Bodo, and G. Kish. Mosaicplasty for the treatment of articular defects of the knee and ankle. *Clin Orthop* 391 Suppl: S328-336, 2001.
9. Johnson, L.L. Arthroscopic abrasion arthroplasty: a review. *Clin Orthop* 391 Suppl: S306-317, 2001.
10. Jomha, N. *Cryopreservation of human articular cartilage*, in *Experimental Surgery, Masters Thesis*. University of Alberta: Edmonton, 1996.
11. Kawabe, N. and M. Yoshinao. Cryopreservation of cartilage. *Int Orthop* 14, 3: 231-235, 1990.

12. Kreklau, B., M. Sittinger, M.B. Mensing, C. Voigt, G. Berger, G.R. Burmester, R. Rahmanzadeh, and U. Gross. Tissue engineering of biphasic joint cartilage transplants. *Biomaterials* 20, 18: 1743-1749, 1999.

13. Lovelock, J.F. The mechanism of the protective action of glycerol against haemolysis by freezing and thawing. *Biochimica et Biophysica Acta* 11, 28-36, 1953.

14. Malinin, T. and E.A. Ouellette. Articular cartilage nutrition is mediated by subchondral bone: a long-term autograft study in baboons. *Osteoarthritis Cartilage* 8, 6: 483-491, 2000.

15. Malinin, T.I., J.L. Wagner, J.C. Pita, and H. Lo. Hypothermic storage and cryopreservation of cartilage. An experimental study. *Clin Orthop* 197: 15-26, 1985.

16. Mankin, H.J., V.C. Mow, J.A. Buckwalter, J.P. Iannotti, and A. Ratcliffe. *Form and function of articular cartilage* in *Orthopaedic Basic Science*, S.R. Simon, Editor: Chicago. 1-44, 1994.

17. McGann, L.E. and J. Farrant. Survival of tissue culture cells frozen by a two-step procedure to -196 degrees C. I. Holding temperature and time. *Cryobiology* 13, 3: 261-268, 1976.

18. McGann, L.E. and J. Farrant. Survival of tissue culture cells frozen by a two-step procedure to -196 degrees C. II. Warming rate and concentration of dimethyl sulphoxide. *Cryobiology* 13, 3: 269-273, 1976.

19. Meryman, H.T. Osmotic stress as a mechanism of freezing injury. *Cryobiology* 8, 5: 489-500, 1971.

20. Muldrew, K., M. Hurtig, K. Novak, N. Schachar, and L.E. McGann. Localization of freezing injury in articular cartilage. *Cryobiology* 31, 1: 31-38, 1994.

21. Ogata, K., L.A. Whiteside, and P.A. Lesker. Subchondral route for nutrition to articular cartilage in the rabbit. Measurement of diffusion with hydrogen gas in vivo. *J Bone Joint Surg [Am]* 60, 7: 905-910, 1978.

22. Ohlendorf, C., W.W. Tomford, and H.J. Mankin. Chondrocyte survival in cryopreserved osteochondral articular cartilage. *J Orthop Res* 14, 3: 413-416, 1996.

23. Rajotte, R.V., H.L. Stewart, W.A. Voss, and T.K. Shnitka. Viability studies on frozen--thawed rat islets of Langerhans. *Cryobiology* 14, 1: 116-120, 1977.

24. Schachar, N.S. and L.E. McGann. Investigations of low-temperature storage of articular cartilage for transplantation. *Clin Orthop* 208: 146-150, 1986.

25. Schreiber, R.E., B.M. Ilten-Kirby, N.S. Dunkelman, K.T. Symons, L.M. Rekettye, J. Willoughby, and A. Ratcliffe. Repair of osteochondral defects with allogeneic tissue engineered cartilage implants. *Clin Orthop* 367 Suppl: S382-395, 1999.

26. Smith, A.U. Survival of frozen chondrocytes isolated from cartilage of adult mammals. *Nature* 205, 782-784, 1965.

27. Steadman, J.R., W.G. Rodkey, and J.J. Rodrigo. Microfracture: surgical technique and rehabilitation to treat chondral defects. *Clin Orthop* 391 Suppl: S362-369, 2001.

28. Tomford, W.W., G.R. Fredericks, and H.J. Mankin. Studies on cryopreservation of articular cartilage chondrocytes. *J Bone Joint Surg [Am]* 66, 2: 253-259, 1984.

Chapter Four

Effects of Increasing Concentrations of Dimethyl Sulfoxide during Cryopreservation of Porcine Articular Cartilage

NM Jomha, PC Anoop, K Bagnall, LE McGann

A version of this chapter has been published in Cell Preservation Technology.

Jomha, N.M., P.C. Anoop, K. Bagnall, and L.E. McGann. Effects of increasing concentrations of dimethyl sulfoxide during cryopreservation of porcine articular cartilage. *Cell Pres Tech* 1, 2: 111-120, 2002.

4.1 Introduction

Large, unconfined joint defects are a significant cause of osteoarthritis resulting in significant disability and cost to the health care system. Currently, the only treatment alternative shown to treat this problem effectively is fresh osteochondral transplantation (3-5). Difficulties such as tissue availability, size and contour mismatching (4, 20) and possibility of transmission of infectious diseases (31) have significantly limited the use of this treatment. Cryopreservation of articular cartilage (AC) is a method by which tissues can be collected and stored to enhance the long-term outcomes of osteochondral tissue transplantation.

The ultimate objective of cryopreservation of intact AC is to provide a source of tissues for joint transplantation to treat large joint defects. For successful long-term results of joint transplantation, the chondrocytes must survive so they can maintain the cartilage matrix. In general, cryopreservation has been successful for cells in suspension (27, 29, 32) as well as for simple multiple cell tissues (6); however, complex tissues have proven more difficult (10, 12, 16, 26). A 2-stage cryopreservation technique (17, 18) has demonstrated some success in an ovine model with intact AC (21) but significant cell death restricts the use of the tissue. There also has been an inability to reproduce these results on human AC (10). It has been postulated that exclusion of solutes during ice formation leads to high, localized solute concentrations that are damaging to cell membranes (15, 19). In addition, high solute concentrations result in constitutional supercooling within the matrix (23). This results in rapid intracellular ice formation, which is also detrimental to cell survival (14, 22).

Vitrification is one method of limiting the damaging effects of ice formation and high solute concentrations. By eliminating ice crystal formation and proceeding directly to a glassy state, vitrification may provide a viable method of cryopreserving intact AC. Vitrification has worked successfully on isolated cells (11, 13) as well as some tissues (2, 30). Unfortunately, problems persist with respect to achieving high cryoprotectant concentrations without producing toxicity (32), achieving acceptable cooling and warming rates due to tissue mass, and devitrification (8). If these problems can be solved, then a viable method for storing AC appears plausible.

The objective of this study was to investigate the effect of increasing concentrations of dimethyl sulfoxide (Me_2SO) in porcine AC using a rapid cryopreservation technique. It was hypothesized that an optimal concentration of Me_2SO could be identified that would provide protection against ice formation as well as high, localized solute concentrations without producing excessive toxicity to the chondrocytes. A balance between the protective effect of vitrification and the toxic effect of high cryoprotectant concentration would result in increased chondrocyte recovery.

4.2 Materials and Methods

Tissues

Intact stifle joints were harvested from 20 healthy, sexually mature pigs killed for meat consumption. In this study, pigs were selected because the cartilage thickness in the stifle joint is the closest to the exceptionally thick cartilage in human knee joints. The joints were immersed in 1X Dulbecco's phosphate buffered solution (pH=7.0) (PBS, Gibco, BRL, MD) maintained at 4°C until 10mm diameter osteochondral dowels (OCDs) were harvested using a hand held coring device (within 12 hours of death of the animal). The OCDs were harvested from the central weight-bearing portion of the medial femoral condyle and consisted of the full thickness of AC (3-4mm) perched on a 5-10mm bone base. Three OCDs were harvested from each joint.

Three groups were defined – 1) fresh control, 2) cryoprotectant toxicity control, and 3) experimental group. The fresh control OCDs were immersed in 1X PBS (50ml) for 30 minutes until sectioning and staining (described below). The remaining OCDs from all the joints were randomly placed into beakers containing different Me_2SO (Sigma, St. Louis, MO) concentrations (1*M*, 3*M*, 5*M*, 6*M*, and 7*M* (w/v) (10 dowels in each concentration except 3*M* which contained 11 dowels)) at 4°C. After 30 minutes of exposure to allow penetration of the cryoprotectant (24), one half of the samples were removed as cryoprotectant toxicity controls. The remaining samples underwent the procedure described below as the experimental group. Additionally, an extra sample was prepared from the 3*M* and 6*M* Me_2SO solutions after cryopreservation and underwent freeze substitution and scanning electron microscopy (SEM) described below.

Cryopreservation Protocol

Each OCD was placed into a polypropylene test-tube (17x100mm culture tube, VWR Can Lab, Ontario, Ca) with sufficient cryoprotectant solution at 4°C to immerse the OCD completely (5ml). Samples were cooled in an ice-water bath for 10 minutes, plunged directly into liquid nitrogen (LN) (180-60°C/min cooling rate depending on the concentration of Me_2SO – 1*M* Me_2SO = 180°C/min, 7*M* Me_2SO = 60°C/min) and held there for at least 1 hour. These samples were thawed in a 37°C water bath (85-100°C/min warming rate) until the ice/glass just began to reform to a liquid state (approximately 30 seconds); once removed from their test-tubes, the samples were placed in 1X PBS (50ml) and taken through sample preparation for fluorescence microscopy (approximately 30 minutes).

Cell Assessment

Samples from all three groups were sectioned using a Vibratome® (TPI, St. Louis, Missouri) cutting vertically across the dowel from the articular surface towards the cartilage-bone junction. Slices sectioned to a thickness of 70μm were taken from the widest portion of the dowels (Figure 4-1a). Each slice was stained using membrane integrity dyes of ethidium bromide (EB; Sigma, St. Louis, MO) and Syto 13 (Molecular Probes, Eugene, OR)(0.1% EB with 0.45% Syto mixed in PBS (vol/vol)). Cells with intact membranes fluoresced green due to the absorption of the Syto stain with the exclusion of the EB stain. Cells with disrupted membranes could not exclude the EB stain and therefore fluoresced red. The 70μm slices were viewed under a Leitz Dialux 22 fluorescence (440-480nm) microscope (Leitz, Germany) at 125X magnification (10X objective and 12.5X eyepiece). The images were recorded by digital camera (Pixera DiRactor, Pixera Corporation, Los Gatos, CA) and stored on computer for later analysis. Membrane integrity dyes were used because cell membranes have been shown to be a primary target of injury during the cryopreservation process (1). Membrane integrity dyes also have been shown to be the most reliable predictor of long-term transplantation results (28).

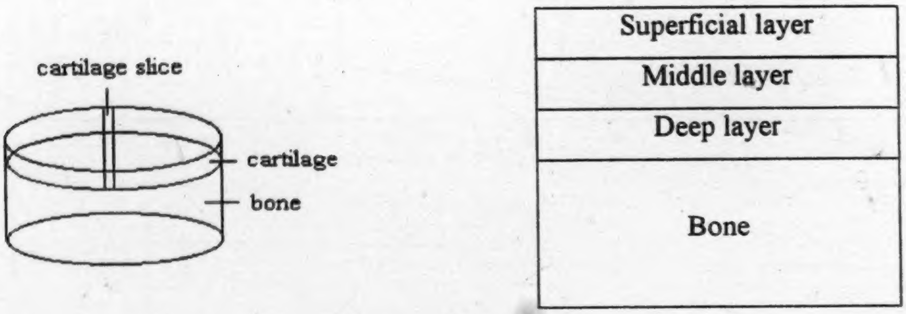

(a) (b)

Figure 4-1. Schematic diagrams of an osteochondral dowel.

(a) Osteochondral dowel with a $70\mu m$ slice removed from the widest portion

(b) Schematic diagram detailing the division of the AC as it sits on the bone base. The cartilage was divided into three equal layers for determination of cell recovery as a function of location within the slice.

A customized computer counting program calculated the percent recovery of intact cells compared to total cells using minimum thresholds for green and red pixel intensity. The total number of green pixels above the minimum intensity was divided by the {total green and red pixels above minimum intensity} to provide a percent recovery of intact cells. Each sample slice was divided into three equal layers (superficial, middle and deep) (Figure 4-1b) to examine recovery as a function of location. Statistical analysis was performed using a two-tailed Univariate analysis of variance and post hoc Bonferroni tests with $P < 0.05$ determined as significant confirmed by 95% confidence intervals using SPSS-10.07 (SPSS Inc, San Rafael, CA).

Scanning Electron Microscopy (SEM)

Samples cooled in 3*M* and 6*M* Me$_2$SO solutions underwent freeze substitution once removed from the liquid nitrogen. This involved manually removing the extramatrix ice from each dowel, which was then immersed in methanol (Sigma, St. Louis, MO) at -80°C. As ice was displaced, the methanol was exchanged at 1-2 day intervals to compensate for dilution. Once the ice was completely displaced (typically seven days), the dowels were immersed in 1% osmium tetroxide (Marivac Ltd, NS, Canada) in methanol at -60°C for two days. The dowels, while still in osmium tetroxide solution, were placed into a container with 100% methanol at -40°C suspended over dry ice. Over the next 24 hours, the dry ice was allowed to vaporize thus allowing the methanol, osmium tetroxide and dowels to warm to approximately -10°C. The sample was removed from the osmium tetroxide, placed into 100% methanol, and sectioned into 70μm slices as previously described. These slices were transferred into 100% ethanol and prepared for the scanning electron microscope by application of a sputter coat (Sputter Coater, Edwards, Model S15B) of gold. Scanning electron microscopy (Hitachi, S-2500) was performed (magnification = 3500 times, voltage used for capturing = 15KV) on representative sections of focusing on the matrix of the three layers and micrographs were taken (Figure 4-2).

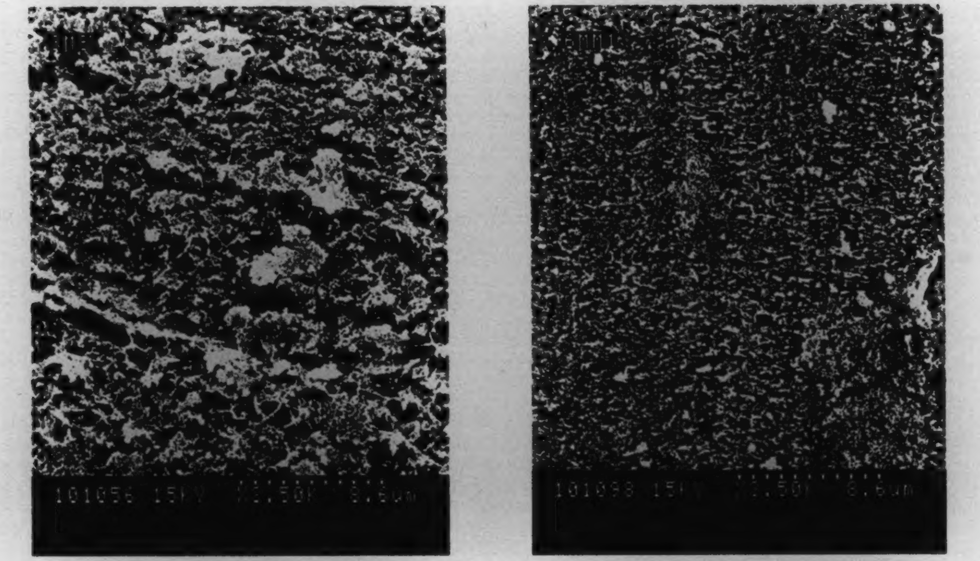

Figure 4-2A Figure 4-2B

Figure 4-2. Scanning electron micrographs (magnification = 3500 times, voltage used for capturing = 15KV) after freeze substitution of osteochondral dowels rapidly cooled in 3*M* Me_2SO solution (4-2A) and 6*M* Me_2SO solution (4-2B). The sample from 3*M* Me_2SO solution demonstrates a significant number of pores outlined (using Batch Imaging Processor, Peter Kelly, University of Calgary, Canada) representing the location and size of ice crystals within the cartilage matrix. The 6*M* Me_2SO solution sample in Figure 4-2B demonstrates a homogeneous appearance suggesting either minimal or no ice formation within the cartilage matrix.

4.3 Results

The fresh controls (n = 7) consistently demonstrated high intact cell recovery in all three layers (total = 79 ± 10%, superficial = 68 ± 6%, middle = 84 ± 8%, deep = 84 ± 8%). To examine the toxicity of Me_2SO exposure, toxicity controls for all concentrations were used. The cryoprotectant toxicity controls demonstrated increasing toxicity (decreased intact cell recovery) with increasing Me_2SO concentrations after 30 minutes of exposure at 4°C (Figure 4-3). There was a significant decrease in intact cell recovery between 1*M* and 3*M* Me_2SO solutions (77 ± 21%, 84 ± 21%, respectively) and the 5*M* Me_2SO solution (53 ± 28%) ($P < 0.001$) (Figure 4-3 – dotted line). There was another significant increase in toxicity between the 6*M* Me_2SO solution (59 ± 25%) and 7*M* Me_2SO solution (25 ± 17%) ($P < 0.001$). The toxic effects were consistent through all three layers in all five concentrations used (Figure 4-3 – solid lines) with the superficial zone experiencing significantly more toxicity than the middle and deep zones ($P < 0.001$).

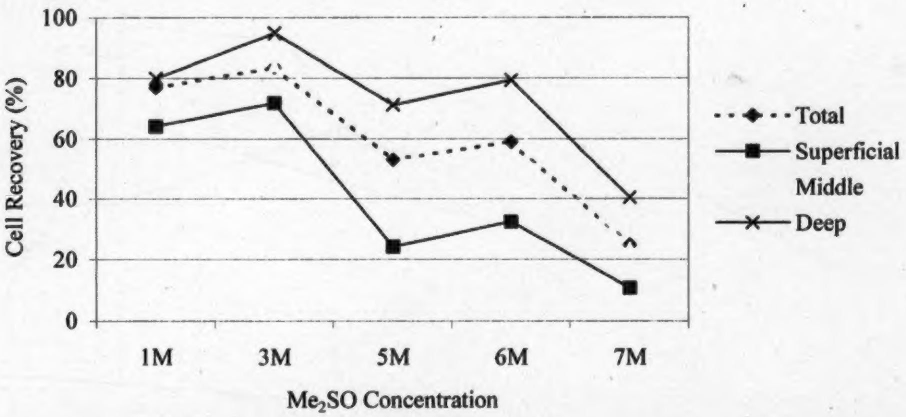

Figure 4-3. Intact chondrocyte recovery relative to fresh controls after 30 minutes of exposure to different concentrations of Me_2SO at 4°C. The cartilage matrix was divided into three layers (superficial, middle, and deep) and cell recovery was noted for each layer as well as the combined total cell recovery for that Me_2SO concentration (dotted line = Total). There is a significant increase in toxicity noted as the Me_2SO concentration increases from 3*M* to 5*M* and from 6*M* to 7*M*, consistent in all three layers.

The toxic effect of the Me_2SO was factored out by using toxicity controls to allow specific focus on the effect of the cooling rate/protocol used in this experiment. Essentially, the toxicity controls provided an indication of the number of cells remaining intact after exposure to the Me_2SO but just before proceeding through the cryopreservation protocol. The intact cell recovery from the 6*M* and 7*M* Me_2SO solutions after the cryopreservation protocol (60 ± 33%, 48 ± 40%, respectively) were significantly higher ($P < 0.001$) than the lower concentration Me_2SO solutions (1*M* = 6 ± 7%, 3*M* = 7 ± 12%, 5*M* = 1 ± 3%) (Figure 4-4 – dotted lines). Once again, this was consistent in all three layers (Figure 4-4 – solid line).

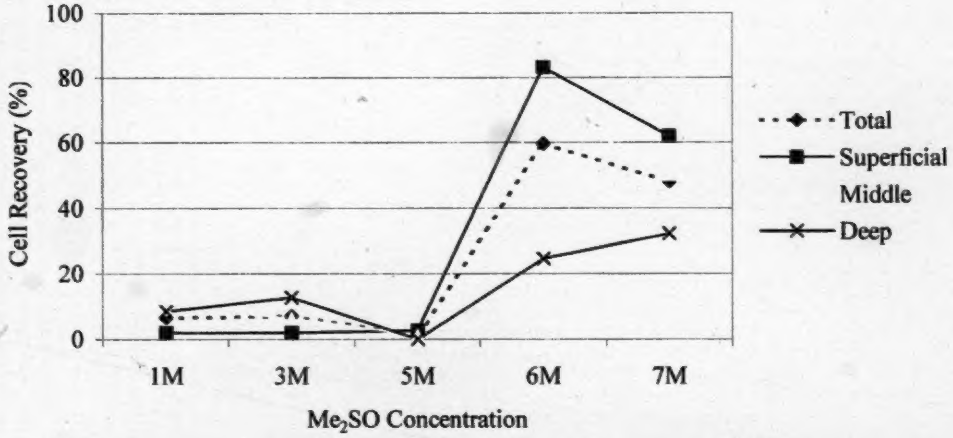

Figure 4-4. Intact chondrocyte recovery relative to toxicity controls (determined from cell recovery in Figure 4-3) after proceeding through the cryopreservation protocol. The thickness of the cartilage matrix was divided into 3 layers (superficial, middle, and deep) with the cell recovery documented for each layer. The total result for all three layers is also described by the dotted line (Total). This figure has factored out the damage that has already occurred due to Me_2SO toxicity therefore the values are not compared to fresh controls. Solutions that underwent vitrification (6*M* and 7*M*) demonstrated the highest intact cell recovery relative to their toxicity controls, consistent in all three layers.

The combined effects of cryoinjury and toxicity represented by cell recovery relative to fresh controls are exhibited in Figure 4-5. Cell recovery from 6*M* Me_2SO (42 ± 21%) was significantly increased ($P < 0.001$) compared with all other concentrations used (1*M* = 7 ± 7%, 3*M* = 8 ± 14%, 5*M* = 1 ± 1%, 7*M* = 14 ± 18%). This was consistent in all three layers and most marked in the middle layer of the 6*M* Me_2SO sample (56 ± 20%).

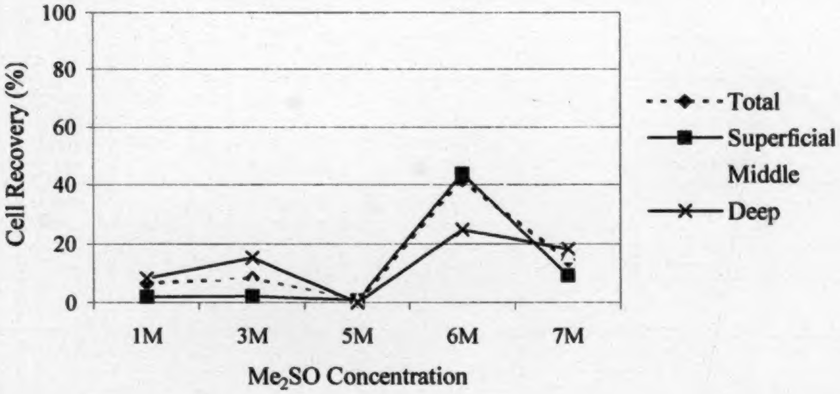

Figure 4-5. Intact chondrocyte recovery relative to fresh controls after cryopreservation in different concentrations of Me_2SO. There was a significant increase in cell recovery with 6*M* Me_2SO when compared to all the other Me_2SO concentrations used. This was consistent in all three layers and most notable in the middle layer of the 6*M* Me_2SO solution.

Figure 4-2 demonstrates the scanning electron micrographs of AC taken from the 3*M* and 6*M* Me_2SO samples. The open spaces within the matrix seen on SEM after freeze substitution are thought to represent matrix deformation due to ice crystal formation. Increased numbers and size of these proposed ice crystals are noted throughout the 3*M* sample which are noticeably absent from the 6*M* Me_2SO sample.

4.4 Discussion

The range of Me_2SO concentrations used in this study included concentrations similar to those of routine cryopreservation techniques (21, 26, 32) as well as concentrations sufficient to achieve vitrification (7). Lower concentrations have decreased cell toxicity but decrease the amount of ice formed at all temperatures. The highest concentrations have the highest toxicity but eliminate ice crystal formation by the process of vitrification (7).

This study demonstrated increased toxicity with increasing Me_2SO concentration exposure at 4°C for 30 minutes, especially at concentrations greater than 3*M* and then 6*M* (Figure 4-3). The toxic effect at lower concentrations (1*M* and 3*M*) after 30 minutes of exposure was small with approximately 75-85% cell recovery compared to fresh controls. As the cryoprotectant concentrations increased to 5*M*, there was a significant decrease in cell recovery down to 25% using 7*M* Me_2SO. This pattern of increasing toxicity was consistent in the superficial, middle, and deep layers. In addition, the superficial layer demonstrated significantly increased toxicity when compared to the middle and deeper layers. This was likely due to exposure to cryoprotectant for a longer period of time (and possibly to a higher concentration) compared to the deeper layers due to time-dependent diffusion through the matrix to reach the middle and deep layers.

Even though cartilage matrix is 65-80% water and is often thought to act as an aqueous solution, the results from this experiment demonstrated that the matrix has interactions and properties that make it distinct from a solution. Chondrocytes in isolation have been successfully cryopreserved (27, 32). Chondrocytes contained with very thin slices of intact AC have been successfully cryopreserved as shown by Jomha (10) in 70μm thick human AC after a 2-stage cryopreservation technique using 1*M* Me_2SO and Oegema *et. al.* (25) using 100μm thick pieces of rabbit articular tissue using a slow freezing technique with 2*M* Me_2SO. Unfortunately, increasing difficulties occur with increasing thickness of the cartilage has been demonstrated by Muldrew *et. al.* (23) on ovine AC, Ohlendorf *et. al.* (26) on calve AC, and Jomha (10) on human AC. The difficulties with cryoprotectant penetration and the matrix interactions that occur with the phase separation during ice formation are not amenable to current slow-cooling, ice-forming cryopreservation techniques commonly used.

Solutions that vitrified (6*M* and 7*M*) demonstrated increased cell recovery relative to toxicity controls compared to solutions that did not vitrify (1*M*, 3*M*, and 5*M*). In the 1*M* and 3*M* solutions, there was low cell recovery despite only mild cryoprotectant toxicity. Dowels immersed in 5*M* Me_2SO demonstrated moderate toxicity but there was significant additional loss of cell recovery during rapid cooling. One consistent observation with the 1*M*, 3*M*, and 5*M* Me_2SO solutions was ice crystal formation with rapid cooling. Conversely, the 6*M* and 7*M* solutions vitrified with rapid cooling as noted by direct observation of glass formation. Dowels contained in 6*M* and 7*M* solutions demonstrated 48-60% recovery overall with up to 70-83% recovery in the superficial and middle layers in the 6*M* solution (relative to toxicity controls) (Figure 4-4). It is likely that vitrification of the surrounding solution due to high cryoprotectant concentration and rapid cooling rate limited the amount and size of ice crystals within the matrix.

The micrographs supported the theory of decreased ice formation within the matrix with higher cryoprotectant concentrations. The micrograph of the sample from the 3*M* Me_2SO solution demonstrated multiple large pores throughout the matrix representing the location and size of the ice crystals that formed (Figure 4-2A). The sample from the 6*M* Me_2SO solution demonstrated a homogeneous appearance (Figure 4-2B). We cannot be sure that vitrification occurred throughout the matrix of the 6*M* sample (indeed, the deep layer probably did not vitrify noted by the lower cell recovery); if ice did form in the matrix from samples from the 6*M* Me_2SO solution, the crystals were smaller, and likely less damaging, than the larger ice crystals formed in the 3*M* Me_2SO samples.

In the 6*M* Me_2SO sample, the deep layer demonstrated lower cell recovery than the superficial and middle layers. Without complete cryoprotectant equilibration throughout the matrix, there would be a lower concentration of Me_2SO in the deep layer resulting in increased ice formation if vitrification did not occur. This is consistent with the lowest recovery in the 6*M* and 7*M* Me_2SO samples in the deep layer (Figure 4-4) and supports the theory that vitrification of the matrix is beneficial to intact cell recovery.

Minimizing cryoprotectant toxicity is essential. The 6*M* and 7*M* Me_2SO solutions vitrified and subsequently showed good cell recovery that would have likely been higher if the toxicity could be minimized. Unfortunately, concentrations greater than 3*M* Me_2SO demonstrated significant toxicity and, if cells could not tolerate exposure to the cryoprotectant (i.e. 7*M* Me_2SO), then survival through vitrification would be irrelevant (Figure 4-5). For example, using the 7*M* Me_2SO solution samples, approximately 50% of the cells that remained after 7*M* cryoprotectant exposure tolerated vitrification. Unfortunately, overall recovery was only 10% relative to fresh controls because there was only approximately 20% of the cells remaining after cryoprotectant exposure due to toxicity.

Conversely, low concentrations of cryoprotectant (1*M* and 3*M*) did not cause excessive toxicity but also did not provide protection against cryoinjury (cell recovery <10%). As the concentration increased to 5*M*, there was increased toxicity combined with a lack of protection from cryoinjury (cell recovery ≤1%). Samples from the 6*M* Me_2SO solution provided the highest cell recovery with respect to fresh controls (42%). It is probable that this concentration of Me_2SO was sufficient to induce vitrification with rapid cooling (at least in the surrounding solution and possibly in the superficial and middle layers) while, at the same time, not being too toxic to kill all the cells. Even though 6*M* Me_2SO had the highest cell recovery, there was still a suboptimal balance between protection of vitrification with the risk of toxicity due to the higher Me_2SO concentration necessary. This requires further investigation.

Cells in different layers of the cartilage matrix experienced different cryopreservation conditions. There was no difference in cell recovery between the three layers (superficial, middle and deep – Figure 4-3) in the fresh controls. Yet, intact cell recovery was consistently highest in the superficial layer and lowest in the deep layer with all Me_2SO concentrations used, and cell recovery was more marked with the higher concentrations (Figure 4-3). This suggests that Me_2SO had difficulty penetrating the full thickness of the cartilage matrix resulting in less time of exposure and exposure to a lower cryoprotectant concentration in the deep layer. This contradicts Muldrew *et. al.* (21) who performed a study using intact 10mm diameter ovine OCDs and a 2-stage cryopreservation technique. Using similar staining methods, it was concluded that the Me_2SO penetrated the cartilage completely after 30 minutes noted by recovery of intact chondrocytes in the superficial and deep layers. It was thought that chondrocytes in the middle layer contained cellular or environmental differences that made them more sensitive to freeze injury. The current study does not agree with Muldrew *et. al.*'s conclusion because the intact cell recovery in the middle layer exceeds that of the deep layer in this experiment. The cells in all three layers in this experiment appear to respond in a similar manner, which is supported by a recent paper by Muldrew *et. al.* (23). This article evaluated cells of all three layers that were closely associated with a cut edge of cartilage and clearly demonstrated that cells of all three layers reacted similarly to freeze injury if closely associated with the edge of the cartilage matrix.

If penetration of the cartilage matrix by the Me_2SO is inhibited, the deeper layers would be more protected from cryoprotectant toxicity but less likely to vitrify. If approximately 6*M* concentration of Me_2SO is required for vitrification and the relative concentration of Me_2SO in the deep layer is lower due to incomplete penetration, then the deep layer may not vitrify and not afford the protection of vitrification to the cells located there. This is consistent with the lower recovery noted in the deep layers of 6*M* and 7*M* solutions (Figure 4-4).

Incomplete Me_2SO penetration can be due to a number of reasons. Exposure for 30 minutes was selected due to information on the penetration of Me_2SO in pig AC as shown by Muldrew (24). Based on the molecular weight of Me_2SO, it should be able to penetrate 3-4mm thick AC very quickly but this does not appear to occur. It could be possible that the negatively charged Me_2SO is repelled by the similarly charged proteoglycans in the matrix. This is unlikely, as there seems to be good penetration in the superficial and middle layers, which contain significant amounts of proteoglycans. It is more likely that the physiologic constraints of the densely packed deeper layers with higher osmolarity and solute concentrations (9) interferes with the penetration of the Me_2SO.

There are physiological and mechanical methods that can be used to "open up" the matrix and make it more amenable to Me_2SO penetration. Physiologically, decreasing the osmolarity of the solution surrounding the cartilage will hydrate the matrix, thereby increasing the distance between the proteoglycan and collagen elements of the matrix and decreasing the force of the negative charges from the proteoglycans. This will also effectively dilute the solutes within the matrix and these changes may allow for more complete Me_2SO penetration. Mechanically, drilling a hole in the bone base would provide exposure of the deep surface of the AC to Me_2SO and release the high osmotic pressure and electrolyte concentration within the deep matrix (9). These methods may provide a more equitable distribution of the Me_2SO throughout the matrix possibly providing increased protection to the cells in the deep layer.

Minimizing the toxic effects of cryoprotectants can be accomplished in two ways. Decreasing the time of exposure is difficult with AC because time is required for adequate penetration of the cryoprotectant into the intact matrix (24). Combining lower concentrations of different cryoprotectants can provide the high overall solute concentration required for vitrification (7). Different cryoprotectant solutions induce toxicity by different mechanisms, therefore combining different cryoprotectants at lower concentrations may minimize or eliminate toxic effects. This technique has been successful in other tissues (2, 30) and requires investigation with respect to AC.

Devitrification can be the cause of cell damage during the preservation process. Devitrification occurred with both the 6*M* and 7*M* Me_2SO concentrations with the warming rate used in this study. Sixty percent of the cells that tolerated the initial exposure to 6*M* Me_2SO survived the vitrification process suggesting that factors such as devitrification are important. It will be essential to investigate the effects of devitrification to maximize intact cell recovery by increasing the warming rate to eliminate devitrification.

Heat transfer can cause difficulty in vitrifying larger tissues due to the inability of obtaining a satisfactory cooling rate in all areas of the tissue. Fortunately, AC is only 3-4mm thick and is attached to bone, which is a good heat conductor. Therefore it is thought that heat transfer is likely to play only a minor role in cell damage during the vitrification of AC. Nevertheless, the lower recovery rate of cells in the deepest layer in this experiment suggests heat transfer effects require investigation to maximize the intact cell recovery during vitrification.

The recovery of 42% of cells compared to fresh control, (60% compared to 6*M* Me_2SO control) is not optimal but this study provided important information about the possibilities of preserving intact AC. It is evident that vitrification is a potential method for preserving intact AC. In this study, 6*M* Me_2SO provided the highest cell recovery. Me_2SO toxicity caused the majority of cell damage during the experimental procedure with vitrification/devitrification and heat transfer accounting for secondary detrimental effects. Further research is required to investigate combinations of lower concentrations of cryoprotectants, as well as alteration of the physiological and mechanical properties of the matrix to enhance chondrocyte recovery.

4.5 Acknowledgements

The authors thank Dr. Marc Moreau for review of the paper and Lauren Beaupre for statistical analysis. The research was supported by the Edmonton Civic Employees Charitable Assistance Fund, the Edmonton Orthopaedic Research Society and the University of Alberta Hospital Foundation.

4.6 References

1. Acker, J.P. and L.E. McGann. Membrane damage occurs during the formation of intracellular ice. *Cryo Letters* 22, 4: 241-254, 2001.
2. Armitage, W.J. and S.J. Rich. Vitrification of organized tissues. *Cryobiology* 27, 5: 483-491, 1990.
3. Aubin, P.P., H.K. Cheah, A.M. Davis, and A.E. Gross. Long-term followup of fresh femoral osteochondral allografts for posttraumatic knee defects. *Clin Orthop* 391 Suppl: S318-327, 2001.
4. Bugbee, W.D. and F.R. Convery. Osteochondral allograft transplantation. *Clin Sports Med* 18, 1: 67-75, 1999.
5. Chu, C.R., F.R. Convery, W.H. Akeson, M. Meyers, and D. Amiel. Articular cartilage transplantation. Clinical results in the knee. *Clin Orthop* 360: 159-168, 1999.
6. Elliot, K. and J. Whelan, eds. CIBA Foundation Symposium. Vol. 52. Elsevier: Amsterdam, 1977.
7. Fahy, G.M. Vitrification: a new approach to organ cryopreservation. *Prog Clin Biol Res* 224, 305-335, 1986.
8. Fahy, G.M., J. Saur, and R.J. Williams. Physical problems with the vitrification of large biological systems. *Cryobiology* 27, 5: 492-510, 1990.
9. Hall, A.C., E.R. Horwitz, and R.J. Wilkins. The cellular physiology of articular cartilage. *Exp Physiol* 81, 3: 535-545, 1996.
10. Jomha, N. *Cryopreservation of human articular cartilage*, in *Experimental Surgery, Masters Thesis*. University of Alberta: Edmonton, 1996.
11. Jutte, N.H., P. Heyse, H.G. Jansen, G.J. Bruining, and G.H. Zeilmaker. Vitrification of human islets of Langerhans. *Cryobiology* 24, 5: 403-411, 1987.
12. Kawabe, N. and M. Yoshinao. Cryopreservation of cartilage. *Int Orthop* 14, 3: 231-235, 1990.
13. Kurata, H., K. Takakuwa, and K. Tanaka. Vitrification of hematopoietic progenitor cells obtained from human cord blood. *Bone Marrow Transplant* 14, 2: 261-263, 1994.

14. Leibo, S. Preservation of mammalian cells and embryos by freezing. *Cryoimmunology* 62, 311-34, 1977.

15. Lovelock, J.F. The mechanism of the protective action of glycerol against haemolysis by freezing and thawing. *Biochimica et Biophysica Acta* 11, 28-36, 1953.

16. Malinin, T.I., J.L. Wagner, J.C. Pita, and H. Lo. Hypothermic storage and cryopreservation of cartilage. An experimental study. *Clin Orthop* 197: 15-26, 1985.

17. McGann, L.E. and J. Farrant. Survival of tissue culture cells frozen by a two-step procedure to -196 degrees C. I. Holding temperature and time. *Cryobiology* 13, 3: 261-268, 1976.

18. McGann, L.E. and J. Farrant. Survival of tissue culture cells frozen by a two-step procedure to -196 degrees C. II. Warming rate and concentration of dimethyl sulphoxide. *Cryobiology* 13, 3: 269-273, 1976.

19. Meryman, H.T. Freezing injury and its prevention in living cells. *Annu Rev Biophys Bioeng* 3, 0: 341-363, 1974.

20. Meyers, M.H., W. Akeson, and F.R. Convery. Resurfacing of the knee with fresh osteochondral allograft. *J Bone Joint Surg [Am]* 71, 5: 704-713, 1989.

21. Muldrew, K., M. Hurtig, K. Novak, N. Schachar, and L.E. McGann. Localization of freezing injury in articular cartilage. *Cryobiology* 31, 1: 31-38, 1994.

22. Muldrew, K. and L.E. McGann. Mechanisms of intracellular ice formation. *Biophys J* 57, 3: 525-32, 1990.

23. Muldrew, K., K. Novak, H. Yang, R. Zernicke, N.S. Schachar, and L.E. McGann. Cryobiology of articular cartilage: ice morphology and recovery of chondrocytes. *Cryobiology* 40, 2: 102-109, 2000.

24. Muldrew, K., B. Sykes, S. N., and L.E. McGann. Permeation kinetics of dimethol sulfoxide in articular cartilage. *Cryo-letters* 17, 311-340, 1996.

25. Oegema, T.R., Jr., L.B. Deloria, M.M. Fedewa, J.C. Bischof, and J.L. Lewis. A simple cryopreservation method for the maintenance of cell viability and mechanical integrity of a cultured cartilage analog. *Cryobiology* 40, 4: 370-375, 2000.

26. Ohlendorf, C., W.W. Tomford, and H.J. Mankin. Chondrocyte survival in cryopreserved osteochondral articular cartilage. *J Orthop Res* 14, 3: 413-416, 1996.

27. Schachar, N.S. and L.E. McGann. Investigations of low-temperature storage of articular cartilage for transplantation. *Clin Orthop* 208: 146-150, 1986.

28. Schachar, N.S., K. Novak, M. Hurtig, K. Muldrew, R. McPherson, G. Wohl, R.F. Zernicke, and L.E. McGann. Transplantation of cryopreserved osteochondral Dowel allografts for repair of focal articular defects in an ovine model. *J Orthop Res* 17, 6: 909-919, 1999.

29. Smith, A.U. Survival of frozen chondrocytes isolated from cartilage of adult mammals. *Nature* 205, 782-784, 1965.

30. Song, Y.C., P.O. Hagen, F.G. Lightfoot, M.J. Taylor, A.C. Smith, and K.G. Brockbank. In vivo evaluation of the effects of a new ice-free cryopreservation process on autologous vascular grafts. *J Invest Surg* 13, 5: 279-288, 2000.

31. Tomford, W.W. Transmission of disease through transplantation of musculoskeletal allografts. *J Bone Joint Surg Am* 77, 11: 1742-1754, 1995.

32. Tomford, W.W., G.R. Fredericks, and H.J. Mankin. Studies on cryopreservation of articular cartilage chondrocytes. *J Bone Joint Surg [Am]* 66, 2: 253-259, 1984.

Chapter Five

The Effect of Changing Tonicity on the Cryopreservation of Porcine Articular Cartilage in High Concentrations Of Cryoprotectant

Jomha NM, Anoop PC, Bagnall K, McGann LE

A version of this chapter has been submitted to Cryobiology.

5.1 Introduction

Large, untreated, articular cartilage (AC) defects degenerate into osteoarthritis (3, 62), the second leading cause of disability in the United States (25). The treatment with the longest satisfactory outcomes is clearly osteochondral allografts (both frozen (12, 18) and fresh (6, 10, 14, 15, 23, 33, 43)) but the availability of repair tissue limits its use. The creation of an osteochondral tissue bank of cryopreserved tissues could enhance the long-term results by maintaining viable cells in a preserved matrix, allowing accurate size/contour matching, permitting thorough infectious disease testing and enabling the surgical procedure to be performed at a time when both the surgical team and the patient are well prepared.

Cryopreservation of cells in solution (2, 32, 35, 39, 51, 54, 56, 61), including chondrocytes (2, 54, 56, 61) has been successful but extension to more complex tissues, such as intact AC, has proven difficult. Investigation of the cryopreservation of intact AC initially produced dismal cell recovery (<10%) (11, 26, 49, 60). However, more recent attempts including the 2-stage cryopreservation technique (36, 37, 45) and the stepped cryopreservation technique (47) have shown much promise. Both of these techniques start with 1*M* cryoprotectant concentration and use a slow, controlled cooling rate. Despite relatively good intact cell recovery (approximately 60% (45, 47)), transplantation studies of AC cryopreserved with these methods have demonstrated significant cartilage degeneration within 1 year in a sheep model (47, 55). This indicates that either insufficient numbers of cells remain to maintain the matrix after transplantation or that the matrix is irreversibly damaged by the ice formation and deteriorates once transplanted. Either way, improvements in cryopreservation techniques are required for continued progress.

The use of high concentration of cryoprotectant may be an alternative strategy to successfully cryopreserving intact AC. Using initial high concentration of cryoprotectant will decrease the amount of ice formed at all temperatures. If the cooling rate is sufficiently rapid, vitrification (formation of an amorphous glass) may occur and completely eliminate ice formation and the problems inherent with phase separation (membrane damage (1, 31, 32, 36, 37), osmotic fluxes with excessive dehydration and shrinkage (24, 41, 42, 46), generation of electrical and chemical gradients (16, 58, 63), destruction of biologic integrity (19), and physical damage from the ice itself (20, 21)). Indeed, vitrification of intact AC, if possible, may be the ultimate solution to cryopreserving AC as noted by the success in individual cells (28, 30) and some small tissues (22, 52, 57).

Vitrification of the entire intact AC matrix may not occur if cryoprotectant penetration into the matrix is incomplete. A recent article investigating high dimethyl sulfoxide (Me_2SO) concentration in combination with a rapid cooling rate for cryopreserving porcine AC (27) identified cryoprotection permeation as a limiting factor. The difficulty in achieving full penetration of Me_2SO in porcine AC has been also demonstrated by Muldrew *et. al.* (48) although this has been disputed (50). With incomplete penetration of Me_2SO, ice may form in portions of the matrix while the remainder vitrifies. However, high concentrations of cryoprotectant without complete vitrification may still provide adequate protection to maintain cell viability and to minimize matrix perturbation of the matrix by ice formation after rapid cooling. This study investigates facilitation of cryoprotectant penetration into the matrix using hypotonic solutions. It was hypothesized that matrix hydration by equilibration in hypotonic solution would result in an increase in cell recovery and expose a depth-dependent relationship for cell recovery based on cryoprotectant concentration and solution tonicity.

5.2 Materials and Methods

Tissues

Intact stifle joints were harvested from 53 sexually mature pigs sacrificed for meat consumption. In this study, pigs were selected because the cartilage thickness in the stifle joint is the closest to the exceptionally thick cartilage in human knee joints. The joints were immersed in 1X Dulbecco's phosphate buffered saline solution (pH = 7.0) (PBS, Gibco, BRL, MD) and maintained at 4°C until 10mm diameter osteochondral dowels (OCDs) were harvested using a hand-held coring device (within 12 hours of death of the animal). The OCDs were harvested from the central weight-bearing portion of the medial femoral condyle and consisted of the full thickness of AC (3-4mm) perched on a 5-10mm bone base. Three OCDs were harvested from each joint.

Control groups were maintained for each Me_2SO (Sigma, St. Louis, MO) concentration (Me_2SO toxicity control groups - 1*M*, 5*M*, and 6*M* (wt/vol)) and for each PBS solution (PBS toxicity control groups - 1X (300mOsm), 0.5X (150mOsm), 0.25X (75mOsm)). The Me_2SO control samples were immersed in 1*M*, 5*M*, or 6*M* Me_2SO (50ml) at 4°C for 30 minutes. The PBS control samples were immersed in 1X, 0.5X, or 0.25X PBS solution maintained at 4°C without cryoprotectant. All control samples underwent sectioning, staining and cell counting (described below) without any experimental protocol.

The 1X PBS (300mOsm) solution was used as the primary reference for all recoveries related to "fresh controls" (in both the control and experimental groups) to provide a single reference value for all solutions. The other toxicity control samples were used to determine any detrimental effect from the cryoprotectant agent or hypotonic solutions themselves.

There were nine experimental groups determined by combinations of the three cryoprotectant concentrations and the three PBS solutions as shown in Table 5-1. There were either five or six samples in all groups.

Cryopreservation Protocol

The experimental OCDs were randomly assigned to the groups described and immersed in one step into one of nine solutions (50 ml) (Table 5-1) for 30 minutes at 4°C. Each OCD was transferred into 5ml of the same solution at 4°C in a polypropylene test-tube (17x100mm culture tube, VWR Can Lab, Ontario, Ca). The experimental samples were cooled in an ice-water bath for 10 minutes, plunged directly into liquid nitrogen (LN) and held there for at least one hour. The cooling rate depended on the concentration of Me_2SO with 1*M* Me_2SO = 180°C/min and 6*M* Me_2SO = 65°C/min. All the experimental samples were warmed in a 37°C water bath (85-100°C/min warming rate) until the ice/glass just began to reform to a liquid state (~30 seconds). Once removed from their test-tubes, the experimental samples were placed in 1X PBS (50ml) and taken through sample preparation (described below) for fluorescence microscopy (~30 minutes).

Cell Assessment

Samples from all groups (control and experimental) were sectioned using a Vibratome® (TPI, St. Louis, Missouri) cutting vertically across the dowel from the articular surface towards the cartilage-bone junction. Slices sectioned to a thickness of 70μm were taken from the widest portion of the dowels (Figure 5-1a). Each slice was stained using the membrane integrity dyes ethidium bromide (EB; Sigma, St. Louis, MO) and Syto 13 (Molecular Probes, Eugene, OR) (0.1% EB with 0.45% Syto mixed in PBS (vol/vol)). Cells with intact membranes fluoresced green due to the absorption of the Syto stain with the exclusion of the EB stain. Cells with disrupted membranes could not exclude the EB stain and therefore fluoresced red. The 70μm slices were viewed under a Leitz Dialux 22 fluorescence (440-480nm) microscope (Leitz, Germany) at 125X magnification (10X objective and 12.5X eyepiece). The images were recorded by digital camera (Pixera DiRactor, Pixera Corporation, Los Gatos, CA) and stored on computer for later analysis. Membrane integrity dyes were used because cell membranes have been shown to be a primary target of injury during the cryopreservation process (1) and the most reliable predictor of long-term transplantation results (55).

A customized computer counting program was designed based on the principles of colorimetry (44). This program was used to calculate the percentage of green pixels (Syto 13 stain) compared to red pixels (EB stain) using minimum thresholds for green and red pixel intensity after elimination of the background in a digitized image. Percent recovery was determined by:

$$\frac{\text{\# of green pixels}}{\text{\# of green pixels + \# of red pixels}} \times 100$$

Each sample slice was divided into three approximately equal layers (superficial, middle and deep) (Figure 5-1b) to examine recovery as a function of location. Statistical analysis was performed using a two-tailed, one-way and three-way analysis of variance and post hoc Bonferroni tests with $P<0.05$ determined as significant using SPSS-10.07 (SPSS Inc, San Rafael, CA).

5.3 Results

The fresh controls from the 1X PBS solution demonstrated 77 ± 2% (overall mean ± S.E.) intact cell recovery (Figure 5-3). This solution was used as the reference for all other control and experimental solutions because it was the closest to physiologic solution and most closely resembled the clinical scenario. Each region of the experimental samples was compared to the same region of the control samples. Figure 5-2 documents the toxicity due to Me_2SO concentration exposure. Of note is the significant increase in toxicity in the 5*M* and 6*M* solutions compared to the 1*M* solution. The toxicity was most severe in the superficial layer of all Me_2SO concentrations. Figure 5-3 documents the toxicity due to exposure to PBS of different tonicities. Again, the most significant loss of cells was in the superficial layer.

There was a significant difference in cell recovery when the three solution concentrations were compared by ANOVA ($P = 0.006$). Post hoc Bonferroni analysis demonstrated a significant increase in recovery from the 6*M* Me_2SO solution compared to the 5*M* Me_2SO solution ($P = 0.017$). One-way ANOVA on the combined effects of tonicity and concentration that compared the overall results from the 6 solution combinations (excluding the 1*M* solutions due to their extremely low cell recovery) described maximal recovery noted in the 6*M*/1X solution (39 ± 6%; $P = 0.012$ compared to 5*M*/0.25X solution, $P < 0.001$ compared to 6*M*/0.5X, 6*M*/0.25X, 5*M*/1X, and 5*M*/0.25X solution samples) (Figure 5-4).

Three-way ANOVA demonstrated that depth within the matrix ($P < 0.001$) and the interaction of depth with concentration ($P = 0.026$) were significant variables in cell recovery as demonstrated in Figures 5-4 and 5-5. In both concentrations (5*M* and 6*M* Me_2SO) the middle layer consistently had the highest recovery of cells. Figure 5-4 shows that cell recovery in the 6*M* Me_2SO solution was the highest in the middle layer (56 ± 8% in the 6*M*/1X solution) in all three solution tonicities followed by the superficial layer and then the deep layer. Figure 5-5 demonstrates that cell recovery from the samples in the 5*M* Me_2SO solution was also highest in the middle layer. Interestingly, the deep layer was second in cell recovery compared to the middle layer while the superficial layer had the lowest recovery of cells.

There was a significant interaction between the concentration of $\mathrm{Me_2SO}$ used and the tonicity of the solution ($P < 0.001$). In the samples from the 6*M* $\mathrm{Me_2SO}$ solution, cell recovery decreased with decreased tonicity (1X > 0.5X and 0.25X; $P < 0.001$) (Figure 5-4). In the 5*M* $\mathrm{Me_2SO}$ solution, the reverse occurred with increased cell recovery accompanying decreased tonicity (0.25X and 0.5X > 1X; $P < 0.001$) (Figure 5-5).

Figures 5-6 and 5-7 demonstrate the recovery of intact cells relative to their own toxicity control. This was determined by calculating the recovery of intact cells after cryopreservation by recovery of intact cells after initial exposure to the cryoprotectant solution (just before rapid cooling). These Figures illustrate the recovery of cells after cryopreservation and, therefore, provides an indication of the cryopreservation specific injury. The recovery relative to toxicity controls in the 6*M*/1X solution (Figure 5-6) was 75% with maximal recovery in the superficial and middle zones. The next best recovery relative to toxicity controls was from the hypotonic 5*M* solutions (0.5X and 0.25X) (Figure 5-7).

The recovery of intact cells from the 1*M* $\mathrm{Me_2SO}$ solutions using the rapid cooling technique (1*M*/1X = 6%, 1*M*/0.5X = 1%, 1*M*/0.25X = 1%) was uniformly low in all layers. These values were unacceptably low and will not be considered further.

	1X (300mOsm)	0.5X (150mOsm)	0.25X (75mOsm)
6*M* Me$_2$SO	6*M* / 1X	6*M* / 0.5X	6*M* / 0.25X
5*M* Me$_2$SO	5*M* / 1X	5*M* / 0.5X	5*M* / 0.25X
1*M* Me$_2$SO	1*M* / 1X	1*M* / 0.5X	1*M* / 0.25X

Table 5-1. Combinations of Me$_2$SO concentrations and PBS solutions used to create the nine experimental solutions

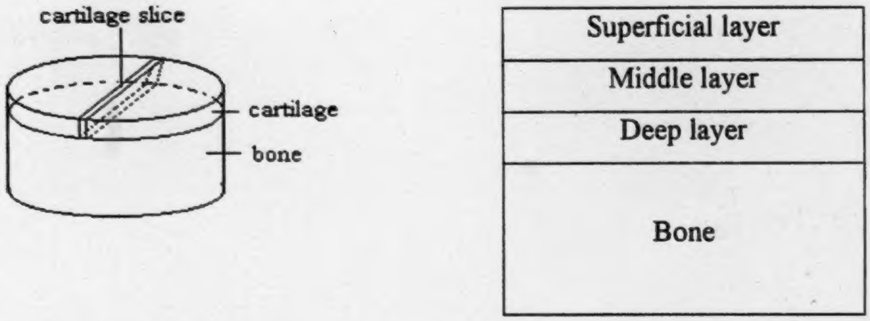

(a) (b)

Figure 5-1. Schematic diagrams of an osteochondral dowel and 70μm section

(a) Osteochondral dowel with a 70μm slice removed from the widest portion.

(b) Schematic diagram detailing the division of the AC as it sits on the bone base. The cartilage was divided into three approximately equal layers for determination of cell recovery as a function of location within the slice.

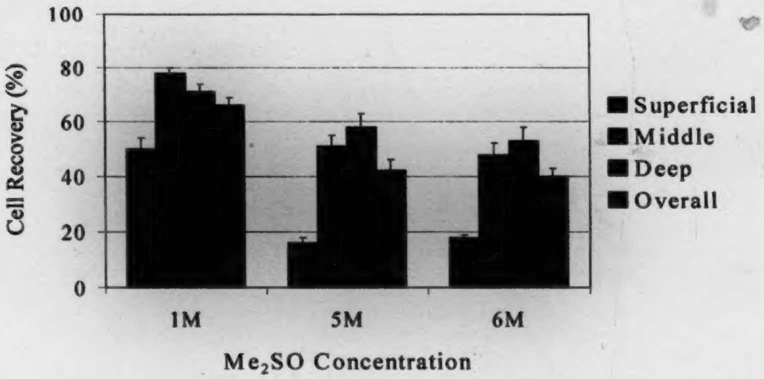

Figure 5-2. The percent recovery of intact cells from toxicity controls (relative to fresh controls) after exposure to Me_2SO at 4°C, illustrating the recovery from the different Me_2SO concentrations as a function of depth within the matrix (mean ± S.E.).

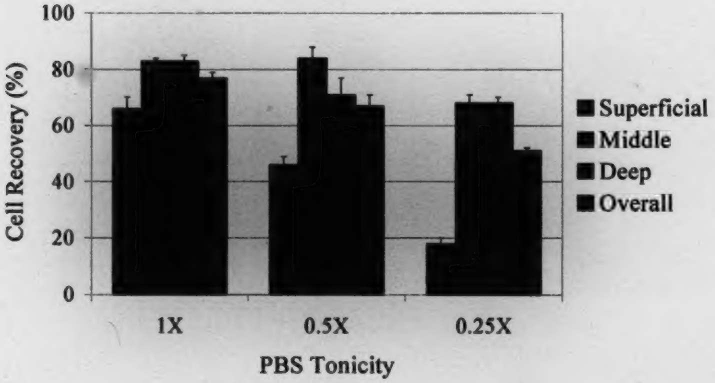

Figure 5-3. The percent recovery of intact cells from toxicity controls (relative to fresh controls) after exposure to PBS at 4°C, illustrating the recovery from the different solution tonicities as a function of depth within the matrix (mean ± S.E.).

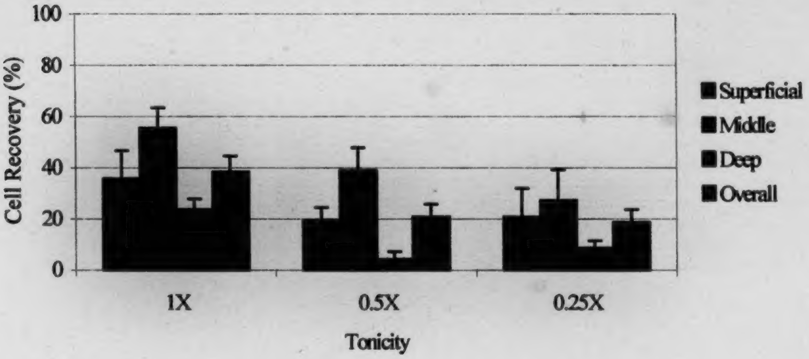

Figure 5-4. The percent recovery of intact cells relative to fresh controls from the three 6*M* Me_2SO solutions (mean ± S.E.). Each layer is represented, as is the final overall recovery of intact cells.

Figure 5-5. The percent recovery of intact cells relative to fresh controls from the three 5*M* Me_2SO solutions (mean ± S.E.). Each layer is represented, as is the final overall recovery of intact cells.

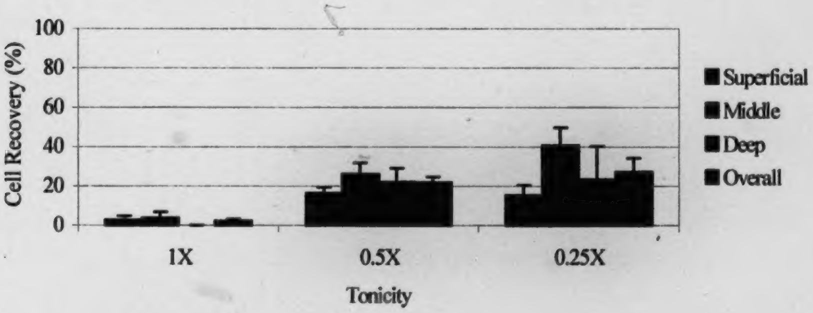

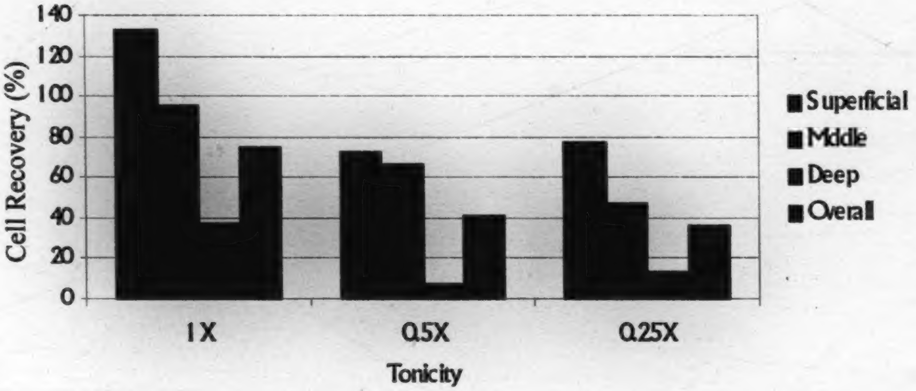

Figure 5-6. The percent recovery of intact cells compared to toxicity controls from the three 6*M* Me_2SO solutions to illustrate cryopreservation specific injury.

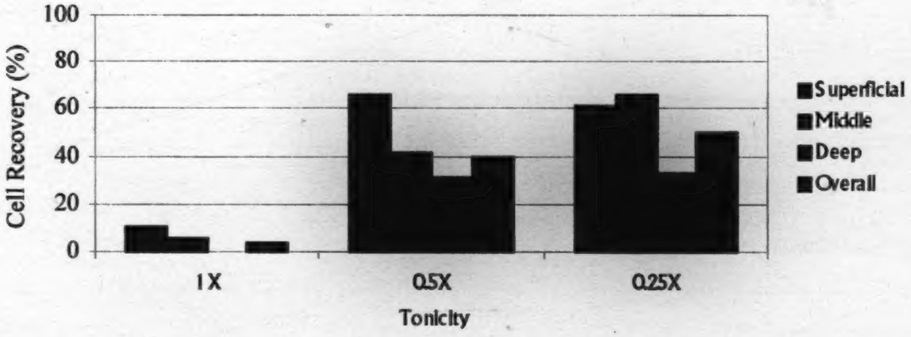

Figure 5-7. The percent recovery of intact cells compared to toxicity controls from the three 5*M* Me_2SO solutions to illustrate cryopreservation specific injury.

5.4 Discussion

The results of this study support the hypothesis of a depth-dependent relationship for cell recovery depending on the concentration and tonicity of the cryopreservation solution. The 5*M* and 6*M* concentrations of Me_2SO were selected due to the results of a previous article that demonstrated a significant difference in cell recovery between these two concentrations, and the observation that the 5*M* solution formed ice outside the tissue while the 6*M* solution vitrified (27). The 1*M* solution was selected because it is commonly used clinically in rapid, uncontrolled cooling of osteochondral tissues.

There was a significant difference in cell recovery between the 5*M* and 6*M* solutions ($P = 0.017$) with the highest overall recovery of intact cells was from the 6*M*/1X solution (39% overall compared to the fresh controls; $P = 0.012$) with maximal recovery located in the middle layer (56% compared to the fresh controls) (Figure 5-4). These results indicated that use of high concentrations of cryoprotectants in intact AC with a rapid cooling protocol provided some protection to the chondrocytes *in situ* and that changing the solution tonicity altered the cell recovery.

The primary difficulty with using high concentrations of Me_2SO is toxicity. The 5*M* and 6*M* Me_2SO solutions demonstrated markedly increased toxicity when compared to the 1*M* Me_2SO solution (Figure 5-2). The toxic effects were most evident in the superficial layer with cell recovery falling to 18%. This initial loss of cells due to toxicity limited the opportunity to recover high numbers of chondrocytes after the cryopreservation procedure. If Me_2SO toxicity is taken into account and the results in Figure 5-2 are used as cryoprotectant toxicity controls (documented the numbers of cells intact after exposure to the cryoprotectant but before any cooling protocol is initiated), the cryopreservation specific toxicity was 25% from samples in the 6*M*/1X solution (75% cell recovery relative to the toxicity controls; Figures 5-6 and 5-7). This indicated that the majority of cells that survived the exposure to the cryoprotectant were able to remain intact after the rapid cooling and warming protocol.

This high cell recovery from cells that survived cryoprotectant exposure may be due to protection by high concentration of cryoprotectant or by vitrification. Vitrification of the 6*M* Me_2SO solution that surrounded the samples during the cooling process was noted by direct observation (17, 30, 64) and may have extended into the superficial and middle layers resulting in high recovery of intact cells in these layers (approximately 100% cell recovery compared to toxicity controls – the exceptionally high recovery in the 6*M*/1X superficial layer was due to the large variation that occurred during testing combined with a very low starting recovery from the toxicity control (18%)). In contrast, the best results from the 5*M* solutions, despite similar toxicity after initial exposure to the Me_2SO (Figure 5-2), was only approximately 50% (5*M*/0.25X) relative to toxicity controls (Figure 5-7). It is important to note that ice formation occurred in the 5*M* Me_2SO solution that surrounded the samples and this solution did not vitrify, as did the 6*M* Me_2SO solution, suggesting that vitrification in the sample from the 6*M* solution may have provided the beneficial effect. Enhanced cryoprotectant penetration in the hypotonic 5*M* Me_2SO solutions (0.5X and 0.25X) may have accounted for the increased cell recovery. It is important to note that even low concentrations of cryoprotectants will increase to levels sufficient to effect vitrification in the residual liquid as ice forms (29) due to exclusion of cryoprotectant from the crystalline ice structure. The 5*M* Me_2SO would enhance this likelihood, because of the presence of initial, high osmolality. However, the concentration of Me_2SO required to provide cell protection induced significant toxicity prior to effectively protecting the cells during rapid cooling.

Depth was another significant variable with respect to cell recovery ($P < 0.001$). The middle layer consistently had the highest number of intact cells after cryopreservation in both the 5*M* and 6*M* Me_2SO solutions, in direct contrast to the minimal middle layer cell recovery in the presence of lower (1*M*) concentration of cryoprotectant in another study (45). Although the cells in both the superficial and middle layers had excellent cell recovery compared to toxicity controls, the middle layer had higher cell recovery compared to fresh controls. This indicated that the cells in the superficial layer were damaged by Me_2SO toxicity or by osmotic stresses on addition/removal of the cryoprotectant.

In addition, there was an interaction between the concentration of Me_2SO used and depth within the slice ($P = 0.026$). The samples in the 6*M* Me_2SO solutions had increased numbers of intact cells in the superficial layer compared to the deep layer and this was reversed in the samples from the 5*M* Me_2SO solution (Figures 5-4 and 5-5). The low recovery of cells from the deep layer of the 6*M* Me_2SO solutions, relative to toxicity controls, suggested that Me_2SO diffusion into the cartilage was the limiting factor. This was supported by the suspected increased Me_2SO penetration noted in the hypotonic 5*M* Me_2SO solutions resulting in increased recovery of cells (Figure 5-5).

Finally, there was a significant interaction between concentration and tonicity ($P < 0.001$). Samples cooled in the presence of 6*M* Me_2SO solutions demonstrated decreased intact cell recovery with decreased solution tonicity (Figure 5-4). Conversely, the samples in the 5*M* Me_2SO solutions demonstrated increased intact cell recovery with decreased solution tonicity (Figure 5-5). In the 6*M* Me_2SO solution, toxicity appeared to be the primary cause of cell loss and therefore, increased penetration due to lower solution tonicity would account for the lower cell recovery. By contrast, lowering the tonicity of the solution using 5*M* Me_2SO resulting in increased cell recovery. The samples from the 5*M*/1X solution had very low recovery in all layers indicating that the cryoprotectant concentration within the matrix was insufficient to provide protection to the cells. As the solution tonicity decreased, the cell recovery increased and this was more marked in the superficial and middle layers (40-56% cell recovery compared to toxicity controls) compared to the deep layers (28-30% cell recovery compared to toxicity controls). These results are consistent with the theory that lowering the solution tonicity increased the penetration of Me_2SO into the matrix resulting in higher Me_2SO concentrations and increased cell protection. This data supported the hypothesis that lower tonicity solutions increased cryoprotectant penetration into intact AC.

The recovery of intact cells from the 1*M* Me_2SO concentration in all PBS solutions was extremely low (<6%), consistent with other studies using uncontrolled cooling with low concentrations of cryoprotectancts (11, 26, 49). The minor toxicity of the low concentration

Me_2SO combined with the increasing toxicity of the hypotonic PBS solutions and the inability to vitrify prior to excessive ice formation likely resulted in the severe cell loss.

The problems with using high concentrations of cryoprotectants with intact AC in this study included Me_2SO toxicity, osmotic fluxes, and temperature- and time-dependent penetration of Me_2SO. The differing results in the various layers provided some insight into potential mechanisms of cell death during the rapid cooling protocol. Cryoprotectant toxicity was noted with the higher Me_2SO concentrations and was most prominent in the superficial layers. Toxicity and/or osmotic stresses significantly decreased the number of intact chondrocytes that were present even prior to initiation of the cryopreservation protocol thus limiting the ability to recover a high percentage of chondrocytes after cryopreservation.

Methods need to be incorporated to decrease cryoprotectant toxicity and osmotic stresses. As cryoprotectants act by different mechanisms, combining cryoprotectants at lower concentrations (so that their additive molarity is sufficient to provide cell protection) may decrease cryoprotectant toxicity. This has been applied to other tissues (28, 40, 52, 57) and may be effective in intact AC. In addition, increasing the temperature of the solution at the time of removal will increase the rate of dilution of the cryoprotectant out of the cells and reduce the exposure of the cells to the cryoprotectant. Osmotic fluxes may occur at the time of addition of the cryoprotectant or at the time of exposure to hypotonic solutions. The Me_2SO was added in one step in this study because it was thought that the matrix would protect the cells from severe osmotic fluxes. This appeared to be true for most of the matrix but was not true for the superficial layer. Addition of the cryoprotectant in stages may limit the efflux of water from the cells and thereby limit the severity of the osmotic fluxes (7, 28, 57). Subsequent removal of the cryoprotectant, which can be done step-wise as well (4, 7, 28, 57, 65), can be aided by addition of a nonpenetrating cryoprotectant solution to protect against reverse osmotic fluxes.

The ability of Me_2SO to penetrate the cartilage matrix remains controversial (48, 50). Incomplete penetration after exposure for 30 minutes was suggested by the results of this study. Increasing the water content of the matrix may have facilitated diffusion of the cryoprotectant into the matrix resulting in the increased cell recovery in the 5*M* hypotonic solutions. The negatively charged Me_2SO used in this study, due to numerous experimental reports with this cryoprotectant (5, 13, 38, 48, 53, 56, 59), may have difficulty penetrating the matrix due to the strong negative charge on the proteoglycans within the matrix (34). Methods to increase cryoprotectant penetration while decreasing the length of time of exposure may help minimize these problems. Non-polarized cryoprotectants such as 1,2-propanediol or formamide may enhance penetration through the negatively-charged matrix. This may allow cryoprotectant equilibration in a shorter period of time. The addition of cryoprotectants with higher glass forming tendencies (i.e. 1,2-propandiol) may enhance the vitrification (8, 9, 65) within the matrix and result in increased cell recovery. In addition, adding the cryoprotectant in a stepwise manner can also limit the length of exposure to high concentrations while allowing more time for deeper penetration.

In conclusion, the results of this study demonstrated that initial exposure to Me_2SO and PBS solutions caused the majority of cell loss. The 6*M*/1X solution demonstrated the highest recovery of intact cells (39%) with the middle layer producing the best results (56%) of the three layers examined. Approximately 75% of the cells that survived the initial exposure to the Me_2SO and PBS solutions survived the rapid cooling and warming processes and evidence suggested that vitrification of a portion of the matrix occurred. Primary causes of cell injury were proposed to be Me_2SO toxicity, osmotic fluxes and the temperature/time-dependency of Me_2SO penetration throughout the intact cartilage matrix. Mechanisms to reduce the primary injury and enhance the recovery of intact cells may include combining cryoprotectants of lower concentration, use of better glass forming cryoprotectants, and step-wise addition and dilution of cryoprotectants (with or without a nonpenetrating cryoprotectant). The results of this study suggest that cryopreservation of intact articular cartilage with high concentrations of cryoprotectants is a viable option and its use in the treatment of AC injuries remains a very real possibility.

5.5 Acknowledgements

The authors thank Lauren Beaupre for statistical analysis and Ouellette Packers Ltd., Edmonton for supplying the tissue. Financial support was provided by Edmonton Orthopaedic Research Society, Edmonton Civic Employees Charitable Assistance Fund, and the University of Alberta Hospital Foundation.

5.6 References

1. Acker, J.P. and L.E. McGann. Membrane damage occurs during the formation of intracellular ice. *Cryo Letters* 22, 4: 241-254, 2001.
2. Almqvist, K.F., L. Wang, C. Broddelez, E.M. Veys, and G. Verbruggen. Biological freezing of human articular chondrocytes. *Osteoarthritis Cartilage* 9, 4: 341-350, 2001.
3. Anderson, A.F. and M.J. Pagnani. Osteochondritis dissecans of the femoral condyles. Long-term results of excision of the fragment. *Am J Sports Med* 25, 6: 830-834, 1997.
4. Armitage, W.J. and S.J. Rich. Vitrification of organized tissues. *Cryobiology* 27, 5: 483-491, 1990.
5. Ashwood-Smith, M.J. Radioprotective and cryoprotective properties of dimethyl sulfoxide in cellular systems. *Ann N Y Acad Sci* 141, 1: 45-62, 1967.
6. Bell, R.S., A. Davis, D.G. Allan, F. Langer, A.A. Czitrom, and A.E. Gross. Fresh osteochondral allografts for advanced giant cell tumors at the knee. *J Arthroplasty* 9, 6: 603-609, 1994.
7. Bourne, W.M. and L.R. Nelson. Human corneal studies with a vitrification solution containing dimethyl sulfoxide, formamide, and 1,2-propanediol. *Cryobiology* 31, 6: 522-530, 1994.
8. Boutron, P., *Non-equilibrium formation of ice in aqueous solutions: Efficiency of polyalcohol solutions for vitrification*, in *The biophysics of organ cryopreservation*, D.E. Pegg and A.M.J. Karow, Editors. Plenum: New York. p. 201-228, 1987.
9. Boutron, P., P. Mehl, A. Kaufmann, and P. Angibaud. Glass-forming tendency and stability of the amorphous state in the aqueous solutions of linear polyalcohols with four carbons. I. Binary systems water-polyalcohol. *Cryobiology* 23, 5: 453-469, 1986.
10. Bugbee, W.D. and F.R. Convery. Osteochondral allograft transplantation. *Clin Sports Med* 18, 1: 67-75, 1999.

11. Bujia, J., D. Kremer, H. Sudhoff, E. Viviente, C. Sprekelsen, and E. Wilmes. Determination of viability of cryopreserved cartilage grafts. *Eur Arch Otorhinolaryngol* 252, 1: 30-34, 1995.

12. Clohisy, D.R. and H.J. Mankin. Osteoarticular allografts for reconstruction after resection of a musculoskeletal tumor in the proximal end of the tibia. *J Bone Joint Surg Am* 76, 4: 549-554, 1994.

13. Cocks, F.H. and W.E. Brower. Phase diagram relationships in cryobiology. *Cryobiology* 11, 4: 340-358, 1974.

14. Convery, F.R., M.H. Meyers, and W.H. Akeson. Fresh osteochondral allografting of the femoral condyle. *Clin Orthop* 273: 139-145, 1991.

15. Czitrom, A.A., F. Langer, N. McKee, and A.E. Gross. Bone and cartilage allotransplantation. A review of 14 years of research and clinical studies. *Clin Orthop* 208: 141-145, 1986.

16. Daw, A., J. Farrant, and G.J. Morris. Membrane leakage of solutes after thermal shock or freezing. *Cryobiology* 10, 2: 126-133, 1973.

17. Fahy, G.M., J. Saur, and R.J. Williams. Physical problems with the vitrification of large biological systems. *Cryobiology* 27, 5: 492-510, 1990.

18. Flynn, J.M., D.S. Springfield, and H.J. Mankin. Osteoarticular allografts to treat distal femoral osteonecrosis. *Clin Orthop* 303: 38-43, 1994.

19. Franks, F. and D. Eagland. The role of solvent interactions in protein conformation. *CRC Crit Rev Biochem* 3, 2: 165-219, 1975.

20. Fujikawa, S. Lamellar to hexagonal II phase transitions in tonoplasts of mushroom hyphae caused by mechanical stress resulting from the formation of extracellular ice crystals. *Cryobiology* 28, 191-202, 1991.

21. Fujikawa, S. and K. Miura. Plasma membrane ultrastructural changes caused by mechanical stress in the formation of extracellular ice as a primary cause of slow freezing injury in fruit-bodies of Basidiomycetes (Lyophyllum ulmarium). *Cryobiology* 23, 371-382, 1986.

22. Fujita, T., Y. Takami, K. Ezoe, T. Saito, A.K. Sato, N. Takeda, Y. Yamamoto, K. Homma. Successful preservation of human skin by vitrification. *J Burn Care Rehabil* 21, 4: 304-309, 2000.

23. Ghazavi, M.T., K.P. Pritzker, A.M. Davis, and A.E. Gross. Fresh osteochondral allografts for post-traumatic osteochondral defects of the knee. *J Bone Joint Surg Br* 79, 6: 1008-1013, 1997.

24. Hechter, O. The role of water structure in the molecular organization of cell membranes. *Fed Proc* S15, S91-102, 1965.

25. Jackson, D.W., T.M. Simon, and H.M. Aberman. Symptomatic articular cartilage degeneration: the impact in the new millennium. *Clin Orthop* 391 Suppl: S14-25, 2001.

26. Jomha, N.*Cryopreservation of human articular cartilage* in *Experimental Surgery, Masters Thesis*. University of Alberta: Edmonton, 1996.

27. Jomha, N.M., P.C. Anoop, K. Bagnall, and L.E. McGann. Effects of increasing concentrations of dimethyl sulfoxide during cryopreservation of porcine articular cartilage. *Cell Pres Tech* 1, 2: 111-120, 2002.

28. Jutte, N.H., P. Heyse, H.G. Jansen, G.J. Bruining, and G.H. Zeilmaker. Vitrification of human islets of Langerhans. *Cryobiology* 24, 5: 403-411, 1987.

29. Karlsson, J.O. Cryopreservation: freezing and vitrification. *Science* 296, 5568: 655-656, 2002.

30. Kurata, H., K. Takakuwa, and K. Tanaka. Vitrification of hematopoietic progenitor cells obtained from human cord blood. *Bone Marrow Transplant* 14, 2: 261-263, 1994.

31. Lovelock, J.E. The haemolysis of human red blood cells by freezing and thawing. *Biochimica Et Biophysica Acta* 10, 414-426, 1953.

32. Lovelock, J.F. The mechanism of the protective action of glycerol against haemolysis by freezing and thawing. *Biochimica et Biophysica Acta* 11, 28-36, 1953.

33. Mahomed, M.N., R.J. Beaver, and A.E. Gross. The long-term success of fresh, small fragment osteochondral allografts used for intraarticular post-traumatic defects in the knee joint. *Orthopedics* 15, 10: 1191-1199, 1992.

34. Mankin, H.J., V.C. Mow, J.A. Buckwalter, J.P. Iannotti, and A. Ratcliffe, *Form and function of articular cartilage*, in *Orthopaedic Basic Science*, S.R. Simon, Editor: Chicago. p. 1-44, 1994.

35. McGann, L.E. Optimal temperature ranges for control of cooling rate. *Cryobiology* 16, 3: 211-216, 1979.

36. McGann, L.E. and J. Farrant. Survival of tissue culture cells frozen by a two-step procedure to -196 degrees C. I. Holding temperature and time. *Cryobiology* 13, 3: 261-268, 1976.

37. McGann, L.E. and J. Farrant. Survival of tissue culture cells frozen by a two-step procedure to -196 degrees C. II. Warming rate and concentration of dimethyl sulphoxide. *Cryobiology* 13, 3: 269-273, 1976.

38. McGann, L.E., D. McAllister, K. Muldrew, and N.S. Schachar. Permeability of isolated chondrocytes to dimethyl sulfoxide. *Orthop Res Soc* 34 annual meeting, 1988.

39. McGann, L.E., A.R. Turner, M.J. Allalunis, and J.M. Turc. Cryopreservation of human peripheral blood stem cells: optimal cooling and warming conditions. *Cryobiology* 18, 5: 469-472, 1981.

40. Mehl, P. and P. Boutron. Glass-forming tendency and stability of the amorphous state in the aqueous solutions of linear polyalcohols with four carbons. II. Ternary systems with water, 1,2-propanediol or 1,3-butanediol or 2,3-butanediol. *Cryobiology* 24, 355-367, 1987.

41. Meryman, H.T., *The exceeding of a minimum tolerable cell volume in hypertonic suspension as a cause of freezing injury*, in *The frozen cell*, G.E.W. Westenholme and M. O'Conner, Editors. Churchill: London. p. 51-64, 1970.

42. Meryman, H.T. Osmotic stress as a mechanism of freezing injury. *Cryobiology* 8, 5: 489-500, 1971.

43. Meyers, M.H., W. Akeson, and F.R. Convery. Resurfacing of the knee with fresh osteochondral allograft. *J Bone Joint Surg [Am]* 71, 5: 704-713, 1989.

44. Mosmann, T. Rapid colorimetric assay for cellular growth and survival: Application to proliferation and cytotoxicity assays. *J Immunol Methods* 65, 55-63, 1963.

45. Muldrew, K., M. Hurtig, K. Novak, N. Schachar, and L.E. McGann. Localization of freezing injury in articular cartilage. *Cryobiology* 31, 1: 31-38, 1994.

46. Muldrew, K. and L.E. McGann. Mechanisms of intracellular ice formation. *Biophys J* 57, 3: 525-532, 1990.

47. Muldrew, K., K. Novak, C. Studholme, G. Wohl, R. Zernicke, N.S. Schachar, and L.E. McGann. Transplantation of articular cartilage following a step-cooling cryopreservation protocol. *Cryobiology* 43, 3: 260-267, 2001.

48. Muldrew, K., B. Sykes, S. N., and L.E. McGann. Permeation kinetics of dimethol sulfoxide in articular cartilage. *Cryo-letters* 17, 311-340, 1996.

49. Ohlendorf, C., W.W. Tomford, and H.J. Mankin. Chondrocyte survival in cryopreserved osteochondral articular cartilage. *J Orthop Res* 14, 3: 413-416, 1996.

50. Pegg, D.E. Cryobiology of cells in situ: Experiments with ovine articular cartilage. *Cryobiology* 37, 4: 381-382, 1998.

51. Rajotte, R.V., H.L. Stewart, W.A. Voss, and T.K. Shnitka. Viability studies on frozen--thawed rat islets of Langerhans. *Cryobiology* 14, 1: 116-120, 1977.

52. Rall, W.F. and G.M. Fahy. Ice-free cryopreservation of mouse embryos at -196 degrees C by vitrification. *Nature* 313, 6003: 573-575, 1985.

53. Rall, W.F., P. Mazur, and J.J. McGrath. Depression of the ice-nucleation temperature of rapidly cooled mouse embryos by glycerol and dimethyl sulfoxide. *Biophys J* 41, 1: 1-12, 1983.

54. Schachar, N., M. Nagao, T. Matsuyama, D. McAllister, and S. Ishii. Cryopreserved articular chondrocytes grow in culture, maintain cartilage phenotype, and synthesize matrix components. *J Orthop Res* 7, 3: 344-351, 1989.

55. Schachar, N.S., K. Novak, M. Hurtig, K. Muldrew, R. McPherson, G. Wohl, R.F. Zernicke, and L.E. McGann. Transplantation of cryopreserved osteochondral Dowel allografts for repair of focal articular defects in an ovine model. *J Orthop Res* 17, 6: 909-919, 1999.

56. Smith, A.U. Survival of frozen chondrocytes isolated from cartilage of adult mammals. *Nature* 205, 782-784, 1965.

57. Song, Y.C., P.O. Hagen, F.G. Lightfoot, M.J. Taylor, A.C. Smith, and K.G. Brockbank. In vivo evaluation of the effects of a new ice-free cryopreservation process on autologous vascular grafts. *J Invest Surg* 13, 5: 279-288, 2000.

58. Steponkus, P., D. Stout, J. Wolfe, and R. Lovelace. Freeze-induced electrical transients and cryoinjury. *Cryo Lett* 5, 343-348, 1984.

59. Tavakol, K., R.G. Miller, D.P. Bazett-Jones, W.S. Hwang, L.E. McGann, and N.S. Schachar. Ultrastructural changes of articular cartilage chondrocytes associated with freeze-thawing. *J Orthop Res* 11, 1: 1-9, 1993.

60. Tomford, W.W. Transmission of disease through transplantation of musculoskeletal allografts. *J Bone Joint Surg Am* 77, 11: 1742-1754, 1995.

61. Tomford, W.W., G.R. Fredericks, and H.J. Mankin. Studies on cryopreservation of articular cartilage chondrocytes. *J Bone Joint Surg [Am]* 66, 2: 253-259, 1984.

62. Twyman, R.S., K. Desai, and P.M. Aichroth. Osteochondritis dissecans of the knee. A long-term study. *J Bone Joint Surg Br* 73, 3: 461-464, 1991.

63. Workman, E. and S. Reynolds. Electrical phenomena occurring during the freezing of dilute aqueous solutions and their possible relationship to thunderstorm electricity. *Phys Rev* 78, 254-259, 1950.

64. Wowk, B., E. Leitl, C.M. Rasch, N. Mesbah-Karimi, S.B. Harris, and G.M. Fahy. Vitrification enhancement by synthetic ice blocking agents. *Cryobiology* 40, 3: 228-236, 2000.

65. Wusteman, M.C., D.E. Pegg, M.P. Robinson, L.H. Wang, and P. Fitch. Vitrification media: toxicity, permeability, and dielectric properties. *Cryobiology* 44, 1: 24-37., 2002.

Chapter Six

Comparison of High Cryoprotectant Concentrations for Cryopreservation of Porcine Articular Cartilage

NM Jomha, PC Anoop, K Bagnall, LE McGann

A version of this chapter has been submitted to Cell Preservation Technology.

6.1 Introduction

Large, untreated articular cartilage (AC) defects degenerate into osteoarthritis (2, 22), the second leading cause of disability in the United States (5). Cryopreservation of intact AC may improve treatment outcome by providing a bank of viable and functional osteochondral tissues that can be used in transplantation procedures. A tissue bank can provide cartilage for optimal size/contour matching, extensive testing for infectious diseases, and appropriate operating conditions for the patient and surgical team. In addition, viable chondrocytes essential to maintain intact cartilage matrix over long periods of time will be available.

Proper functioning of AC depends on two variable 1) intact matrix and 2) chondrocytes to maintain the matrix. Studies on intact ovine AC utilizing slow-cooling techniques with a low concentration of cryoprotectant (1*M* dimethyl sulfoxide (Me_2SO)) (2-staged (12) and stepped (13) cooling) have demonstrated up to 60% intact cell recovery using membrane integrity stains (12, 13). However, even with this relatively high recovery rate, long-term transplantation results have demonstrated significant deterioration one year after transplantation (13, 17). It is likely that the matrix damage that occurs with ice formation is irreparable by the remaining intact cells. An alternative to this is vitrification that avoids ice formation and may leave the matrix relatively intact. Even with an intact matrix, viable cells are still required to maintain the matrix over the long term. A recent study has demonstrated that a rapid-cooling technique using a high concentration of Me_2SO (6*M*) can achieve moderate recovery of cells (42%) (7). These results have encouraged further investigation of the high-concentration rapid-cooling methodology because it is felt that higher cell viability will lead to improved matrix maintenance and more successful transplants experienced.

The most appropriate cryoprotectant for AC has not been defined, and different cryoprotectants have different properties and exert different responses in chondrocytes and the matrix. Recent literature has focused on Me_2SO, propylene glycol (PD), and VS-55, although other cryoprotectants also have been used. Me_2SO is the most commonly used cryoprotectant on cartilage tissue (6, 9, 11, 12, 14-16, 20, 21) while PD has a higher glass forming tendency (4) and has been successful on very thin slices of AC (6). VS-55 is a combination solution that includes 3.1M Me_2SO, 2.2M PD, and 3.1M formamide in EuroCollins carrier, and has been used successfully to vitrify vascular grafts (18). All of these solutions have been successful in other tissues and it is important to evaluate the effectiveness of these cryoprotectant solutions on intact AC to maximize cell recovery while maintaining the intact matrix.

This study was designed to compare three different cryoprotectant solutions (Me_2SO, PD, and a combination solutoin of Me_2SO, PD, and formamide (MPF) in the same concentrations as VS-55 but using a phosphate buffered (PBS) carrier) on porcine AC using a rapid-cooling protocol. It was hypothesized that the MPF combination solution would provide the highest recovery of intact cells after the rapid-cooling/warming protocol because the low concentration of individual cryoprotectants would induce less toxicity while the combination of cryoprotectants would provide sufficient molality to achieve vitrification throughout the tissue.

6.2 Materials and Methods

Tissues

Intact stifle joints were harvested from 12 sexually mature pigs sacrificed for meat consumption. In this study, pigs were selected because the cartilage thickness in the stifle joint is the closest to the exceptionally thick cartilage in human knee joints. The joints were immersed in 1X Dulbecco's PBS solution (pH = 7.0) (Gibco, BRL, MD) and maintained at 4°C until 10mm diameter osteochondral dowels (OCDs) were harvested using a hand-held coring device (within 12 hours of death of the animal). The OCDs were harvested from the central weight-bearing portion of the medial femoral condyle and consisted of the full thickness of AC (3-4mm) perched on a 5-10mm bone base. Three OCDs were harvested from each joint.

Cryopreservation Protocol

The OCDs were randomly assigned to one of seven groups. A fresh control group consisted of OCDs immersed in 1X PBS at 4°C. Toxicity control groups were created for each of the three cryoprotectant solutions. OCDs samples were immersed in 50ml of 6*M* Me_2SO or 5*M* PD in a one-step addition, or in MPF solution in a multi-step addition for 30 minutes at 4°C. These control samples were removed from the cryoprotectant solutions (one-step with Me_2SO and PD, multi-step with MPF) and assessed as described below.

There were three experimental groups consisting of the 6*M* Me_2SO, 5*M* PD, and MPF. The Me_2SO and PD samples were immersed in the appropriate solutions in a one-step addition and dilution process while the MPF samples underwent a multistep addition and dilution process as per the recommended protocol (8). Briefly, the samples were consecutively immersed in 50ml of solution for 10 minutes in 15%, 30%, 50%, 80%, and 100% MPF concentration. After immersion in 50ml of the full concentration of the appropriate solution for 30 minutes at 4°C, samples were transferred into polypropylene test-tubes (17x100mm culture tube, VWR Can Lab, Ontario, Ca) with 5ml of solution. The samples in test-tubes were placed in an ice-water bath at 0°C for 10 minutes and then rapidly cooled by plunging into liquid nitrogen (LN) (~ 65°C/min). Samples were held in the LN for at least one hour and then rapidly warmed in a 37°C water bath (~ 120°C/min) until the liquid reformed. The OCDs randomly assigned to the MPF group underwent a stepwise dilution of the cryoprotectant solution after warming as per the protocol (8). Briefly, the samples were immersed consecutively in 50ml of solution for 10 minutes in 50%, 40%, 30%, 20%, 10%, and 0% MPF solution. Once warmed, all samples were immersed in 1X PBS at 4°C until cell assessment, which occurred within one hour.

Cell Assessment

Samples from all groups (fresh controls, toxicity controls and experimental samples) were sectioned using a Vibratome® (TPI, St. Louis, Missouri) cutting vertically across the dowel from the articular surface towards the cartilage-bone junction. Slices sectioned to a thickness of 70µm were taken from the widest portion of the dowels. Each slice was stained using the membrane integrity dyes ethidium bromide (EB; Sigma, St. Louis, MO) and Syto 13 (Molecular Probes, Eugene, OR) (0.1% EB with 0.45% Syto mixed in PBS (vol/vol)). Cells with intact membranes fluoresced green due to the absorption of the Syto stain with the exclusion of the EB stain. Cells with disrupted membranes were permeable to EB and therefore fluoresced red. The 70µm slices were viewed under a Leitz Dialux 22 fluorescence (440-480nm) microscope (Leitz, Germany) at 125X magnification (10X objective and 12.5X eyepiece). The images were recorded by digital camera (Pixera DiRactor, Pixera Corporation, Los Gatos, CA) and stored on computer for later analysis. Membrane integrity dyes were used because cell membranes have been shown to be a primary target of injury during the cryopreservation process (1), and membrane integrity was shown to be the most reliable predictor of long-term transplantation results for AC (17).

A customized computer counting program was used to calculate the percent recovery of intact cells compared to total cells using minimum thresholds for green and red pixel intensity. Percent recovery of intact cells was determined by:

$$\frac{\text{\# of green pixels}}{\text{\# of green pixels} + \text{\# of red pixels}} \quad \times 100$$

Each sample slice was divided into three approximately equal layers (superficial, middle and deep) to examine recovery as a function of location. Statistical analysis was performed using a two-tailed, three-way analysis of variance and post hoc Bonferroni tests with $P < 0.05$ determined as significant using SPSS-10.07 (SPSS Inc, San Rafael, CA).

6.3 Results

The results of the fresh controls from the 1X PBS solution (no cryoprotectant or cooling performed) demonstrated 76 ± 2% (mean ± S.E.) intact cell recovery with no difference between the three layers as determined by the pixel intensity program. This was used as the reference for the toxicity controls and the experimental samples. Figure 6-1 demonstrates the toxicity controls for each solution as a function of location compared with fresh controls. In these samples, the cryoprotectant was added rapidly in a single step for Me_2SO and PD, but stepwise for MPF prior to cell evaluation. Although there was significantly more toxicity in the superficial layer ($P = 0.001$) when compared with the deeper layers, there was no significant difference in recovery in the superficial layer between the three groups. Overall, there was no significant difference in toxicity between the three cryoprotectant control solutions (P > 0.05) although the difference between MPF and PD solutions approached significance (P = 0.062) mainly due to the excellent recovery in the middle and deep layers in the MPF solution.

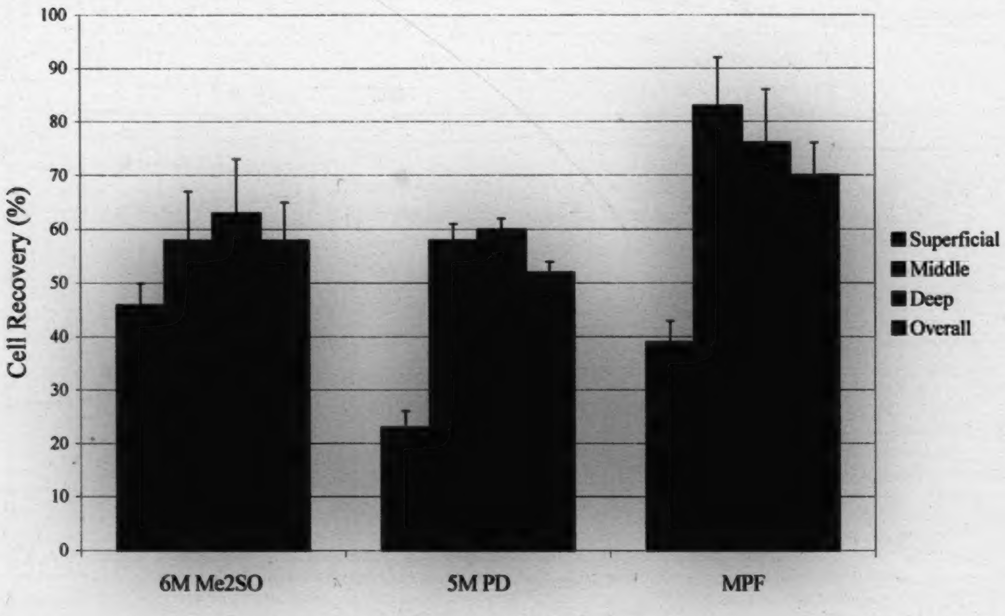

Figure 6-1. Intact cell recovery from the three toxicity control solutions as a percentage of the fresh control by layers. Overall, the MPF solution samples demonstrated the least cell toxicity but this was not statistically significant. Maximal toxicity was noted in the superficial layer in all three solutions (P = 0.001).

Figure 6-2 demonstrates the results from the experimental samples that underwent rapid cooling. The cryoprotectant used and the depth of the cells within the matrix were significant determinants of cell recovery. The 6*M* Me_2SO solution samples had the highest recovery in all layers (overall = 33 ± 2%). The 6*M* Me_2SO solution samples and the 5*M* PD solution samples demonstrated significantly higher recovery of intact cells in all layers compared to the MPF solution samples (P = 0.024). The difference in recovery between the 6*M* Me_2SO and 5*M* PD samples was not significant (P > 0.05). Figure 6-2 also demonstrates that the middle layer had a significantly higher recovery of intact cells compared to the other layers (P < 0.001) when all solution samples were considered.

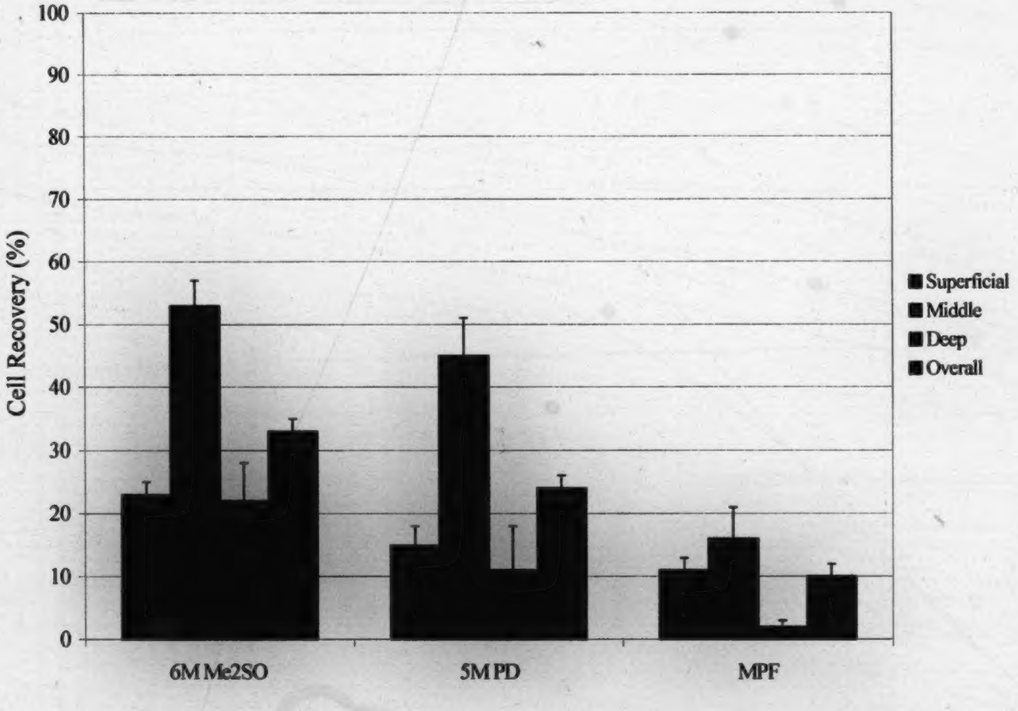

Figure 6-2. Demonstration of the intact cell recovery from the experimental solutions by layers after rapid cooling. The cell recovery from the MPF solution was significantly lower than the other two solutions in all three layers. The 6*M* Me_2SO solution had the highest overall recovery (33 ± 2%). The middle layer had the highest recovery of intact cells in all three solution samples and was close to 100% in the 6*M* Me_2SO samples when compared to the toxicity controls.

6.4 Discussion

The results of this study demonstrated that the recovery of intact cells was higher in the 6*M* Me_2SO and 5*M* PD solutions when compared to the MPF combination solution (P = 0.024), even though there was no significant difference in the cellular toxicity of the three solutions. The 6*M* Me_2SO solution samples had the highest recovery of intact cells followed closely by the 5*M* PD solution samples. This did not support the hypothesis that the MPF combination solution would provide the highest intact cell recovery.

The recovery from the 6*M* Me_2SO solution samples confirmed the results of previous studies (7) and indicated that cryopreservation of intact cartilage by rapid cooling in high concentrations of Me_2SO can result in moderate cell recovery. The low recovery from the MPF solution samples was surprising, possibly due to inadequate penetration from lower concentration gradients of the MPF constituent solutes. The inability of the MPF solution to penetrate throughout the matrix is consistent with the low toxicity observed in the deeper layers.

The length of cryoprotectant exposure was based on Muldrew *et. al.*'s experience that 30 minutes provided complete cryoprotectant penetration of Me_2SO at 4°C in ovine AC (12). Cryoprotectant penetration is dependent on temperature, time, and concentration gradient. All cryoprotectant exposure was at 4°C to limit toxicity but penetration may have increased with higher temperatures. The length of exposure could also be increased but, once again, toxicity would increase. Finally, the most probably cause for the poor results from the MPF solution was the concentration gradient. The deep portion of the matrix has high electrolyte concentration and osmotic pressure (10, 23) and the lower concentration of the individual components may not have been able to overcome these concentration barriers.

Toxicity was a major contributor to cell loss, in addition to difficulties with cryoprotectant penetration. The initial toxicity in all three solutions was significant and was most evident in the superficial layer (Figure 6-1). Indeed, if the initial cell loss due to toxicity was taken into account, the overall recovery of cells from the 6*M* Me_2SO solution samples was 60%, rising to 90% in the middle layer, which shows excellent promise for future development and studies.

In the superficial layer, toxicity, and not osmotic stress, was the primary damaging variable. There was no significant difference in cell recovery from the superficial layer of MPF when compared to Me_2SO or PD. If osmotic stresses had significant deleterious effects, it would be expected that the superficial layer of the Me_2SO and PD samples would have lower cell recovery because of the single step addition of the solution to the cartilage but this did not occur. It is possible that the matrix mitigated the effect of the large osmotic shifts suggesting that stepwise addition of the cryoprotectant may not be necessary in AC.

The MPF solution demonstrated less toxicity than the other solutions although this was not statistically significant, which was surprising (Figure 6-1). It was thought that the lower concentrations of the individual cryoprotectants would decrease toxicity as noted in other studies (3, 7, 24). It is possible that the overall increased molarity (8.4*M* in the MPF solution compared to 6*M* in the Me_2SO solution and 5*M* in the PD solution) was the main damaging variable. Combinations of cryoprotectants with lower overall molarities (compared to MPF) that result in vitrification may have lower toxicity and may be required for use in AC.

Cell recovery was the highest in the middle layer of the cartilage in all solutions (Figure 6-2). Cell loss in the superficial layer was likely due to significant cryoprotectant toxicity from prolonged exposure. Cell loss in the deep layer was likely due to ice formation because of inadequate cryoprotectant penetration. Therefore, cryoprotectant penetration remains the most essential issue to resolve in order to increase cell recovery after cryopreservation of AC.

In conclusion, this study has demonstrated that a combination solution (MPF) using cryoprotectant concentrations similar to a solution previously successful in vitrifying vascular tissues (18) and thin rabbit AC (19) (VS-55) was not successful in porcine AC. The 6*M* Me_2SO (33 ± 2%) and 5*M* PD (23 ± 2%) solutions samples demonstrated the highest overall intact cell recovery with up to 53% recovery from the middle layer. The superficial layer demonstrated the most significant toxicity from the control solutions while the MPF solution was not significantly less toxic than the other two solutions tested. Therefore, cryoprotectant toxicity and diffusion in the matrix remain the primary obstacles to achieving higher cell recovery.

6.5 Acknowledgements

The authors thank Lauren Beaupre for statistical analysis and Ouellette Packers Ltd., Edmonton for supplying the tissue. Funding was provided by the Edmonton Orthopaedic Research Society, Edmonton Civic Employees Charitable Assistance Fund, and University of Alberta Hospital Foundation.

6.6 References

1. Acker, J.P. and L.E. McGann. Membrane damage occurs during the formation of intracellular ice. *Cryo Letters* 22, 4: 241-254., 2001.
2. Anderson, A.F. and M.J. Pagnani. Osteochondritis dissecans of the femoral condyles. Long-term results of excision of the fragment. *Am J Sports Med* 25, 6: 830-834, 1997.
3. Armitage, W.J. and S.J. Rich. Vitrification of organized tissues. *Cryobiology* 27, 5: 483-491, 1990.
4. Boutron, P. and A. Kaufmann. Stability of the amorphous state in the system water--1,2-propanediol. *Cryobiology* 16, 6: 557-568, 1979.
5. Jackson, D.W., T.M. Simon, and H.M. Aberman. Symptomatic articular cartilage degeneration: the impact in the new millennium. *Clin Orthop* 391 Suppl: S14-25, 2001.
6. Jomha, N.*Cryopreservation of human articular cartilage* in *Experimental Surgery, Masters Thesis*. University of Alberta: Edmonton, 1996.
7. Jomha, N.M., P.C. Anoop, K. Bagnall, and L.E. McGann. Effects of increasing concentrations of dimethyl sulfoxide during cryopreservation of porcine articular cartilage. *Cell Pres Tech* 1, 2: 111-120, 2002.
8. Khirabadi, B.S., Y.C. Song, and K.G.M. Brockbank.*Method of cryopreservation of blood vessels by vitrification* in *United States Patent*. Organ Recovery Systems, Inc. (Chicago, IL): United States. p. 18, 2001.
9. Kiefer, G.N., K. Sundby, D. McAllister, and e. al. The effect of cryopreservation on the biomechanical behavior of bovine articular cartilage. *J Orthop Res* 7, 494-501, 1989.
10. Maroudas, A., M.T. Bayliss, and M.F. Venn. Further studies on the composition of human femoral head cartilage. *Ann Rheum Dis* 39, 5: 514-523, 1980.
11. McGann, L.E., D. McAllister, K. Muldrew, and N.S. Schachar. Permeability of isolated chondrocytes to dimethyl sulfoxide. *Orthop Res Soc* 34 annual meeting, 1988.
12. Muldrew, K., M. Hurtig, K. Novak, N. Schachar, and L.E. McGann. Localization of freezing injury in articular cartilage. *Cryobiology* 31, 1: 31-38, 1994.

13. Muldrew, K., K. Novak, C. Studholme, G. Wohl, R. Zernicke, N.S. Schachar, and L.E. McGann. Transplantation of articular cartilage following a step-cooling cryopreservation protocol. *Cryobiology* 43, 3: 260-267, 2001.

14. Muldrew, K., B. Sykes, S. N., and L.E. McGann. Permeation kinetics of dimethol sulfoxide in articular cartilage. *Cryo-letters* 17, 311-340, 1996.

15. Ohlendorf, C., W.W. Tomford, and H.J. Mankin. Chondrocyte survival in cryopreserved osteochondral articular cartilage. *J Orthop Res* 14, 3: 413-416, 1996.

16. Schachar, N.S. and L.E. McGann. Investigations of low-temperature storage of articular cartilage for transplantation. *Clin Orthop* 208: 146-150, 1986.

17. Schachar, N.S., K. Novak, M. Hurtig, K. Muldrew, R. McPherson, G. Wohl, R.F. Zernicke, and L.E. McGann. Transplantation of cryopreserved osteochondral Dowel allografts for repair of focal articular defects in an ovine model. *J Orthop Res* 17, 6: 909-919, 1999.

18. Song, Y.C., P.O. Hagen, F.G. Lightfoot, M.J. Taylor, A.C. Smith, and K.G. Brockbank. In vivo evaluation of the effects of a new ice-free cryopreservation process on autologous vascular grafts. *J Invest Surg* 13, 5: 279-288, 2000.

19. Song, Y.C., F.G. Lightfoot, C.Y. Li, J.M. Boggs, M.J. Taylor, Y.H. An, and K.G.M. Brockbank. Successful cryopreservation of articular cartilage by vitrification. *Thirty-eigth annual meeting of the society for cryobiology* Edinburgh, United Kingdom, July 29-Aug1: 2001.

20. Tavakol, K., R.G. Miller, D.P. Bazett-Jones, W.S. Hwang, L.E. McGann, and N.S. Schachar. Ultrastructural changes of articular cartilage chondrocytes associated with freeze-thawing. *J Orthop Res* 11, 1: 1-9, 1993.

21. Tomford, W.W., G.R. Fredericks, and H.J. Mankin. Studies on cryopreservation of articular cartilage chondrocytes. *J Bone Joint Surg [Am]* 66, 2: 253-259, 1984.

22. Twyman, R.S., K. Desai, and P.M. Aichroth. Osteochondritis dissecans of the knee. A long-term study. *J Bone Joint Surg Br* 73, 3: 461-464, 1991.

23. Urban, J. and A. Hall, *Physical modifiers of cartilage metabolism*, in *Articular cartilage and osteoarthritis*, K. K.E., *et al.*, Editors. Raven Press: New York. p. 393-406, 1992.

24. Wusteman, M.C., D.E. Pegg, M.P. Robinson, L.H. Wang, and P. Fitch. Vitrification media: toxicity, permeability, and dielectric properties. *Cryobiology* 44, 1: 24-37, 2002.

Chapter Seven

MRI and Biochemical Assessments of Changes in Porcine Articular Cartilage after Different Freezing Protocols

L Laouar[1,2], K Fishbein[2], NM Jomha[1], LE McGann[1], WE Horton[3] &
RGS Spencer[2]

[1]University of Alberta, Department of Medicine & Pathology, Edmonton, Alberta, Canada; [2]NIH/National Institute on Aging, Baltimore, Maryland USA; [3]Northeastern Ohio Universities, College of Medicine, Ohio, USA.

A version of this chapter has been submitted to Osteoarthritis and Cartilage.

This study was designed by myself and one of my supervisors (LEM) and was performed by our research associate (LL) in Baltimore where facilities were available for the MRI portion of the study.

7.1 Introduction

Osteochondral disease and injury are a significant cause of pain and disability. Progression leads to osteoarthritis, the second leading cause of work disability in the United States with an estimated cost of $65 billion in the U.S. in 1997 (13). Currently, the only definitive treatment for large, unconfined osteochondral defects in young patients is osteochondral transplantation (2, 5, 8, 19, 21). Although some success has been achieved, there are still significant difficulties with this treatment including accurate size and contour matching of the transplant tissue (5, 8, 9, 26), transmission of infectious diseases (6, 44), and difficulties in operative timing. Cryopreservation of articular cartilage (AC) with maintenance of matrix integrity and cell viability would represent a major step towards resolving these problems by allowing storage of the tissue for long periods of time for appropriately selective utilization.

Cryopreservation of chondrocytes in isolation has been successful (1, 34, 36, 45) but cryopreservation of more complex matrix tissue has proven difficult (14, 15, 20). Experiments with intact AC using uncontrolled cooling rates have resulted in minimal cell viability (20, 30). A 2-stage cryopreservation technique (24, 25) that controls the cooling rate has demonstrated promising results on ovine AC (27) with up to 60% recovery of intact cells. Transplantation studies have shown that transplanted osteochondral dowels cryopreserved with this 2-stage cryopreservation procedure demonstrate superior results compared to dowels preserved with an uncontrolled freezing protocol, though the results were still inferior to that of fresh autografts (38).

While an increased number of viable cells available at the time of transplantation does correlate with longer survival time of transplanted cartilage, matrix integrity is also likely to play a significant role in transplant viability and performance, due to functional role of the matrix and the importance of matrix-chondrocyte interactions. These considerations may be particularly problematic after cryopreservation and transplantation, as chondrocytes in the transplanted graft may have a reduced capacity for matrix repair. Conclusions from the few studies available with respect to the consequences to the matrix of cryopreservation have been varied. Tavakol *et. al.* (43) found no ultrastructural changes using transmission electron microscopy while Schiller (39), using MR spectroscopy and relaxometry, noted biophysical changes secondary to freezing and thawing. Finally, Stevenson (42) demonstrated a significant loss of glycosaminoglycan content but no change in hydroxyproline after cryopreservation.

Magnetic resonance imaging (MRI) is a noninvasive technique with the ability to assess a variety of biophysical properties of AC. MR-derived parameters such as proton relaxation times, magnetization transfer contrast (MTC) (11, 16), water diffusion coefficient, and fixed charged density (4) can provide insight into the properties of matrix components as well as interactions between those components. In particular, MR techniques can provide information on collagen and proteoglycan content, matrix fixed charge density (32, 40), and the ability of water to diffuse through the matrix (31). Furthermore, because MRI is noninvasive and allows three-dimensional assessment of the tissue, it has the potential to evaluate transplanted AC *in vivo*.

This study examined porcine AC using MRI and biochemical analysis to determine consequences to the structure and composition of the cartilage matrix after different freezing protocols. Varying ice-forming conditions were created ranging from no ice (fresh controls), to extensive ice formation resulting from direct plunging of hydrated tissue into liquid nitrogen (LN) (14). Intermediate ice-forming conditions were created by slow-cooling to dehydrate the tissue while extramatrix ice formed, and by adding a cryoprotectant, which decreases the amount of ice formed at all subzero temperatures (18, 33). It was hypothesized that these cryopreservation protocols would have different, measurable effects on the structure and composition of cartilage matrix. Biochemical assessment was performed in order to relate MRI findings with standard assays of matrix components.

7.2 Materials and Methods

Tissue

AC was harvested from the distal femoral condyles of sexually mature pigs within twelve hours of sacrifice for meat consumption. Osteochondral dowels (OCD's) of 10mm diameter were cored using a drillpress and subjected to four different cryopreservation protocols. One group of dowels was immersed in 1X Dulbecco's Phosphate Buffer Saline (PBS) (Gibco-BRL 1 X PBS pH=7.0) as a fresh control group (control group – CTR). A second group was immersed in 5ml of 1X PBS, placed into polypropylene test tubes (17x100mm culture tube, VWR Can Lab, Ontario, Ca) and directly plunged in LN (snap frozen group – SF). A third group of dowels was immersed in 1*M* dimethyl sulfoxide (50ml) (Me_2SO, Sigma, St. Louis, MO) for 30 minutes (slow-cooled Me_2SO group – SC-Me_2SO). The fourth group was immersed in 1X PBS (slow-cooled PBS group – SC-PBS). The dowels in the third and fourth groups were placed into polypropylene test tubes with 5ml of solution and treated in accordance with the following protocol (24, 25). Samples were placed in an ice water-bath at 0°C for 10 minutes followed by 5 minutes in an alcohol bath at –7°C, and then ice-nucleated in the suspending solution with ice crystals from forceps dipped in LN. The samples were held at –7°C for 10 minutes to allow dissipation of the latent heat of fusion, cooled at 1°C/min. to –30°C, then plunged in LN where they were stored.

The cooled samples were warmed in a water bath at 37°C for 5 minutes, and the Me_2SO was removed using two washes and overnight storage in PBS prior to MRI. Osteochondral dowels were then immersed in 20ml PBS containing 0.2 units penicillin G sulfate, 200ug streptomycin sulfate (Gibco-BRL), 10ug Fungizone (Biofluids) and 0.4mg Gentamycin sulfate (Biowhitaker). The whole procedure was repeated in triplicate for each experimental condition.

Water proton MRI microscopy

The fresh control samples were imaged within 24 hours while the cooled samples were imaged immediately after warming. All MRI experiments were performed on a Bruker DMX spectrometer (Bruker Analytik, Rheinstetten, Germany) coupled to a super-widebore magnet (bore diameter 104.7 mm) operating at 9.4T (400.1 MHZ for ^{1}H) using a Bruker self-shielded microimaging gradient set with 20 mm diameter resonator coil. The imaging plane was parallel to the long axis of the cartilage. A 20mm field of view, 1mm slice thickness, and 256 x 256 matrix was used to acquire each image. The temperature of the sample was maintained at 37°C by a stream of heated air, and was monitored by a thermocouple in close proximity to the tissue.

Several imaging contrast modalities were implemented to obtain quantitative maps of MRI-measurable parameters. These contrast modalities were: longitudinal (T_1) and transverse (T_2) relaxation times, magnetization transfer contrast (MTC), from which a rate (k_m) was derived to describe the interaction of free and bound water, and the water diffusion coefficient (D).

The theoretical signal intensity of a simple spin-echo imaging sequence with echo time (TE) and repeat time (TR) is:

$$I = \mathrm{A}\rho \exp(-\,TE/T_2)[1 - \exp(-\,TR/T_1)]$$

where A is an overall system gain factor and ρ is the local mobile proton density.

A T_1 map was obtained by fitting the signal intensity of 16 images obtained with TRs ranging between 0.3 and 16 seconds, with a fixed TE of 6.7 msec, to the function $I = k\,[1 - \exp(-\,TR/T_1)]$. A T_2 map was calculated from 16 images acquired with a multi-echo (16 echos) sequence with an echo spacing of 6.66 seconds, with TR fixed at 5 seconds, to the functional form $I = k' \exp(-\,TE/T_2)$.

The magnetization transfer rate between bound and free water was obtained from the following equation: $k_m = 1/T_{1sat}\,[1 - I_s/I_o]$, where I_s and I_o denote, respectively, the amplitude of the narrow free water resonance in the presence or absence of a 5 s, 12 μT saturation pulse applied 6 kHz away from that resonance. T_{1sat} denotes T_1 in the presence of off-resonance saturation (12). $T_{1\,sat}$ was obtained by fitting a series of images acquired with saturating pulses of variable duration, $t_p = 0.01 - 5$ s, to the appropriate functional form (12).

Water diffusion coefficient maps were calculated from a series of 16 images acquired with the pulse gradient spin echo sequence (41). Typical values of the diffusion (Δ) and gradient duration (δ) times were 10 msec and 5 msec, respectively. Diffusion coefficients were calculated explicitly incorporating the effect of the readout gradient (29) and normalized to the diffusion coefficient of water at 37°C. Diffusion coefficients were measured both parallel and perpendicular to the cartilage.

Gadolinium-DTPA (GD-DTPA^{2-}) was used as a contrast agent to measure the fixed charged density (FCD) of the AC matrix. GD-DTPA^{2-} is a negatively charged molecule that is excluded from regions of matrix rich in negatively charged proteoglycans (PG) (4).

Figure 7-1 shows three distinct bands across the width of the AC. We denote these as superficial (SB), middle (MB), and deep (DB) bands based on the MR appearance. Each band was demarcated with a cursor and intensities in all pixels in the marked area were used for calculation of local MRI parameters.

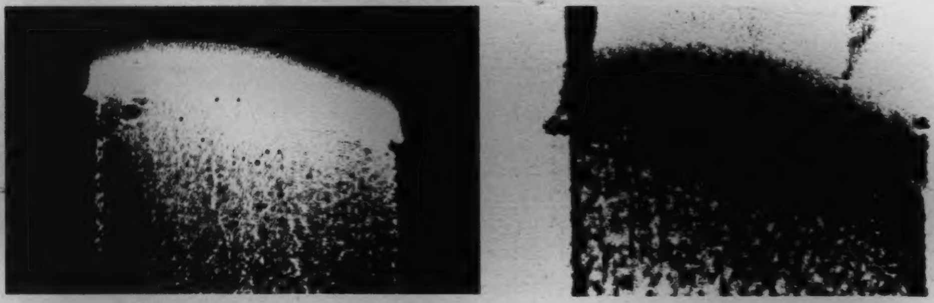

A. MTC-MAP B. MTC-Weighted

Figure 7-1. Digital images illustrating three distinct bands in the cartilage matrix. Proton MRI MTC-map (A) and proton MRI MTC-weighted image (B) in AC cooled in 1*M* Me_2SO. TE =6.7 ms; TR = 5000 ms; saturation pulse = 6000 Hz.

Biochemical Assays

An additional set of OCDs were treated in the same fashion as those prepared for the MRI analysis. In order that the timing of the biochemical assays matched the timing of the MRI studies, these OCD's were incubated for 7 hours in PBS and antibiotics (0.2 units penicillin G sulfate, 200μg streptomycin sulfate, 10μg Fungizone and 0.4mg Gentamycin sulfate at 37°C) prior to processing. The AC was sectioned from the bone using a scalpel and weighed to determine the total wet weight of the tissue. The tissue was then lyophilized to determine dry weight. Tissue hydration was calculated as the weight lost during lyophilization divided by the wet weight of the tissue.

Dried tissue samples (30-40 mg) were digested with papain (Sigma, St. Louis, MO) for 2 hours at 60°C. The digestion solution contained 300μg/ml of papain and 330 μg/ml of N-acetyl cysteine in phosphate buffered EDTA. The quantity of glycosaminoglycan (GAG) per dry weight of the sample was determined using the dimethylmethylene blue dye binding colorimetric assay (10).

Aliquots of the papain digest were hydrolyzed for 8 hours with 6N hydrochloric acid (HCl) at 120°C, and the hydroxyproline per dry weight of the sample was determined using a colorimetric assay (46). The collagen per dry weight was calculated by multiplying the hydroxyproline results per dry weight by a factor of 7.6 (23). The quantities reported in Table 7-1 for GAG and collagen are for the whole tissue.

Aliquots of the papain digest were used in the determination of the DNA per dry weight, using the Puregen protocol for DNA isolation from body fluids (Gentra Systems, Minneapolis, MN). This technique is based on the measurement of optical density (OD) at 260 nm. Typically, 1 OD unit was equivalent to 50μg of double stranded DNA per ml.

Statistical analysis

MRI data (n = 3) and biochemical data (n = 3) are reported as the mean ± standard error. Statistical analysis was performed using 2-way and 1-way analysis of variance and Bon ferroni post hoc analysis with statistical significance assigned at the $P < 0.05$ level (SPSS-10.07, SPSS Inc, San Rafael, CA).

7.3 Results

Proton NMR microimaging

Both calculated maps and weighted images (Figure 7-1) showed three definite bands within the cartilage – a superficial band (SB), a middle band (MB), and a deep band (DB). On MTC map images (Figure 7-1A), the MB appears brighter than both the SB and DB. On the MTC-weighted image (Figure 7-1B), the MB appears darker. The contrast between the three different bands was seen in all four treatments: CTR, SF, SC-Me_2SO, and SC-PBS groups and in all T_1 and T_2 diffusion images and FCD images.

Quantitative MRI data

MRI data from all AC dowels from each treatment were averaged for each band. The results demonstrate that the response to cooling and warming was different in the three experimental groups compared to the fresh control. The properties of the cartilage matrix as determined by microimaging are presented in Figures 7-2 to 7-6.

Figure 7-2 shows that FCD values increased with tissue depth in fresh control AC. There was a significant difference noted by tissue depth ($P < 0.001$), solution used ($P < 0.001$) along with an interaction between tissue depth and solution used ($P < 0.001$). FCD in the SB was significantly lower than in the MB ($P < 0.001$), and also lower in the MB than in the DB ($P = 0.012$). This occurred in CTR and SC-Me_2SO groups. The overall FCD, when tissue depth was not controlled for, was not significantly different between the CTR samples and the SC-Me_2SO samples ($P > 0.05$). However, when controlling for tissue depth, the FCD in the CTR samples was significantly higher than in the SC-Me_2SO samples ($P = 0.001$). In contrast, FCD values were significantly reduced in SF samples and in SC-PBS samples ($P < 0.001$) with and without controlling for the three tissue depths when compared to both the CTR and the SC-Me_2SO groups. In addition, the SF and SC-PBS sample FCD was not significantly different when compared to each other ($P > 0.05$).

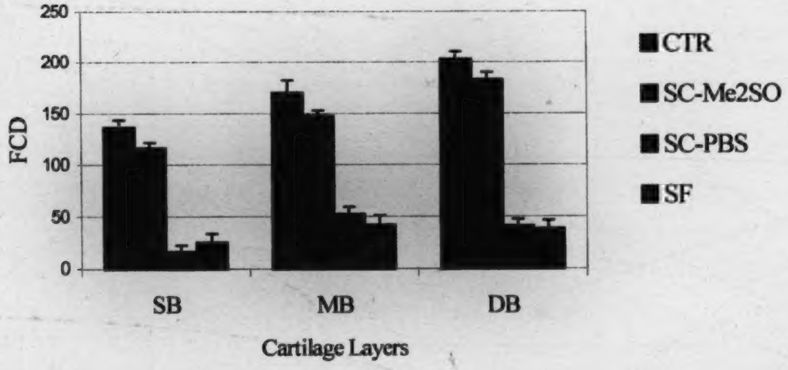

Figure 7-2. Fixed charge density (FCD – mM) of the CTR group along with the three experimental groups characterizing the superficial, middle and deep bands. Errors shown are standard errors (n = 3). There was a significant increase in FCD values with increasing depth in the tissue in the CTR and SC-Me_2SO groups. The FCD value in the CTR group was significantly higher than all experimental groups when controlling for the tissue layers but not different than the SC-Me_2SO group values when overall FCD was recorded. The SF and SC-PBS group values had significantly lower FCD when compared to the CTR and SC-Me_2SO FCD values ($P < 0.001$) and were not different from each other ($P > 0.05$).

There was a significant difference in k_m values with respect to tissue depth ($P < 0.001$) and solution used ($P < 0.001$). The k_m value in the control and the experimental samples was highest in the MB while the k_m value was lowest in the SB ($P < 0.001$) in all groups (Figure 7-3). There was a significant reduction in k_m value in the SC-PBS samples ($P = 0.049$) when compared with the CTR group but not the other two solutions ($P > 0.05$).

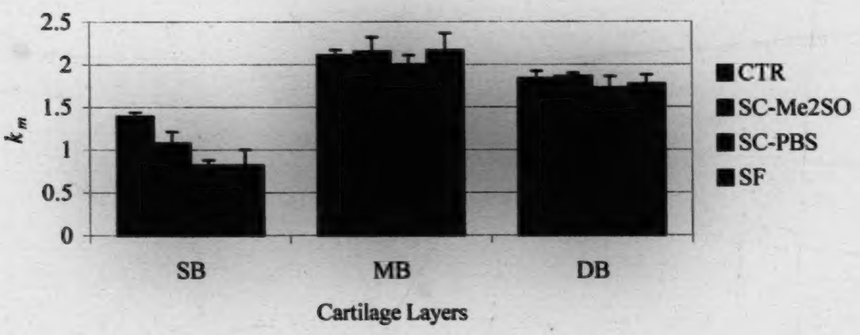

Figure 7-3. k_m (sec^{-1}) values of AC in the three bands from the CTR group and three experimental groups. Errors shown are standard errors ($n = 3$). The highest k_m value was noted in the MB with significant decreases in the SB ($P < 0.001$) and in the DB ($P = 0.002$). There was a significant decrease in the k_m values for the SC-PBS group compared to the CTR group ($P = 0.049$) but, otherwise, there was no difference between the groups.

The T_2 values of the fresh control and all experimental groups are reported in Figure 7-4. There was no significant difference in T_2 in the four different groups.

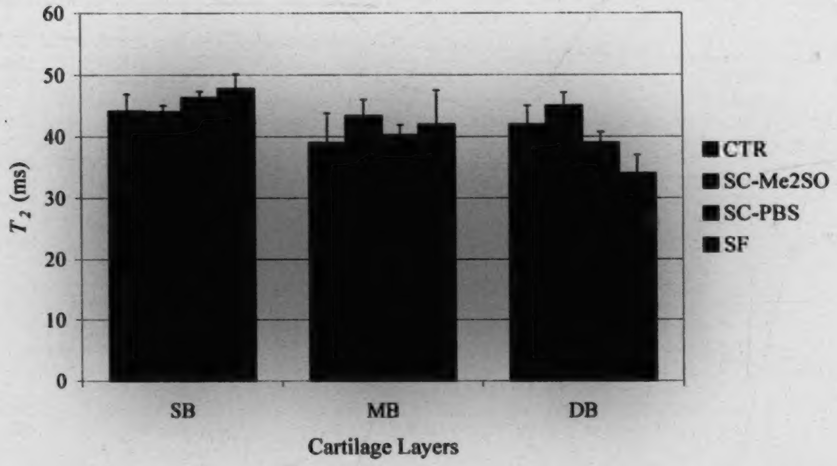

Figure 7-4. T_2 (ms) of AC in the three bands of all four groups. Errors shown are standard errors (n = 3). There was no significant difference between the four groups.

Water diffusion coefficients were determined perpendicular and parallel to the AC surface and data are represented in Figures 7-5 and 7-6. There was a significant different with respect to tissue depth ($P < 0.001$) in the perpendicular and parallel water diffusion coefficient results with the SB significantly higher than the MB ($P < 0.001$) and the DB ($P < 0.001$). In the perpendicular water diffusion coefficient measurements, only the SF group was significantly different than the CTR group ($P = 0.046$). In the parallel water diffusion coefficient measurements, there was no significant differences between any groups.

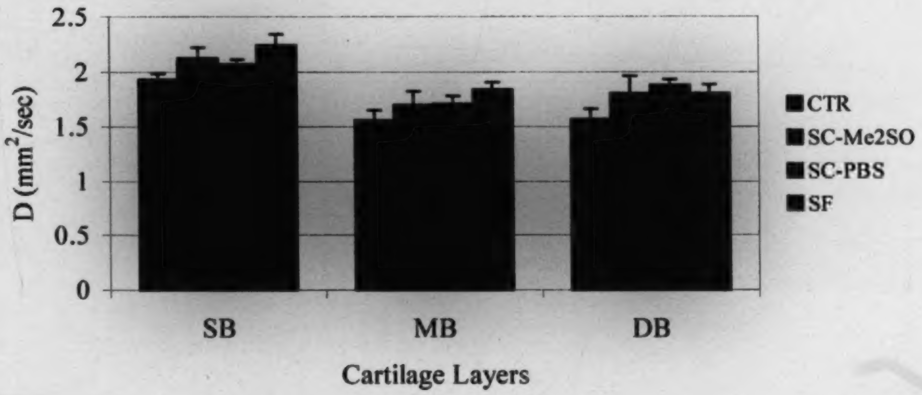

Figure 7-5. Diffusion coefficient of water perpendicular to AC surface in the three bands in all four groups. Errors shown are standard errors (n = 3). There was significant difference between the SB and the MB (P < 0.001) and the DB (P = 0.001). The SF group was significantly higher than the CTR group (P = 0.046) but all other groups were not different.

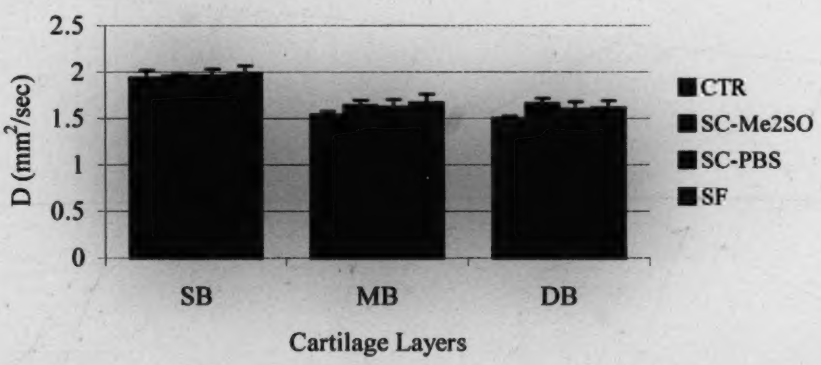

Figure 7-6. Diffusion coefficient of water parallel to AC surface in the three bands in all four groups. Errors shown are standard errors (n = 3). There was a significant difference between the SB and the MB (P < 0.001) and the DB (P = 0.001). There was no difference between the experimental groups and the CTR groups.

There was no significant difference between the T_1 values of any of the four solution groups or three tissue depths.

Biochemical results

Results of biochemical assessments are summarized in Table 7-1. No statistically significant differences were seen between groups in terms of wet/dry weight, hydration, DNA content, hydroxyproline content or chondroitin sulfate content.

	CTR	SC-Me_2SO	SC-PBS	SF
Wet weight mg	121.5 ± 21.22	121.9 ± 6.89	115.5 ± 5.45	118.9 ± 20.31
Dry weight mg	29.2 ± 6.89	27.5 ± 2.15	31.46 ± 1.64	25.6 ± 4.09
% H_20	76.47 ± 1.6	77.45 ± 0.24	72.77 ± 0.17	78.13 ± 0.74
ng HP/µg dry weight	11.48 ± 1.03	14 ± 1.12	13.5 ± 2.49	14.01 ± 3.05
µg CS/µg dry weight	0.19 ± 0.04	0.24 ± 0.04	0.25 ± 0.04	0.33 ± 0.01
ng DNA/µg dry weight	1.59 ± 0.05	1.94 ± 0.16	1.48 ± 0.11	2.02 ± 0.22
µg HP/µg DNA	7.17 ± 0.52	7.2 ± 0.06	9.08 ± 1.43	6.8 ± 1.08
µg CS/µg DNA	120.73 ± 22.9	141.73 ± 26.67	172.56 ± 12.92	162.88 ± 11.39
µg DNA in sample	45.83 ± 9.2	52.83 ± 0.44	46.49 ± 2.36	50.83 ± 3.84

Table 7-1. Biochemical data (mean average ± S.E. for n = 3 in all cases).

7.4 Discussion

In the present study, changes in the extracellular matrix of young porcine AC after cooling and warming were detected by magnetic resonance imaging. Few comparable MRI studies have been published. Schiller *et. al.* (39) investigated the influence of temperature on stored porcine AC at 4°C and -18°C using NMR methods (39). Briefly, porcine AC cores were stored for three days either at 4°C or frozen at –18°C and thawed, then compared to fresh control tissue using NMR-spectroscopy, NMR-relaxometry, and MR-microimaging. T_1 weighted imaging did not detect any changes in the cooled samples compared to fresh controls. However, changes in T_2 relaxation were reported and attributed to degradation of the cartilage matrix. In the sample stored at 4°C, a shift in the distribution to a longer T_2 was reported. Subtle differences in the high resolution proton spectra of the three type of sample were also seen.

No direct comparison could be made between our current study and the data reported by Schiller *et. al.* (39) because the current study is a cryopreservation study of AC monitored by different MR-microimaging parameters reflecting local collagen content, proteoglycan content, and diffusion coefficient as well as combined properties of the extracellular matrix.

In the current study, three distinct bands were consistently identified in the AC with all imaging techniques. These bands were used to identify the location of specific changes in the imaging parameters.

FCD values were determined by T_1 imaging after tissue equilibration with gadolinium ($Gd\text{-}DTPA^{2-}$) and are directly related to tissue glycosaminoglycan concentration (3, 4). Therefore, FCD values reflect proteoglycan loss or other changes reflecting matrix fixed charge density. In the present study, FCD values increased with tissue depth (Figure 7-2), reflecting the known proteoglycan gradient within the tissue (22). There was a significant decrease in FCD values in the SC-Me_2SO group compared with the CTR group with a further significant decrease in the groups without Me_2SO cryoprotectant (SF and SC-PBS) when controlling for the three tissue depths. Overall, FCD values were not significantly different between the CTR and SC-Me_2SO groups ($P > 0.05$) and were not significantly different between groups without cryoprotectant (SF and SC-PBS) ($P > 0.05$). These findings suggest that ice formation during cooling and warming caused alterations in the extracellular matrix, and that these effects were limited, although not completely eliminated, by the presence of Me_2SO. The biochemical analysis supported this concept of an alteration in, rather than a loss of, PG. The potential causes of changes in MRI-determined FCD, independent of concentration changes, are unclear, but may relate to details of molecular size and tertiary structure.

The k_m value reflects the rate of the magnetization transfer (MT) from the relatively fixed protons in collagen to the more mobile protons in the interstices. Previous work has suggested that MTC in cartilage is dominated by collagen, with only minor contribution from proteoglycan (11, 16). In the present study, MT analysis was performed using the common model of a single mobile and a single bound component, operationally defined as a visible, narrow spectral component and a broad, non-observable spectral component, respectively (16). While a more sophisticated analysis is available (17), the two-component model is a well-established phenomenological description of a transfer process that reflects local collagen content. In this study, k_m values were highest in the MB of the cartilage. Cooling and warming of porcine AC tissue significantly affected the k_m value in the SB in all the SC-PBS group compared to the CTR group. The MRI data are consistent with collagen loss from the SB in the SC-PBS group but this was not supported by the biochemical studies. We attribute this to an alteration in the structure of the collagen and its interactions with the rest of the matrix due to the formation of ice in the superficial layer (28).

The water diffusion coefficient gives a measure of the effect of tissue structure on the translational mobility of water molecules, with higher macromolecular content being reflected by a lower diffusion coefficient. Our results showed a significant increase in the water diffusion coefficient in the directions both parallel and perpendicular to the articular surface in the SB but this did not vary amongst the different groups, with the exception of the SF group with respect to the perpendicular water diffusion coefficient. This indicated that the water diffusion coefficient was not strongly sensitive to alterations induced by slow cooling and warming. There was no significant difference between groups for the T_1 and T_2 relaxation times, primarily reflecting molecular motion. Thus, in this study no significant alterations in water mobility and molecular motion within the extracellular matrix were seen.

The biochemical analysis did not demonstrate any changes in any of the experimental groups immediately after cryopreservation. There is little comparable work in the literature. Stevenson *et. al.* (38, 42) documented a significant loss of glycosaminoglycans in transplanted cryopreserved canine AC, but tissue was assessed eleven months postoperatively and compared to fresh controls. No changes were seen in the hydroxyproline content in the cryopreserved samples as compared to controls (42). Schacher *et. al.* (38) showed that frozen ovine allografts and autografts three months after transplantation demonstrated a significant loss in hexuronic acid compared to fresh controls. The main difference between these two studies and the current study is the timing of the assessment of the AC components. Based on this previous work and our current results, we conjecture that matrix components are altered at the time of cooling and warming and are subsequently degraded or lost after transplantation.

The breakdown of matrix proteoglycan and collagen in AC is mainly a proteolytic process (35, 37). Cell injury due to low temperature exposure may activate degradative enzymes by stimulating increased production by the chondrocytes or by induction of the release of previously synthesized enzymes. Our data suggests that alteration, but not loss, of matrix occurs with cryopreservation. The results reported by Stevenson *et. al.* (42) and Schachar *et. al.* (38) suggest that degradation evolves slowly post transplantation; this may be a result of the alteration that occurs during cooling and warming. This is also consistent with the slow deterioration of human allograft tissue (7, 9). Thus, attempts to limit matrix alterations at the time of cryopreservation may represent one approach towards improving long-term transplantation results.

As discussed above, the combination of MRI and biochemical data suggests the occurrence of matrix changes at the molecular level, with attenuation of these changes by

Me_2SO. These structural changes may be due to ice formation, since it is known that 1*M* Me_2SO decreases the amount of ice formed at subzero temperatures (18, 33).

In summary, MRI studies suggested that cooling and warming of intact porcine AC alters collagen microstructure in the superficial region, and proteoglycan microstructure throughout the AC. Me_2SO provided some protection from these changes, indicating that ice formation may be their cause. Biochemical analyses suggested that these alterations were not accompanied by loss of these components. Finally, stability of cryopreserved transplanted AC may be enhanced by prevention of these microstructural alterations.

7.5 Acknowledgements

The authors thank P.C. Anoop for preparation of the samples. This study was funded by the MSI Foundation of Edmonton, the Edmonton Civic Employees Charitable Assistance Foundation, the Edmonton Orthopaedic Research Society and the National Institute of Health.

7.6 References

1. Almqvist, K.F., L. Wang, C. Broddelez, E.M. Veys, and G. Verbruggen. Biological freezing of human articular chondrocytes. *Osteoarthritis Cartilage* 9, 4: 341-350, 2001.
2. Aubin, P.P., H.K. Cheah, A.M. Davis, and A.E. Gross. Long-term followup of fresh femoral osteochondral allografts for posttraumatic knee defects. *Clin Orthop* 391 Suppl: S318-327, 2001.
3. Bashir, A., M.L. Gray, R.D. Boutin, and D. Burstein. Glycosaminoglycan in articular cartilage: in vivo assessment with delayed Gd(DTPA)(2-)-enhanced MR imaging. *Radiology* 205, 2: 551-558, 1997.
4. Bashir, A., M.L. Gray, and D. Burstein. Gd-DTPA2- as a measure of cartilage degradation. *Magn Reson Med* 36, 5: 665-673, 1996.
5. Bugbee, W.D. and F.R. Convery. Osteochondral allograft transplantation. *Clin Sports Med* 18, 1: 67-75, 1999.
6. CDC. Transmission of HIV through bone transplantation: Case report and public health recommendations. *MMWR* 37, 39: 557-568, 1988.
7. Clohisy, D.R. and H.J. Mankin. Osteoarticular allografts for reconstruction after resection of a musculoskeletal tumor in the proximal end of the tibia. *J Bone Joint Surg Am* 76, 4: 549-554, 1994.
8. Convery, F.R., M.H. Meyers, and W.H. Akeson. Fresh osteochondral allografting of the femoral condyle. *Clin Orthop* 273: 139-145, 1991.
9. Flynn, J.M., D.S. Springfield, and H.J. Mankin. Osteoarticular allografts to treat distal femoral osteonecrosis. *Clin Orthop* 303: 38-43, 1994.
10. Goldberg, R.L. and L.M. Kolibas. An improved method for determining proteoglycans synthesized by chondrocytes in culture. *Connect Tissue Res* 24, 3-4: 265-275, 1990.
11. Gray, M.L., D. Burstein, L.M. Lesperance, and L. Gehrke. Magnetization transfer in cartilage and its constituent macromolecules. *Magn Reson Med* 34, 3: 319-325, 1995.

12. Hajnal, J.V., C.J. Baudouin, A. Oatridge, I.R. Young, and G.M. Bydder. Design and implementation of magnetization transfer pulse sequences for clinical use. *J Comput Assist Tomogr* 16, 1: 7-18, 1992.

13. Jackson, D.W., T.M. Simon, and H.M. Aberman. Symptomatic articular cartilage degeneration: the impact in the new millennium. *Clin Orthop* 391 Suppl: S14-25, 2001.

14. Jomha, N.*Cryopreservation of human articular cartilage* in *Experimental Surgery, Masters Thesis*. University of Alberta: Edmonton, 1996.

15. Kawabe, N. and M. Yoshinao. Cryopreservation of cartilage. *Int Orthop* 14, 3: 231-235, 1990.

16. Kim, D.K., T.L. Ceckler, V.C. Hascall, A. Calabro, and R.S. Balaban. Analysis of water-macromolecule proton magnetization transfer in articular cartilage. *Magn Reson Med* 29, 2: 211-215, 1993.

17. Lattanzio, P.J., K.W. Marshall, A.Z. Damyanovich, and H. Peemoeller. Macromolecule and water magnetization exchange modeling in articular cartilage. *Magn Reson Med* 44, 6: 840-851, 2000.

18. Lovelock, J.F. The mechanism of the protective action of glycerol against haemolysis by freezing and thawing. *Biochimica et Biophysica Acta* 11, 28-36, 1953.

19. Mahomed, M.N., R.J. Beaver, and A.E. Gross. The long-term success of fresh, small fragment osteochondral allografts used for intraarticular post-traumatic defects in the knee joint. *Orthopedics* 15, 10: 1191-1199, 1992.

20. Malinin, T.I., J.L. Wagner, J.C. Pita, and H. Lo. Hypothermic storage and cryopreservation of cartilage. An experimental study. *Clin Orthop* 197: 15-26, 1985.

21. Mankin, H.J., S.H. Doppelt, T.R. Sullivan, and W.W. Tomford. Osteoarticular and intercalary allograft transplantation in the management of malignant tumors of bone. *Cancer* 50, 4: 613-630, 1982.

22. Mankin, H.J., V.C. Mow, J.A. Buckwalter, J.P. Iannotti, and A. Ratcliffe, *Form and function of articular cartilage*, in *Orthopaedic Basic Science*, S.R. Simon, Editor: Chicago. p. 1-44, 1994.

23. Maroudas, A., M.T. Bayliss, and M.F. Venn. Further studies on the composition of human femoral head cartilage. *Ann Rheum Dis* 39, 5: 514-523, 1980.

24. McGann, L.E. and J. Farrant. Survival of tissue culture cells frozen by a two-step procedure to -196 degrees C. I. Holding temperature and time. *Cryobiology* 13, 3: 261-268, 1976.

25. McGann, L.E. and J. Farrant. Survival of tissue culture cells frozen by a two-step procedure to -196 degrees C. II. Warming rate and concentration of dimethyl sulphoxide. *Cryobiology* 13, 3: 269-273, 1976.

26. Meyers, M.H., W. Akeson, and F.R. Convery. Resurfacing of the knee with fresh osteochondral allograft. *J Bone Joint Surg [Am]* 71, 5: 704-713, 1989.

27. Muldrew, K., M. Hurtig, K. Novak, N. Schachar, and L.E. McGann. Localization of freezing injury in articular cartilage. *Cryobiology* 31, 1: 31-38, 1994.

28. Muldrew, K., K. Novak, H. Yang, R. Zernicke, N.S. Schachar, and L.E. McGann. Cryobiology of articular cartilage: ice morphology and recovery of chondrocytes. *Cryobiology* 40, 2: 102-109, 2000.

29. Neeman, M., J.P. Freyer, and L.O. Sillerud. Pulsed gradient spin-echo diffusion studies in NMR imaging: effects of the imaging gradients on the determination of diffusion coefficients. *J Mag Reson* 90, 303-312, 1990.

30. Ohlendorf, C., W.W. Tomford, and H.J. Mankin. Chondrocyte survival in cryopreserved osteochondral articular cartilage. *J Orthop Res* 14, 3: 413-416, 1996.

31. Potter, K., J.J. Butler, C. Adams, K.W. Fishbein, E.W. McFarland, W.E. Horton, and R.G. Spencer. Cartilage formation in a hollow fiber bioreactor studied by proton magnetic resonance microscopy. *Matrix Biol* 17, 7: 513-523, 1998.

32. Potter, K., J.J. Butler, W.E. Horton, and R.G. Spencer. Response of engineered cartilage tissue to biochemical agents as studied by proton magnetic resonance microscopy. *Arthritis Rheum* 43, 7: 1580-1590, 2000.

33. Rall, W.F., P. Mazur, and J.J. McGrath. Depression of the ice-nucleation temperature of rapidly cooled mouse embryos by glycerol and dimethyl sulfoxide. *Biophys J* 41, 1: 1-12, 1983.

34. Rendal-Vazquez, M.E., E. Maneiro-Pampin, M. Rodriguez-Cabarcos, O. Fernandez-Mallo, I. Lopez de Ullibarri, C. Andion-Nunez, and F.J. Blanco. Effect of cryopreservation on human articular chondrocyte viability, proliferation, and collagen expression. *Cryobiology* 42, 1: 2-10, 2001.

35. Schachar, N., D. McAllister, M. Stevenson, K. Novak, and L. McGann. Metabolic and biochemical status of articular cartilage following cryopreservation and transplantation: a rabbit model. *J Orthop Res* 10, 5: 603-609, 1992.

36. Schachar, N., M. Nagao, T. Matsuyama, D. McAllister, and S. Ishii. Cryopreserved articular chondrocytes grow in culture, maintain cartilage phenotype, and synthesize matrix components. *J Orthop Res* 7, 3: 344-351, 1989.

37. Schachar, N.S., D.J. Cucheran, L.E. McGann, K.A. Novak, and C.B. Frank. Metabolic activity of bovine articular cartilage during refrigerated storage. *J Orthop Res* 12, 1: 15-20, 1994.

38. Schachar, N.S., K. Novak, M. Hurtig, K. Muldrew, R. McPherson, G. Wohl, R.F. Zernicke, and L.E. McGann. Transplantation of cryopreserved osteochondral Dowel allografts for repair of focal articular defects in an ovine model. *J Orthop Res* 17, 6: 909-919, 1999.

39. Schiller, J., M. Wagner, A. Werner, K. Arnold, and W. Grunder. [The effect of temperature on preservation of swine articular cartilage--an NMR study]. *Biomed Tech (Berl)* 40, 1-2: 19-23, 1995.

40. Stanisz, G.J. and R.M. Henkelman. Gd-DTPA relaxivity depends on macromolecular content. *Magn Reson Med* 44, 5: 665-667, 2000.

41. Stejskal, E.O. and J.E. Tanner. Spin diffusion measurements: spin echoes in the presence of a time-dependent field gradient. *J Chem Pys* 42, 288-292, 1965.

42. Stevenson, S., G.A. Dannucci, N.A. Sharkey, and R.R. Pool. The fate of articular cartilage after transplantation of fresh and cryopreserved tissue-antigen-matched and mismatched osteochondral allografts in dogs. *J Bone Joint Surg [Am]* 71, 9: 1297-1307, 1989.

43. Tavakol, K., R.G. Miller, D.P. Bazett-Jones, W.S. Hwang, L.E. McGann, and N.S. Schachar. Ultrastructural changes of articular cartilage chondrocytes associated with freeze-thawing. *J Orthop Res* 11, 1: 1-9, 1993.

44. Tomford, W.W. Transmission of disease through transplantation of musculoskeletal allografts. *J Bone Joint Surg Am* 77, 11: 1742-1754, 1995.

45. Tomford, W.W., G.R. Fredericks, and H.J. Mankin. Studies on cryopreservation of articular cartilage chondrocytes. *J Bone Joint Surg [Am]* 66, 2: 253-259, 1984.

46. Woessner, J.F. The determination of hydroxyproline in tissue and protein samples containing small proportions of this amino acid. *Arch Biochem Biophys* 93, 440-447, 1961.

Chapter Eight

Intramatrix Events during Cryopreservation of Porcine Articular Cartilage Using Rapid Cooling

NM Jomha, PC Anoop, LE McGann

A version of this chapter has been submitted to Journal of Orthopaedic Research.

8.1 Introduction

Cryopreservation of articular cartilage (AC) may improve long-term transplantation results by providing a bank of tissues that contain live chondrocytes, which can maintain the cartilage matrix over long periods of time. A bank of live tissue would also enable accurate size and contour matching which is essential for good long term results (5, 7-9), extensive testing for infectious diseases (6, 22) and the surgical procedure to be performed at appropriate times. Initial attempts at cryopreserving AC began with cryopreservation of cells in isolation (20) followed by uncontrolled freezing of intact AC (1, 17, 18, 23). Subsequent investigation of staged cooling provided improved results but these methods have not been able to provide good, long-term transplantation results (16, 19). Recent investigation has provided more promising results using a rapid-cooling technique with high concentrations of cryoprotectants (11).

Recent studies, using high concentrations of dimethyl sulfoxide (Me_2SO) and a rapid-cooling rate, have demonstrated a concentration-dependent and depth-dependent recovery of intact chondrocytes *in situ* (11). It was concluded that high concentrations of cryoprotectants could produce a partial or complete vitrification of the AC matrix resulting in 56% chondrocyte recovery from the middle layer of the matrix, which is approximately 100% of the toxicity controls. However, the dependency of recovery on the depth in the cartilage and the concentration of Me_2SO raised questions regarding physical events occurring in the matrix as a result of ice formation. As the viability of cryopreserved AC is below the acceptable level, it was thought that the knowledge of the effects of the cooling process within the matrix would provide information to direct future studies focusing on improved viability.

At lower cooling rates and/or lower concentrations of cryoprotectant agents, ice will form in the solution surrounding the sample and likely nucleate ice formation within the matrix. It is possible that matrix disruption due to ice formation is responsible for poor long-term transplantation results despite obtaining up to 60% intact cell recovery (16, 19). With more rapid cooling rates and high cryoprotectant concentrations, the solution surrounding the sample will vitrify (11), but it remains to be determined what happens within the cartilage matrix itself, during the cooling process.

This study investigated the effects of different concentrations of Me_2SO on the temperature profile and matrix structure using a rapid-cooling technique. It was hypothesized that the temperature within the cartilage matrix would closely follow the temperature in the surrounding solution because cartilage contains a high percentage of water (14), and that increasing the concentration of cryoprotectant would reduce the amount of ice formed and result in less disruption of the matrix. At the higher concentrations of Me_2SO where the surrounding solution vitrifies rather than freezes, disruption of the matrix was expected to be minimal.

8.2 Methods and Materials

Tissues

Intact stifle joints were harvested from seven sexually mature pigs sacrificed for meat consumption. In this study, pigs were selected because the cartilage thickness in the stifle joint is the closest to the exceptionally thick cartilage in human knee joints. The joints were immersed in 1X Dulbecco's phosphate buffered saline solution (pH=7.0) (PBS, Gibco, BRL, MD) and maintained at 4°C until 10mm diameter osteochondral dowels (OCDs) were harvested using a hand-held coring device (within 12 hours of death of the animal). The OCDs were harvested from the central weight-bearing portion of the medial femoral condyle and consisted of the full thickness of AC (3-4mm) perched on a 5-10mm bone base. Three OCDs were harvested from each joint.

Temperature measurements

OCDs were immersed in one step into 50ml of 1*M*, 3*M*, 5*M*, 6*M*, or 7*M* Me_2SO solutions at 4°C for 30 minutes to allow the cryoprotectant to equilibrate. The samples were placed, with 5ml of solution, in polypropylene test-tubes (17x100mm culture tube, VWR Can Lab, Ontario, Ca). Thermocouples (Omega thermocouple-Type T copper constantan; Wire size 30 gauge, Omega Engineering, Inc, Stamford, CT) were inserted into the cryoprotectant solution surrounding the OCD and into the deep, central portion of the

AC. Test-tubes containing the sample and solution were placed into an ice-water bath for 10 minutes, then plunged into liquid nitrogen (LN) until the contents of the testtube reached -190°C. The test-tubes were warmed in a 37°C water bath until the solution became liquid. Temperature measurements were recorded by Daq View USB Data acquisition system (Model OMB-DAQ 55 (Omega Engineering, Inc, Stamford, CT) at 0.35 second intervals. This was repeated in triplicate with different samples in each experimental solution.

Scanning electron microscopy

Two more OCDs were immersed in each solution of 1*M*, 5*M*, or 6*M* Me_2SO for 30 minutes at 4°C and rapidly cooled by plunging into LN as described in the previous section. After storage in LN for a minimum of two hours, samples were freeze-substituted in methanol (Sigma, St. Louis, MO) at -80°C for seven days, with complete methanol changes every one to two days. The dowels were immersed in 1% osmium tetroxide (Marivac Ltd, NS, Canada) in methanol at -60°C for two days, then allowed to warm slowly, while surrounding dry ice vaporized (over 24 hours), to approximately -10°C. Samples were then removed from the osmium tetroxide, placed into 100% methanol, and sectioned into 70μm slices from the widest portion of the dowel at room temperature. These slices were transferred into 100% ethanol and prepared for the scanning electron microscope by application of a sputter coat (Sputter Coater, Edwards, Model S15B) of gold. Scanning electron microscopy (Hitachi, S-2500) was performed (magnification = 3500 times, voltage used for capturing = 15KV) on representative sections of the matrix from the superficial, middle and deep layers and micrographs were taken (three images from each layer) resulting in nine digitized images from each sample. This was repeated twice for each experimental solution. Each digitized image was processed using Batch Processor computer program (Peter Kennedy, University of Calgary) designed specifically to identify open areas within an image by differentiating pixel intensities within the image. The percentage of open areas within the matrix was recorded for the 18 images for each concentration (two samples with nine images each).

Results from the Batch Processor were averaged for each sample and compared using Univariate analysis of variance confirmed with 95% confidence intervals. Post hoc Bonferroni testing was performed using two-tailed testing with $P < 0.05$ indicating statistical significance using SPSS-10.07 (SPSS Inc, San Rafael, CA).

8.3 Results

Figure 8-1 shows the temperature profiles from the central portion of the cartilage matrix. The temperature profile of samples immersed in 1*M* Me_2SO demonstrated early release of the latent heat of fusion, followed by a steady decrease in temperature. With higher concentrations of Me_2SO, the release of the latent heat of fusion was at lower temperatures, consistent with freezing point depression due to increased cryoprotectant concentration. As the concentration of Me_2SO increased, the amount of latent heat of fusion released decreased. During the cooling process, ice formed in the 1*M*, 3*M*, and 5*M* Me_2SO solutions surrounding the sample, while vitrification occurred in the 6*M* and 7*M* solutions (visual observation). The cooling rates for each cryoprotectant concentration shown in Table 8-1 were determined between -20°C and -120°C. There was a progressive decrease in the cooling rate with increased Me_2SO concentration. The warming rates ranged between 64°C/min and 122°C/min without a consistent pattern among the different concentations of Me_2SO.

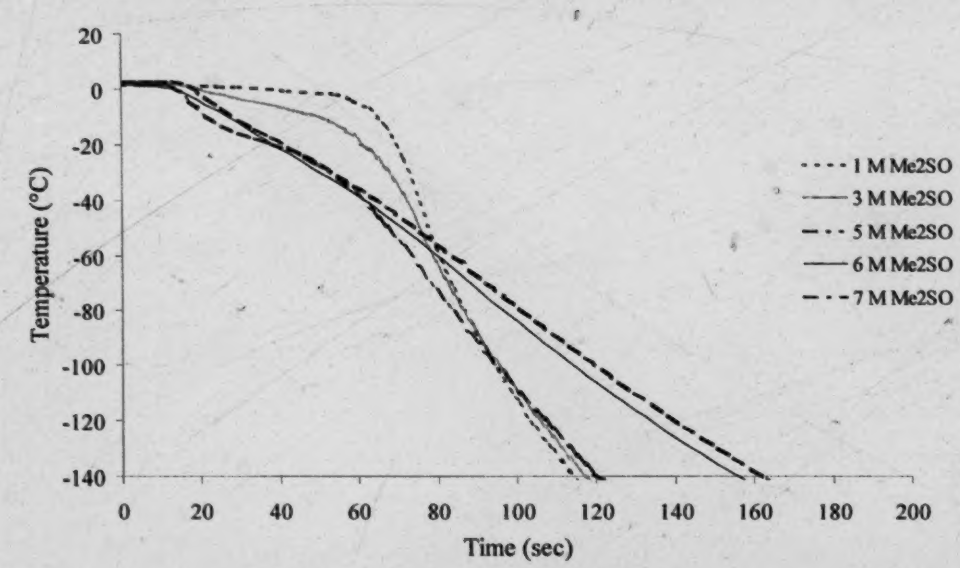

Figure 8-1. Temperature versus time graph of the temperature within the matrix during the rapid-cooling protocol from the different Me_2SO solutions. The 1*M* Me_2SO sample demonstrates the largest release of latent heat of fusion as noted by the largest shoulder to the curve. The release of heat occurs with less intensity and at lower temperatures as the concentration of Me_2SO increases. There is only a slight break in the slope in the 6*M* and 7*M* Me_2SO samples.

	Cooling rate (°C/min)
1*M* Me_2SO	187
3*M* Me_2SO	140
5*M* Me_2SO	89
6*M* Me_2SO	65
7*M* Me_2SO	61

Table 8-1. Cooling rates for each cryoprotectant concentration determined by the time to cool from -20°C to -120°C for each Me_2SO concentration.

Figure 8-2 shows the temperature gradient between the cartilage matrix and the surrounding Me_2SO solution. 1*M* Me_2SO demonstrated the largest temperature gradient that occurred at the highest temperature. As the Me_2SO concentration increased, there was a decreased temperature gradient between the matrix and the surrounding solution and the peak temperature gradient occurred at progressively lower temperatures. In addition, each curve has two peaks, one corresponding to the expected ice formation temperature and the other corresponding to the glass transformation temperature.

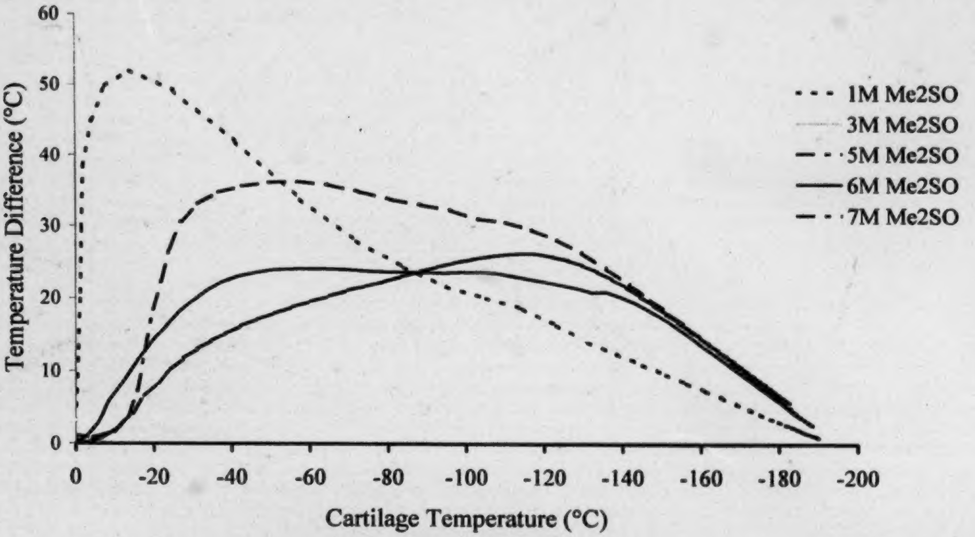

Figure 8-2. Temperature gradient graph using matrix temperature as the reference point. Each Me_2SO concentration graph contains two areas of significant slope change, one corresponding to the ice formation temperature and one corresponding to the glass transformation temperature. The lower Me_2SO concentrations exhibit larger temperature gradient at warmer temperatures (ice formation). The higher Me_2SO concentrations exhibit larger temperature gradients at cooler temperatures (glass transition – vitrification).

During the experimental procedures, the 6*M* solution surrounding the OCD vitrified while the 5*M* and 1*M* solutions formed ice. Figure 8-3 illustrates representative examples of the scanning electron micrographs of freeze-substituted samples from the 1*M*, 5*M*, and 6*M* Me_2SO solutions after rapid cooling and shows the areas of disruption within the matrix. Table 8-2 records the calculated percent of open areas within the cartilage matrix as determined by the Batch Processor computer program. There was a statistically significant decrease in the open areas in the matrix from the sample in the 6*M* Me_2SO solution when compared to the 1*M* samples ($P = 0.001$) and the 5*M* samples ($P = 0.017$). There was no statistically significant difference between the 1*M* and 5*M* samples ($P = 0.119$).

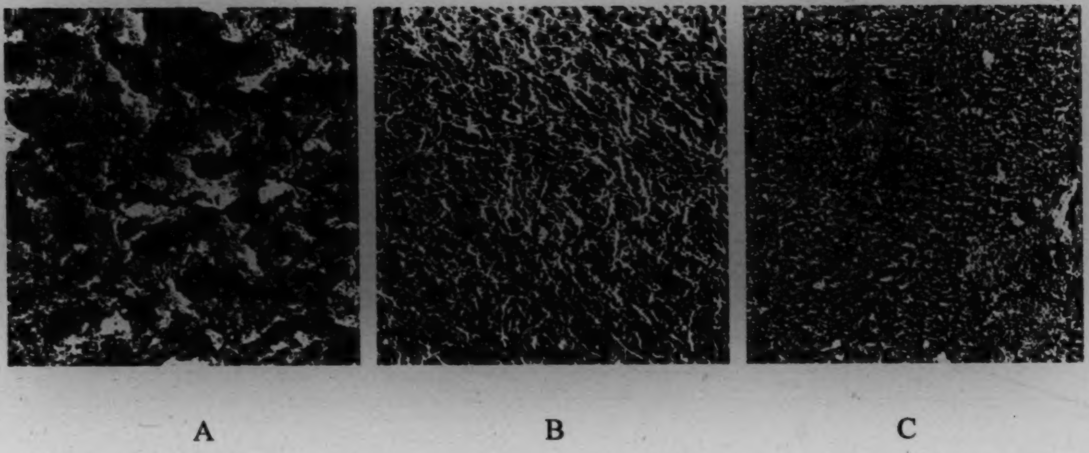

Figure 8-3. Representative scanning electron micrographs (magnification = 3500 times, voltage used for capturing = 15KV) from 1*M* Me_2SO (A), 5*M* Me_2SO (B), and 6*M* Me_2SO (C) samples. Note the larger open areas in the 1*M* Me_2SO sample compared to the homogenous appearance of the 6*M* Me_2SO sample. It is thought that the open areas contained ice crystals after the cooling process.

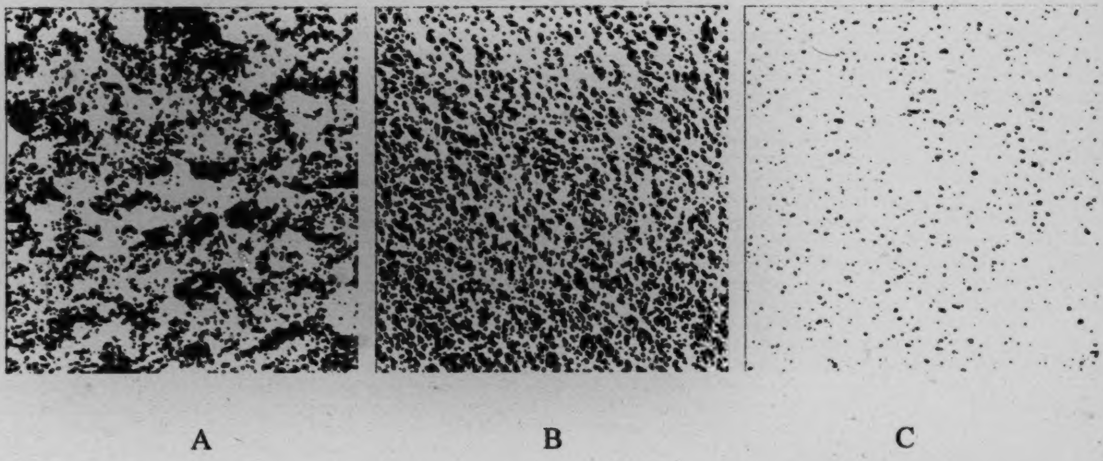

Figure 8-4. Computer generated (Batch Processor) images of the open areas from the same samples as seen in Figure 8-3. Note the larger and more frequent open areas in the 1*M* Me_2SO sample compared to the 5*M* Me_2SO sample and the minute areas in the 6*M* Me_2SO sample.

	Percent open areas (mean ± S.D.)
1*M* Me_2SO	43.3 ± 2.2
5*M* Me_2SO	30.8 ± 7.1
6*M* Me_2SO	10.5 ± 7.0

Table 8-2. Percent of open area as determined by the Batch Processor program, which shows the statistically significant decrease in open areas within the cartilage matrix after cryopreservation in the 6*M* Me_2SO sample compared to the 1*M* and 5*M* Me_2SO samples.

8.4 Discussion

Understanding the events that occur within the matrix during rapid cooling can be useful in developing methods to enhance long-term survival of cryopreserved osteochondral tissues after transplantation. The results of this study described the temperature changes that occurred within the matrix during the rapid-cooling protocol, and provided objective evidence of matrix disruption due to the cooling process.

Evidence of intramatrix ice formation is provided in Figure 8-1, where the shoulder in the curves of the samples from the 1*M* and 3*M* Me_2SO solutions are due to the release of the latent heat of fusion that occurred with ice formation. The longer delay prior to sample cooling in these samples suggested a larger amount of heat was released and therefore more ice was formed. As the Me_2SO concentration increased, the shoulder became smaller and occurred at a lower temperature. This is consistent with increased freezing point depression with higher concentrations of cryoprotectant and decreased amounts of ice formed at all temperatures. Even the 6*M* and 7*M* Me_2SO samples demonstrated a small break in the slope of the curve suggesting that even though these solutions appeared to be vitrified, there was still some ice formed within the matrix.

The proposed ice formation/vitrification events are demonstrated more clearly in Figure 8-2. This graph illustrates the temperature gradients between the solution itself and the temperature within the central portion of the matrix. The 1*M* Me_2SO sample had the largest divergence at a relative high subzero temperature likely corresponding to the large amount of ice formed at higher temperatures. This corresponded to the longer delay prior to sample cooling seen in Figure 8-1. As the concentration of Me_2SO increased, the peak temperature gradient decreased and occurred at progressively lower temperatures. This indicated that less latent heat of fusion was being released corresponding to less ice formation occurring within the matrix. The shift in the initial peak to lower temperatures with higher Me_2SO concentrations correlated well with the freezing point depression expected with higher cryoprotectant concentrations. It is important to note that even though the 6*M* and 7*M* Me_2SO solutions vitrified, there was still a temperature difference between the cartilage and the surrounding solution at temperatures above the glass transformation temperature, suggesting that some ice formation occurred within the matrix even when the surrounding solution vitrified. This was more pronounced for the 6*M* than the 7*M* samples.

The second peak in Figure 8-2 occurred near the glass transition temperature for Me_2SO in water, suggesting that this was the result of the release of latent heat associated with glass transformation. Although the temperature difference near the glass transition temperature was more prominent at the higher Me_2SO concentrations, the smaller peaks in the 1*M* and 3*M* Me_2SO solutions suggested that some vitrification occurred in the matrix even with these lower concentrations of cryoprotectant. It is likely that as ice formed in these low Me_2SO concentration solutions, the Me_2SO became increasingly concentrated by exclusion of Me_2SO by ice until the concentration was sufficient for vitrification to occur in the matrix.

The presence of ice in the matrix of the samples in the 6*M* Me_2SO solution may be surprising because the 6*M* Me_2SO solution surrounding the sample vitrified on rapid cooling. Under these conditions, a recent study has demonstrated up to 100% intact cell recovery compared to toxicity controls from the superficial and middle portions of the cartilage matrix after rapid cooling in 6*M* Me_2SO (11), suggesting that complete vitrification throughout the matrix is not required for high cell recovery.

Most attention from cryopreservation studies of AC has focused on chondrocyte recovery. The scanning electron micrographs in this study introduced important elements to the cryopreservation picture. Previous studies using a slow cooling cryopreservation technique have demonstrated up to 60% intact cell recovery (15, 16), yet long-term transplantation studies were disappointing (16, 19). The present study objectively demonstrated significantly increased matrix disruption with low concentrations of Me_2SO, most likely due to the ice formed during the cryopreservation procedure (Figures 8-3 and 8-4, Table 8-2). Conversely, high concentrations of Me_2SO resulted in minimal disruption either due to miniscule ice crystals or vitrification, consistent with another study (10). It is possible that the cells that survive the cryopreservation process in the previously mentioned studies were not able to repair the damaged matrix resulting in deterioration over the long term. However, post-thaw assessments of the mechanical properties of AC (3, 13) have not demonstrated significant alterations in mechanical properties immediately after cryopreservation. One possibility is that the methods of testing for mechanical changes were not sufficiently sensitive to measure accurately the matrix disruption that occurred with ice formation. Alternatively, it could be that disruption of the matrix is not expressed as altered mechanical properties immediately after cryopreservation and becomes evident only with use and the passage of time. It is now apparent that viable chondrocytes in a normal matrix are essential requirements for successful AC transplantation.

Intramatrix cooling and warming rates are difficult to describe with a single number because the temperature/time curve is nonlinear, and varies for different Me_2SO concentrations. At lower concentrations, there was a long delay prior to sample cooling as the latent heat of fusion was released at high subzero temperatures. The temperature range for calculating the rates of cooling and warming were arbitrarily selected to eliminate most of the delay due to the latent heat of fusion. There was a decreased cooling rate with increased Me_2SO concentration. This was consistent but caution must be used because of the limitations imposed by the different patterns of cooling that occurred.

It has been shown that high concentrations of cryoprotectants with a rapid-cooling protocol can achieve relatively high, intact cell recovery that may be improved with alterations of cryoprotectant concentrations, combinations of cryoprotectants, and the methods of addition and dilution of the cryoprotectant (2, 4, 12, 21, 24). In addition, this study demonstrated that high Me_2SO concentrations resulted in significantly less matrix disruption. This was likely due to partial vitrification within the matrix as noted by the temperature measurements and scanning electron micrographs. The use of high concentrations of cryoprotectants and a rapid-cooling protocol may result in better long-term transplantation results due to a more normal matrix and viable cells to maintain the matrix. Transplantation studies are required to provide conclusive proof.

8.5 Acknowledgements

The authors thank Dr. Keith Bagnall for review of the paper, Lauren Beaupre for statistical analysis and Ouellette Packers Ltd., Edmonton for supplying the tissue. Funding was provided by Edmonton Orthopaedic Research Society, Edmonton Civic Employees Charitable Assistance Fund, and The University of Alberta Hospital Foundation.

8.6 References

1. Almqvist, K.F., L. Wang, C. Broddelez, E.M. Veys, and G. Verbruggen. Biological freezing of human articular chondrocytes. *Osteoarthritis Cartilage* 9, 4: 341-350, 2001.
2. Armitage, W.J. and S.J. Rich. Vitrification of organized tissues. *Cryobiology* 27, 5: 483-491, 1990.
3. Arnoczky, S.P., M. C.A., S. M.B., V.C. Mow, and R.F. Warren. The effect of cryopreservation on canine menisci: a biochemical, morphologic, and biomechanical evaluation. *J of Orthop Res* 6, 1: 1-12, 1988.
4. Bourne, W.M. and L.R. Nelson. Human corneal studies with a vitrification solution containing dimethyl sulfoxide, formamide, and 1,2-propanediol. *Cryobiology* 31, 6: 522-530, 1994.
5. Bugbee, W.D. and F.R. Convery. Osteochondral allograft transplantation. *Clin Sports Med* 18, 1: 67-75, 1999.
6. CDC. Transmission of HIV through bone transplantation: Case report and public health recommendations. *MMWR* 37, 39: 557-568, 1988.
7. Convery, F.R., M.H. Meyers, and W.H. Akeson. Fresh osteochondral allografting of the femoral condyle. *Clin Orthop* 273: 139-145, 1991.
8. Flynn, J.M., D.S. Springfield, and H.J. Mankin. Osteoarticular allografts to treat distal femoral osteonecrosis. *Clin Orthop* 303: 38-43, 1994.
9. Garrett, J.C. Treatment of osteochondral defects of the distal femur with fresh osteochondral allografts: a preliminary report. *Arthroscopy* 2, 4: 222-226, 1986.
10. Hunziker, E.B., J. Wagner, and D. Studer. Vitrified articular cartilage reveals novel ultra-structural features respecting extracellular matrix architecture. *Histochem Cell Biol* 106, 4: 375-382, 1996.
11. Jomha, N.M., P.C. Anoop, K. Bagnall, and L.E. McGann. Effects of increasing concentrations of dimethyl sulfoxide during cryopreservation of porcine articular cartilage. *Cell Pres Tech* 1, 2: 111-120, 2002.
12. Jutte, N.H., P. Heyse, H.G. Jansen, G.J. Bruining, and G.H. Zeilmaker. Vitrification of human islets of Langerhans. *Cryobiology* 24, 5: 403-411, 1987.

13. Kiefer, G.N., K. Sundby, D. McAllister, and e. al. The effect of cryopreservation on the biomechanical behavior of bovine articular cartilage. *J Orthop Res* 7, 494-501, 1989.

14. Mankin, H.J., V.C. Mow, J.A. Buckwalter, J.P. Iannotti, and A. Ratcliffe. *Form and function of articular cartilage.*, in *Orthopaedic Basic Science*, S.R. Simon, Editor: Chicago. 1-44, 1994.

15. Muldrew, K., M. Hurtig, K. Novak, N. Schachar, and L.E. McGann. Localization of freezing injury in articular cartilage. *Cryobiology* 31, 1: 31-38, 1994.

16. Muldrew, K., K. Novak, C. Studholme, G. Wohl, R. Zernicke, N.S. Schachar, and L.E. McGann. Transplantation of articular cartilage following a step-cooling cryopreservation protocol. *Cryobiology* 43, 3: 260-267, 2001.

17. Rendal-Vazquez, M.E., E. Maneiro-Pampin, M. Rodriguez-Cabarcos, O. Fernandez-Mallo, I. Lopez de Ullibarri, C. Andion-Nunez, and F.J. Blanco. Effect of cryopreservation on human articular chondrocyte viability, proliferation, and collagen expression. *Cryobiology* 42, 1: 2-10, 2001.

18. Schachar, N., M. Nagao, T. Matsuyama, D. McAllister, and S. Ishii. Cryopreserved articular chondrocytes grow in culture, maintain cartilage phenotype, and synthesize matrix components. *J Orthop Res* 7, 3: 344-351, 1989.

19. Schachar, N.S., K. Novak, M. Hurtig, K. Muldrew, R. McPherson, G. Wohl, R.F. Zernicke, and L.E. McGann. Transplantation of cryopreserved osteochondral Dowel allografts for repair of focal articular defects in an ovine model. *J Orthop Res* 17, 6: 909-919, 1999.

20. Smith, A.U. Survival of frozen chondrocytes isolated from cartilage of adult mammals. *Nature* 205, 782-784, 1965.

21. Song, Y.C., P.O. Hagen, F.G. Lightfoot, M.J. Taylor, A.C. Smith, and K.G. Brockbank. In vivo evaluation of the effects of a new ice-free cryopreservation process on autologous vascular grafts. *J Invest Surg* 13, 5: 279-288, 2000.

22. Tomford, W.W. Transmission of disease through transplantation of musculoskeletal allografts. *J Bone Joint Surg Am* 77, 11: 1742-1754, 1995.

23. Tomford, W.W. and H.J. Mankin. Investigational approaches to articular cartilage preservation. *Clin Orthop* 174: 22-27, 1983.

24. Wusteman, M.C., D.E. Pegg, M.P. Robinson, L.H. Wang, and P. Fitch. Vitrification media: toxicity, permeability, and dielectric properties. *Cryobiology* 44, 1: 24-37, 2002.

Chapter Nine

General Discussion and Conclusion

9.1 General Discussion

Large, full-thickness osteochondral defects progress to osteoarthritis (2, 14, 41), a significant cause of disability (21). To date, there are no proven good, long-term treatment options. Osteochondral allografting has had some success (4, 8, 11, 13, 17, 19, 26) but problems remain concerning accurate size/contour matching (8, 12, 17, 27), infectious disease prevention (10, 39), and planning for the surgical procedure. Successful cryopreservation of articular cartilage (AC) can provide a bank of appropriate tissues that contain live chondrocytes in a functional matrix. It would also solve the major problems affecting the current practice of osteochondral allografting and likely improve on the long-term transplantation results.

It was determined that numerous studies would be required to resolve the issue of the cryopreservation of AC. Assessment of chondrocyte *in situ* recovery using membrane integrity stains required counting of intact and disrupted cells throughout multiple cartilage slices. Cell counting was an onerous task that required many weeks per study to complete. As well, it was thought that human evaluation was too subjective because of the background interference that occurred when using membrane integrity stains on the cartilage matrix. A custom, computer program had been designed to estimate intact cell recovery based on pixel colour intensity from the fluorescent dyes (ethidium bromide and Syto 13). The initial study in this thesis was performed and this study validated the reliability of using this computer program on chondrocytes *in situ.*

Articular cartilage research began with investigation on cryopreservation of isolated cells (1, 34, 36, 40) followed by chondrocytes *in situ* (9, 22, 32). Despite initial disappointing results with other techniques (9, 22, 32), cryopreservation using a 2-stage technique or a stepped-cooling technique with low concentration of cryoprotectant (28, 29) showed some promise, most noticeably on ovine AC (30, 31). Unfortunately, despite relatively good cell recovery on sheep, attempts to reproduce those results on thicker, human AC were unsuccessful (31, 35). Further investigation of the causes of cell injury suggested that ice formation and the resultant accumulation of solutes within the matrix were the main cause of cell loss during slow-cool, low concentration cryopreservation. The difficulty in controlling ice formation and solute accumulation led to the initial study in this thesis.

To confirm the ice formation/solute concentration theory, the first study physically altered the bone carrier portion of the 10mm osteochondral dowel (OCD) to provide a potential escape route for "trapped" solutes and another entry point for ice nucleation of the matrix. Porcine AC was used in all experiments due to difficulties in obtaining healthy human AC. Porcine AC of the stifle joint is approximately 3-4mm thick and approximates the thickness of AC in the human knee joint. Although ethical approval had been obtained for using donor human tissue, the number of suitable donors available to have tissue donated for research was sporadic and unreliable. Therefore, a constant supply of pig joints was arranged through a local meat packer (Ouellette Packers Ltd., Edmonton). A 2mm hole was drilled through the central portion of the bone base to increase the surface area exposed to cryoprotectant and the contact area exposed to ice nucleation. The results of this experiment supported the ice nucleation theory by demonstrating a significantly increased recovery of intact cells with an altered distribution of recovery. Even though the recovery was higher than the control samples, physically altering the bone base was not a practical option with clinical applicability and alternative physical alterations did not seem viable.

The results of this initial study, along with unpublished work, reinforced the idea that increasing the number of viable cells after slow-cooled, low concentration cryopreservation could not be done using practical methods that would continue to provide viable clinical opportunities. Even though up to 60% intact cell recovery had been demonstrated on ovine AC using this technique, replication on the thicker AC that exists within human joints did not seem realistic. Therefore, a change of philosophy to using high concentrations of cryoprotectant in a rapid cooling protocol (in an attempt to achieve vitrification - consolidation of an aqueous solution into a solid state without crystalline formation) occurred. This was encouraged by the publication of studies successfully vitrifying other tissues (3, 5, 23, 25, 33, 37).

Vitrification avoids phase separation that occurs with ice formation and may eliminate the problems associated with tissue freezing. Vitrification has had some success in cryopreservation of other tissues (3, 5, 23, 25, 33, 37), including a recent report using thin rabbit

AC (38). The first cartilage study in this thesis using the thicker porcine AC and increasing concentrations of cryoprotectant with a rapid cooling rate demonstrated a peak recovery of intact cells at 6*M* dimethyl sulfoxide (Me_2SO) (42%). Lower recovery rates were noted from the lower concentration solutions (1*M*, 3*M*, and 5*M*) likely due to uncontrolled ice formation damaging the cells. Conversely, toxicity was the main problem with higher (5*M*, 6*M*, and 7*M*) concentration solutions. The other difficulty that became apparent was the lack of penetration of the cryoprotectant solutions into the deep portions of the matrix noted by the low recovery of cells from the deep layer.

To enhance the penetration of the Me_2SO into the matrix, the matrix was hydrated by altering the tonicity of the solution. It was hypothesized that hydrating the matrix would accelerate penetration of the Me_2SO into the deep layers, resulting in enhanced protection in the deep layer with less duration of cryoprotectant exposure in the superficial layer. Increased penetration did occur but a concomitant increase in protection was not evident. The 6*M* Me_2SO solution immersed in the isotonic phosphate buffered saline (PBS) solution had the highest recovery of intact cells (39%). Lower tonicity solutions of 6*M* Me_2SO had lower recovery rates of cells, likely due to increased toxicity from increased cryoprotectant exposure. Conversely, the 5*M* Me_2SO solution samples had virtually no recovery in the isotonic solution but increased recovery in the hypotonic solutions supporting the hypothesis that hypotonic solutions increased cryoprotectant penetration. This study demonstrated that cryoprotectant penetration can be altered physiologically but poor cryoprotectant penetration and toxicity continued to be the primary obstacles to successful cryopreservation of thick AC.

The final experiment using high concentrations of cryoprotectants with a rapid-cooling technique compared three solutions – 6*M* Me_2SO, 5*M* 1,2-propanediol (PD), and VS-55 (a combination solution of Me_2SO/PD/formamide). These solutions were selected because of previous studies that had used them as vitrification solutions and the success they have had on tissues including AC. The combination solution (VS-55) was expected to be the least toxic due to the lower concentrations of individual cryoprotectants. Surprisingly, the VS-55 solution was not significantly less toxic than the 6*M* Me_2SO or

5*M* PD solutions. The success of the VS-55 solution in thin rabbit AC led to the expectation of similar results in thicker AC but, unexpectedly, the Me_2SO solution had the highest recovery rate of intact cells. The pattern of toxicity in the superficial layer and inadequate protection in the deep layer with optimal recovery in the middle layer was noted in all three solutions as had been seen in previous studies. Despite alterations in solution tonicity and cryoprotectant solutions, cryoprotectant toxicity and penetration remained the primary issues hindering successful cryopreservation of AC.

Even though the initial studies with low concentrations of cryoprotectants and a slow-cool protocol showed low recovery of intact cells, other reports have demonstrated up to 60% recovery of intact cells in ovine AC (30, 31). However, transplantation results at one year have been poor, even with this level of cell recovery. Intramatrix ice formation, which can be protective to chondrocytes, may cause disruption of the matrix as has been suggested (20). To investigate the intramatrix events during cooling, temperature measurements and scanning electron microscopy were utilized to characterize the environment within the matrix. By measuring the temperature within the matrix and the surrounding solution during the cooling process, the release of heat (either due to latent heat of fusion during ice formation or heat release from the phase change of vitrification) was used to determine whether ice formed within the matrix. Interestingly, even when high concentrations of Me_2SO vitrified surrounding the sample, a small amount of ice still formed within the matrix. When lower concentrations of Me_2SO were used, larger amounts of ice formed.

Concomitant scanning electron micrographs were evaluated for the presence of open areas indicating matrix disruption, likely due to ice formation. Once again, the samples from lower concentrations of Me_2SO produced significantly more matrix disruption when compared with the samples from 6*M* Me_2SO. This was consistent with the MRI study examining structural properties of the cartilage matrix after a slow-cool, low concentration cryopreservation protocol. That study provided confirming evidence of the matrix alteration by ice formation. This information indicated that matrix damage or chondrocyte loss may be responsible for poor, long-term transplantation results.

Accordingly, it is probable that the preservation of intact cartilage matrix with viable chondrocytes *in situ* is required for successful transplantation of cryopreserved AC.

Early work on this thesis indicated that the slow-cool, low concentration cryopreservation protocol can obtain moderate cell recovery but achieving an equivalent or better rate on thicker porcine AC is difficult. The type of physical alterations to the bone structure required to increase the recovery of chondrocytes makes application of this cryopreserved tissue to clinical problems impractical. Drilling multiple holes through the bone to the bone-cartilage junction in a complex geometric shape such as a femoral condyle would be technically difficult and would jeopardize the mechanical integrity of the graft. Furthermore, there is evidence that the protective ice formation that occurs with this technique is detrimental to the matrix structure and may cause the cartilage to deteriorate over time after transplantation. On the other hand, vitrification (using a rapid-cool, high cryoprotectant concentration protocol) seems to hold more promise because it also can obtain recovery of high numbers of intact cells but with significantly less matrix disruption. The primary problems with vitrification that remain are cryoprotectant toxicity and penetration.

Future research in this area should focus on cryoprotectant toxicity and penetration into thick AC matrix. These two obstacles are intimately intertwined as increased exposure to increase cryoprotectant penetration increases the risk of toxicity. Developing a method to allow the cells to tolerate vitrification concentrations of solution may be one answer because cells that survived exposure to high concentrations of cryoprotectant also survived the cryopreservation process. In the current studies, this was most evident in the middle layer where nearly 100% of the cells that survived initial cryoprotectant exposure remained intact after the cryopreservation protocol. Once the primary factors of toxicity and penetration have been dealt with, other factors such as devitrification and heat transfer must also be considered because of their detrimental effects on cell recovery.

Cryoprotectant toxicity can be minimized by various approaches. Although VS-55 was not effective in the thick porcine AC, it has been effective in other tissues such as thin rabbit AC (38) and vascular tissues (37). The combination of three relatively low concentrations of cryoprotectants may have provided an inadequate concentration gradient to the thick porcine AC. The concentration gradient can be increased by combining only two cryoprotectants at moderately higher concentrations, potentially increasing the cryoprotectant penetration. Cryoprotectants other than those used in VS-55 such as 2,3-butanediol (6, 7, 15, 44) or ethylene glycol (43, 44) alone or in combination (16, 18, 23, 33, 37) may be effective by exhibiting different penetration characteristics and chemical interactions. The addition of non-penetrating cryoprotectants may draw water out of the matrix and help concentrate lower molarity solutions of penetrating cryoprotectants, effectively increasing the concentration of the cryoprotectant after initial exposure to lower molarities. Vitrification could still occur despite exposure to lower concentrations of individual cryoprotectants. Further lowering of the concentration required to vitrify can be accomplished with the application of high pressures (24).

Another method to limit toxicity and osmotic stresses is step-wise addition/dilution (3, 5, 23, 37, 44). Initial exposure of the cartilage matrix to lower concentrations of cryoprotectant may permit penetration into the deeper layers with lower cryoprotectant exposure to the superficial layer. Step-wise addition of the cryoprotectant results in progressively higher concentration exposure but results in an overall exposure to high cryoprotectant concentrations of shorter duration. This may be a method to get higher concentrations of cryoprotectants into the deeper layers while limiting superficial layer toxicity. Cryoprotectant toxicity is temperature dependent therefore addition should be done at cooler temperatures. Conversely, dilution can be done in warmer temperatures because cryoprotectant penetration out of cells is more rapid at warmer temperatures. The expeditious removal of the cryoprotectant from the cells may outweigh the cost of increased toxicity due to the warmer temperature. Further investigation into these methods will limit toxicity and enhance cell recovery.

Penetration of the cryoprotectant into the matrix is another problem that remains to be solved. As mentioned previously, the use of two cryoprotectants in combination at moderate concentrations may increase the penetration due to the increased concentration gradient. Various cryoprotectants can be used based on differing mechanisms of action. Other methods of increasing penetration into the matrix can include chemical alteration of the hydroxyl terminal end of cryoprotectants. The hydroxylation of various cryoprotectants decreases cryoprotectant-cryoprotectant interactions making these modified cryoprotectants more effective. This modification also increases the cryoprotectant permeability (42), which may enhance penetration into the matrix as can the application of a pressure gradient. All of these methods, alone or in combination, have the potential to increase cryoprotectant penetration into the cartilage matrix and to increase the recovery of intact chondrocytes.

Many of the methods described here have formed the basis of a Canadian Institutes of Health Research grant currently submitted. It should be noted that membrane integrity assays are not an exact measure of cell viability even though they have been shown to have the best correlation with transplantation outcome (35). Other cell viability assays such as radionuclide incorporation and cell colony culture would be useful and it would be beneficial to investigate the relationship between intact cell recovery using membrane integrity stains and other cell viability methods. Ultimately, the most reliable method to determine the ability of a chondrocyte *in situ* to survive and function is transplantation. The previously mentioned CIHR application will incorporate these additional tests once cell recovery as determined by membrane integrity stains, has improved. Another important question that remains unanswered is the number of cells required to maintain the cartilage over the long term. This can best be answered by correlating cell recovery with long-term outcomes in transplantation studies and will be examined once transplantation procedures begin.

9.2 Conclusion

In conclusion, this research investigated various methods of cryopreserving intact AC. Initial poor results from the slow-cool, low concentration cryoprotectant method were due to inadequate cryoprotectant penetration, uncontrolled ice formation/solute buildup and matrix disruption. Rapid-cool, high concentration cryoprotectant protocols have shown promise with moderate cell recovery and minimal matrix damage. Further investigation will focus on minimizing toxicity, increasing cryoprotectant penetration, and a subsequent transplantation program using AC cryopreserved in a rapid-cooled, highly concentrated cryoprotectant.

9.3 References

1. Almqvist, K.F., L. Wang, C. Broddelez, E.M. Veys, and G. Verbruggen. Biological freezing of human articular chondrocytes. *Osteoarthritis Cartilage* 9, 4: 341-350, 2001.
2. Anderson, A.F. and M.J. Pagnani. Osteochondritis dissecans of the femoral condyles. Long-term results of excision of the fragment. *Am J Sports Med* 25, 6: 830-834, 1997.
3. Armitage, W.J. and S.J. Rich. Vitrification of organized tissues. *Cryobiology* 27, 5: 483-491, 1990.
4. Bell, R.S., A. Davis, D.G. Allan, F. Langer, A.A. Czitrom, and A.E. Gross. Fresh osteochondral allografts for advanced giant cell tumors at the knee. *J Arthroplasty* 9, 6: 603-609, 1994.
5. Bourne, W.M. and L.R. Nelson. Human corneal studies with a vitrification solution containing dimethyl sulfoxide, formamide, and 1,2-propanediol. *Cryobiology* 31, 6: 522-530, 1994.
6. Boutron, P. Levo- and dextro-2,3-butanediol and their racemic mixture: Very efficient solutes for vitrification. *Cryobiology* 27, 55-69, 1990.
7. Boutron, P., *Non-equilibrium formation of ice in aqueous solutions: Efficiency of polyalcohol solutions for vitrification*, in *The biophysics of organ cryopreservation*, D.E. Pegg and A.M.J. Karow, Editors. Plenum: New York. p. 201-228, 1987.
8. Bugbee, W.D. and F.R. Convery. Osteochondral allograft transplantation. *Clin Sports Med* 18, 1: 67-75, 1999.
9. Bujia, J., D. Kremer, H. Sudhoff, E. Viviente, C. Sprekelsen, and E. Wilmes. Determination of viability of cryopreserved cartilage grafts. *Eur Arch Otorhinolaryngol* 252, 1: 30-34, 1995.
10. CDC. Transmission of HIV through bone transplantation: Case report and public health recommendations. *MMWR* 37, 39: 557-568, 1988.
11. Clohisy, D.R. and H.J. Mankin. Osteoarticular allografts for reconstruction after resection of a musculoskeletal tumor in the proximal end of the tibia. *J Bone Joint Surg Am* 76, 4: 549-554, 1994.

12. Convery, F.R., M.H. Meyers, and W.H. Akeson. Fresh osteochondral allografting of the femoral condyle. *Clin Orthop* 273: 139-145, 1991.

13. Czitrom, A.A., F. Langer, N. McKee, and A.E. Gross. Bone and cartilage allotransplantation. A review of 14 years of research and clinical studies. *Clin Orthop* 208: 141-145, 1986.

14. De Smet, A.A., O.A. Ilahi, and B.K. Graf. Untreated osteochondritis dissecans of the femoral condyles: prediction of patient outcome using radiographic and MR findings. *Skeletal Radiol* 26, 8: 463-467, 1997.

15. Fahy, G.M., D.R. MacFarlane, C.A. Angell, and H.T. Meryman. Vitrification as an approach to cryopreservation. *Cryobiology* 21, 4: 407-426, 1984.

16. Fahy, G.M., J. Saur, and R.J. Williams. Physical problems with the vitrification of large biological systems. *Cryobiology* 27, 5: 492-510, 1990.

17. Flynn, J.M., D.S. Springfield, and H.J. Mankin. Osteoarticular allografts to treat distal femoral osteonecrosis. *Clin Orthop* 303: 38-43, 1994.

18. Fujita, T., Y. Takami, K. Ezoe, T. Saito, A.K. Sato, N. Takeda, Y. Yamamoto, K. Homma. Successful preservation of human skin by vitrification. *J Burn Care Rehabil* 21, 4: 304-309, 2000.

19. Ghazavi, M.T., K.P. Pritzker, A.M. Davis, and A.E. Gross. Fresh osteochondral allografts for post-traumatic osteochondral defects of the knee. *J Bone Joint Surg Br* 79, 6: 1008-1013, 1997.

20. Hunziker, E.B., J. Wagner, and D. Studer. Vitrified articular cartilage reveals novel ultra-structural features respecting extracellular matrix architecture. *Histochem Cell Biol* 106, 4: 375-382, 1996.

21. Jackson, D.W., T.M. Simon, and H.M. Aberman. Symptomatic articular cartilage degeneration: the impact in the new millennium. *Clin Orthop* 391 Suppl: S14-25, 2001.

22. Jomha, N.*Cryopreservation of human articular cartilage* in *Experimental Surgery, Masters Thesis*. University of Alberta: Edmonton, 1996.

23. Jutte, N.H., P. Heyse, H.G. Jansen, G.J. Bruining, and G.H. Zeilmaker. Vitrification of human islets of Langerhans. *Cryobiology* 24, 5: 403-411, 1987.

24. Kanno, H. and C.A. Angell. Homogenous nucleatoin and galss formation in aqueous alkali halide solutions at high pressures. *J Phys Chem* 81, 2639-2643, 1977.

25. Kurata, H., K. Takakuwa, and K. Tanaka. Vitrification of hematopoietic progenitor cells obtained from human cord blood. *Bone Marrow Transplant* 14, 2: 261-263, 1994.

26. Mahomed, M.N., R.J. Beaver, and A.E. Gross. The long-term success of fresh, small fragment osteochondral allografts used for intraarticular post-traumatic defects in the knee joint. *Orthopedics* 15, 10: 1191-1199, 1992.

27. Marco, F., C. Leon, F. Lopez-Oliva, A.J. Perez, A. Sanchez-Barba, and L. Lopez-Duran Stern. Intact articular cartilage cryopreservation. In vivo evaluation. *Clin Orthop* 283: 11-20, 1992.

28. McGann, L.E. and J. Farrant. Survival of tissue culture cells frozen by a two-step procedure to -196 degrees C. I. Holding temperature and time. *Cryobiology* 13, 3: 261-268, 1976.

29. McGann, L.E. and J. Farrant. Survival of tissue culture cells frozen by a two-step procedure to -196 degrees C. II. Warming rate and concentration of dimethyl sulphoxide. *Cryobiology* 13, 3: 269-273, 1976.

30. Muldrew, K., M. Hurtig, K. Novak, N. Schachar, and L.E. McGann. Localization of freezing injury in articular cartilage. *Cryobiology* 31, 1: 31-38, 1994.

31. Muldrew, K., K. Novak, C. Studholme, G. Wohl, R. Zernicke, N.S. Schachar, and L.E. McGann. Transplantation of articular cartilage following a step-cooling cryopreservation protocol. *Cryobiology* 43, 3: 260-267, 2001.

32. Ohlendorf, C., W.W. Tomford, and H.J. Mankin. Chondrocyte survival in cryopreserved osteochondral articular cartilage. *J Orthop Res* 14, 3: 413-416, 1996.

33. Rall, W.F. and G.M. Fahy. Ice-free cryopreservation of mouse embryos at -196 degrees C by vitrification. *Nature* 313, 6003: 573-575, 1985.

34. Schachar, N., M. Nagao, T. Matsuyama, D. McAllister, and S. Ishii. Cryopreserved articular chondrocytes grow in culture, maintain cartilage phenotype, and synthesize matrix components. *J Orthop Res* 7, 3: 344-351, 1989.

35. Schachar, N.S., K. Novak, M. Hurtig, K. Muldrew, R. McPherson, G. Wohl, R.F. Zernicke, and L.E. McGann. Transplantation of cryopreserved osteochondral Dowel allografts for repair of focal articular defects in an ovine model. *J Orthop Res* 17, 6: 909-919, 1999.

36. Smith, A.U. Survival of frozen chondrocytes isolated from cartilage of adult mammals. *Nature* 205, 782-784, 1965.

37. Song, Y.C., P.O. Hagen, F.G. Lightfoot, M.J. Taylor, A.C. Smith, and K.G. Brockbank. In vivo evaluation of the effects of a new ice-free cryopreservation process on autologous vascular grafts. *J Invest Surg* 13, 5: 279-288, 2000.

38. Song, Y.C., F.G. Lightfoot, C.Y. Li, J.M. Boggs, M.J. Taylor, Y.H. An, and K.G.M. Brockbank. Successful cryopreservation of articular cartilage by vitrification. *Thirty-eigth annual meeting of the society for cryobiology* Edinburgh, United Kingdom, July 29-Aug1: 2001.

39. Tomford, W.W. Transmission of disease through transplantation of musculoskeletal allografts. *J Bone Joint Surg Am* 77, 11: 1742-1754, 1995.

40. Tomford, W.W., G.R. Fredericks, and H.J. Mankin. Studies on cryopreservation of articular cartilage chondrocytes. *J Bone Joint Surg [Am]* 66, 2: 253-259, 1984.

41. Twyman, R.S., K. Desai, and P.M. Aichroth. Osteochondritis dissecans of the knee. A long-term study. *J Bone Joint Surg Br* 73, 3: 461-464, 1991.

42. Wowk, B., M. Darwin, S.B. Harris, S.R. Russell, and C.M. Rasch. Effects of solute methoxylation on glass-forming ability and stability of vitrification solutions. *Cryobiology* 39, 3: 215-227, 1999.

43. Wowk, B., E. Leitl, C.M. Rasch, N. Mesbah-Karimi, S.B. Harris, and G.M. Fahy. Vitrification enhancement by synthetic ice blocking agents. *Cryobiology* 40, 3: 228-236, 2000.

44. Wusteman, M.C., D.E. Pegg, M.P. Robinson, L.H. Wang, and P. Fitch. Vitrification media: toxicity, permeability, and dielectric properties. *Cryobiology* 44, 1: 24-37, 2002.